

- JAM20: Cammarota, Gamberg, Kang, Miller, Pitonyak, Prokudin, Rogers, Sato, Phys.Rev.D 102 (2020) 5, 054002
- Gamberg, Kang, Pitonyak, Prokudin, Sato, Phys.Lett.B 816 (2021)
- JAM22: Gamberg, Malda, Miller, Pitonyak, Prokudin, Sato, arXiv:2205.00999

THE ORIGIN OF SPIN ASYMMETRIES

Alexei Prokudin

“Experiments with spin have killed more theories than any other single physical parameter”

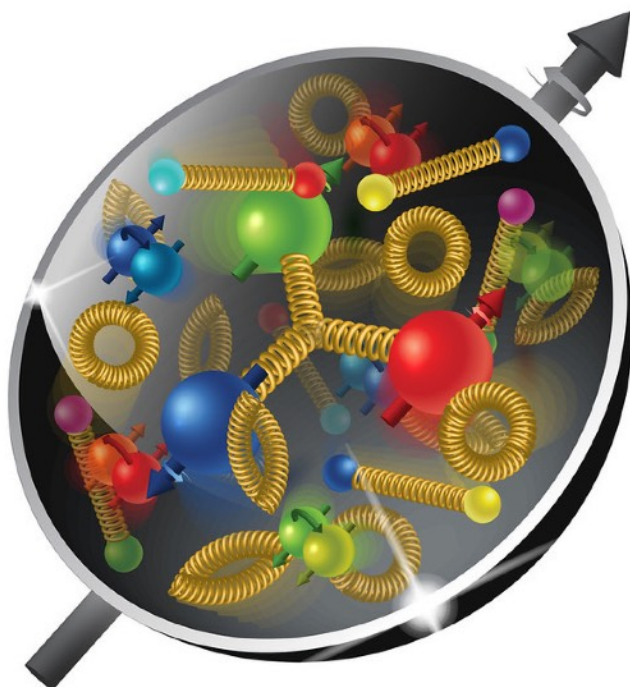
Elliot Leader, Spin in Particle Physics, Cambridge U. Press (2001)

“Polarization data has often been the graveyard of fashionable theories. If theorists had their way they might well ban such measurements altogether out of self- protection”

J. D. Bjorken, Proc. Adv. Research Workshop on QCD Hadronic Processes, St. Croix, Virgin Islands (1987).

WHY SPIN?

Spin is a fundamental degree of freedom originated from the space-time symmetry



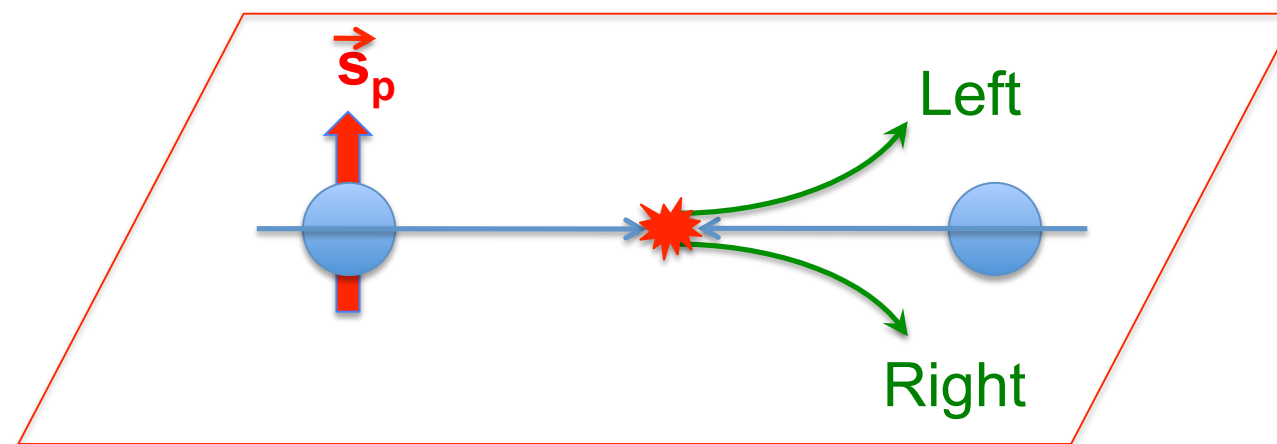
Spin plays a critical role in determining the basic structure of fundamental interactions

Spin provides a unique opportunity to probe the inner structure of a composite system (such as the proton) and hence to test our ability to understand the working of non-perturbative QCD

Test of a theory is not complete without a full exploration of spin-dependent decays and scatterings

SINGLE SPIN ASYMMETRIES

Consider polarized proton - proton collisions



Count pions going to the right or to the left with respect to the spin direction

$$A_N \equiv \frac{\sigma(\vec{s}_P) - \sigma(-\vec{s}_P)}{\sigma(\vec{s}_P) + \sigma(-\vec{s}_P)}$$

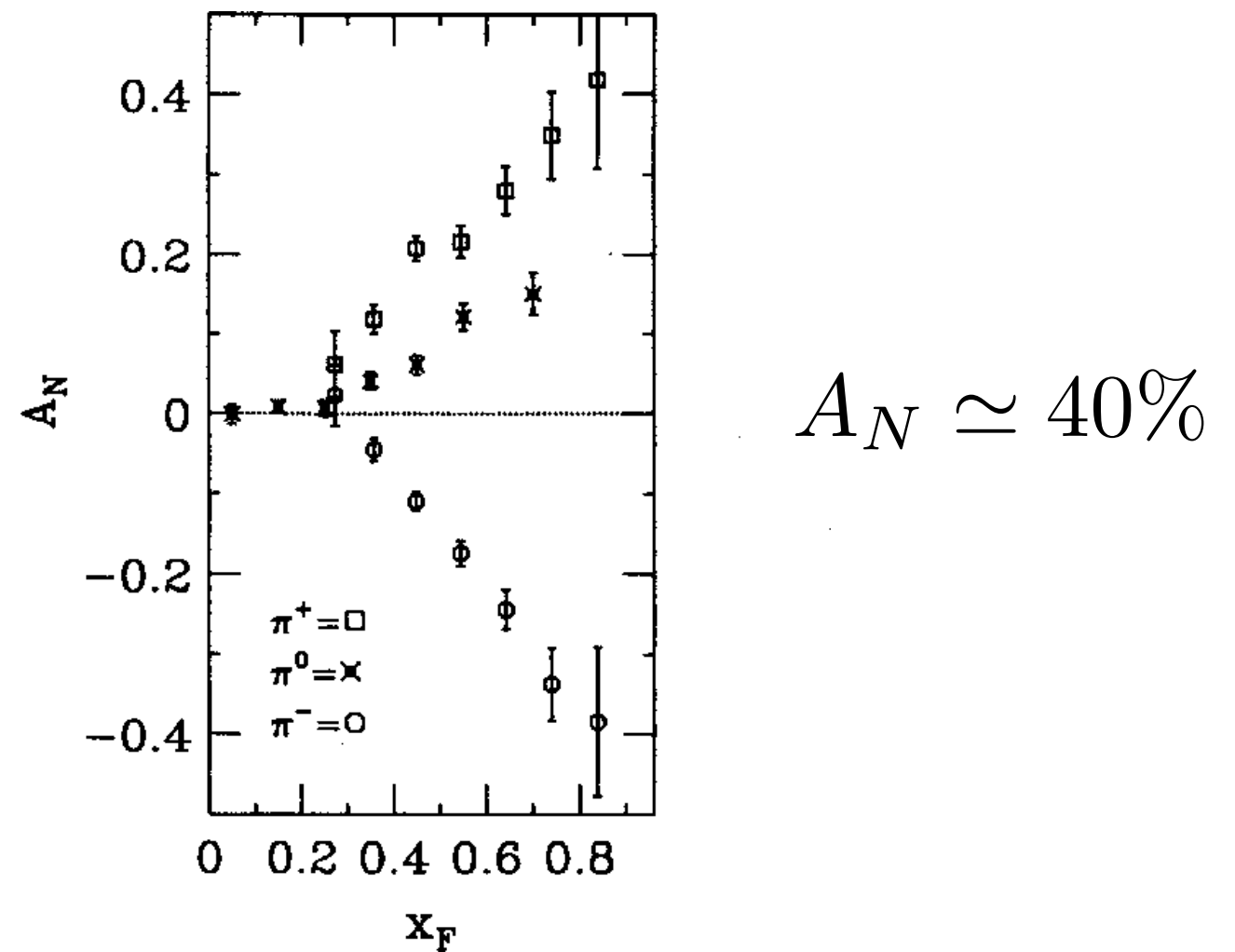
CHALLENGE OF QCD: UNDERSTANDING SPIN ASYMMETRIES

QCD had a very simple prediction

$$A_N \propto \alpha_s \frac{m_q}{P_T} \rightarrow 0$$

Kane, Pumplin, Repko (1978)

Experiment proved this prediction wrong

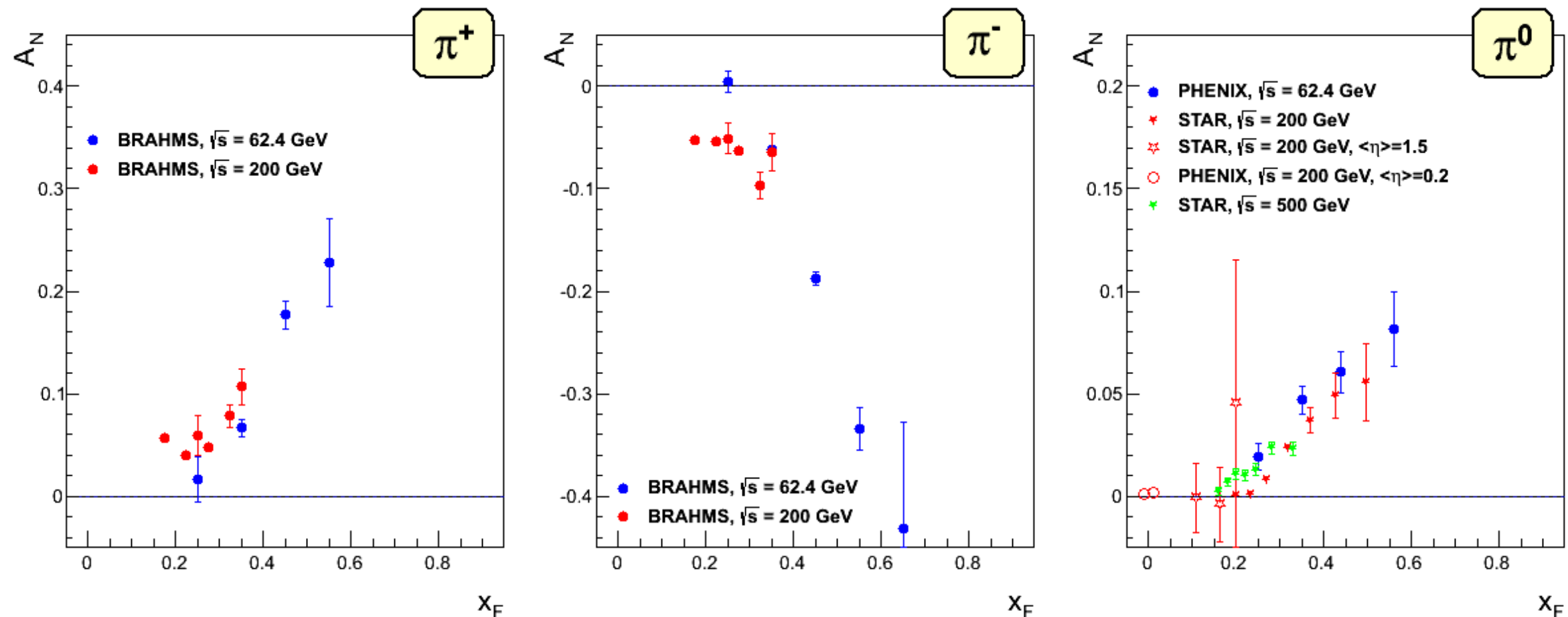


Fermilab experiment E704 (1991)
 $\sqrt{s} \simeq 19$ (GeV)

CHALLENGE OF QCD: UNDERSTANDING SPIN ASYMMETRIES

Asymmetry survives with growing collision energy

RHIC: STAR, BRAHMS, PHENIX



“The RHIC SPIN Program: Achievements and Future Opportunities”, Aschenauer et al (15)

FAILURE OF QCD?



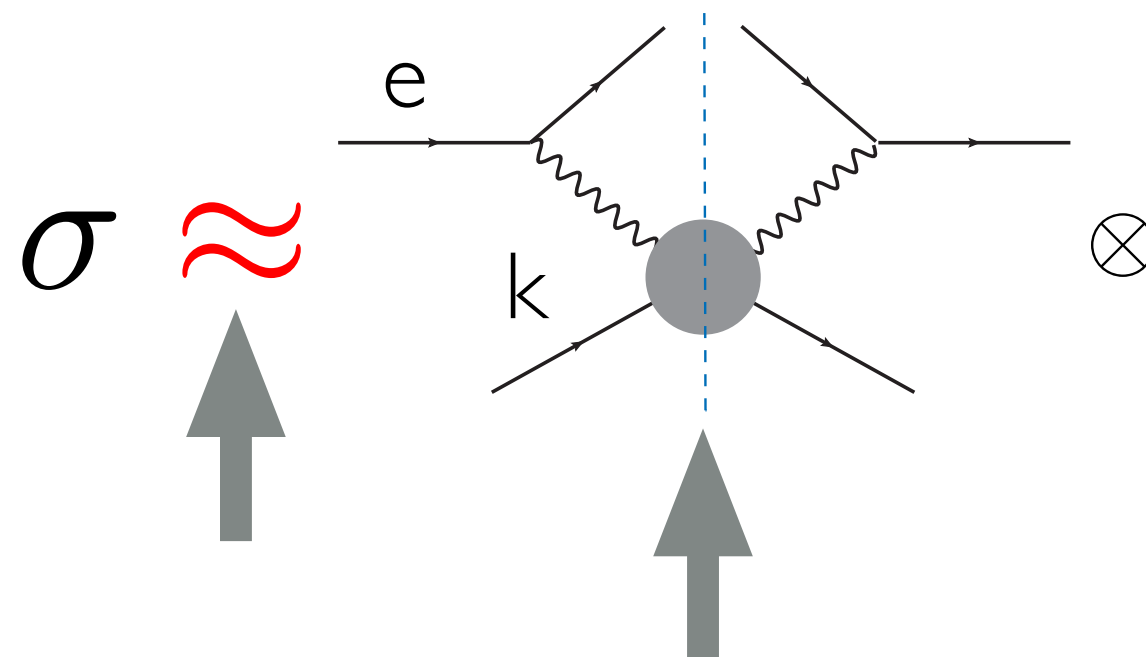
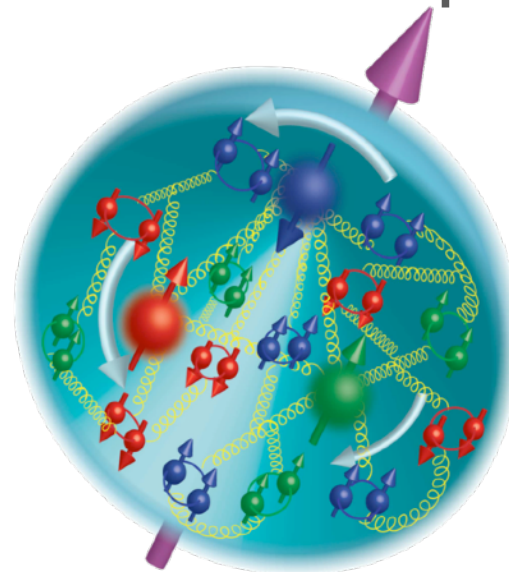
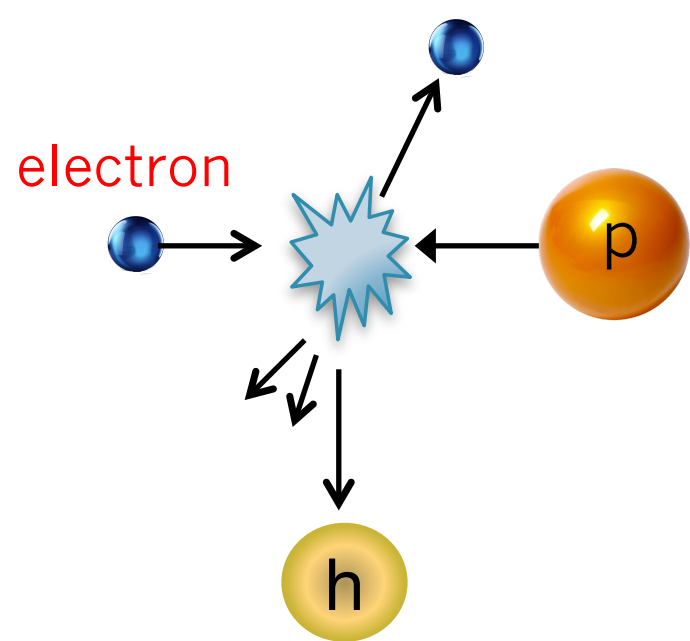


BETTER
UNDERSTANDING OF QCD!

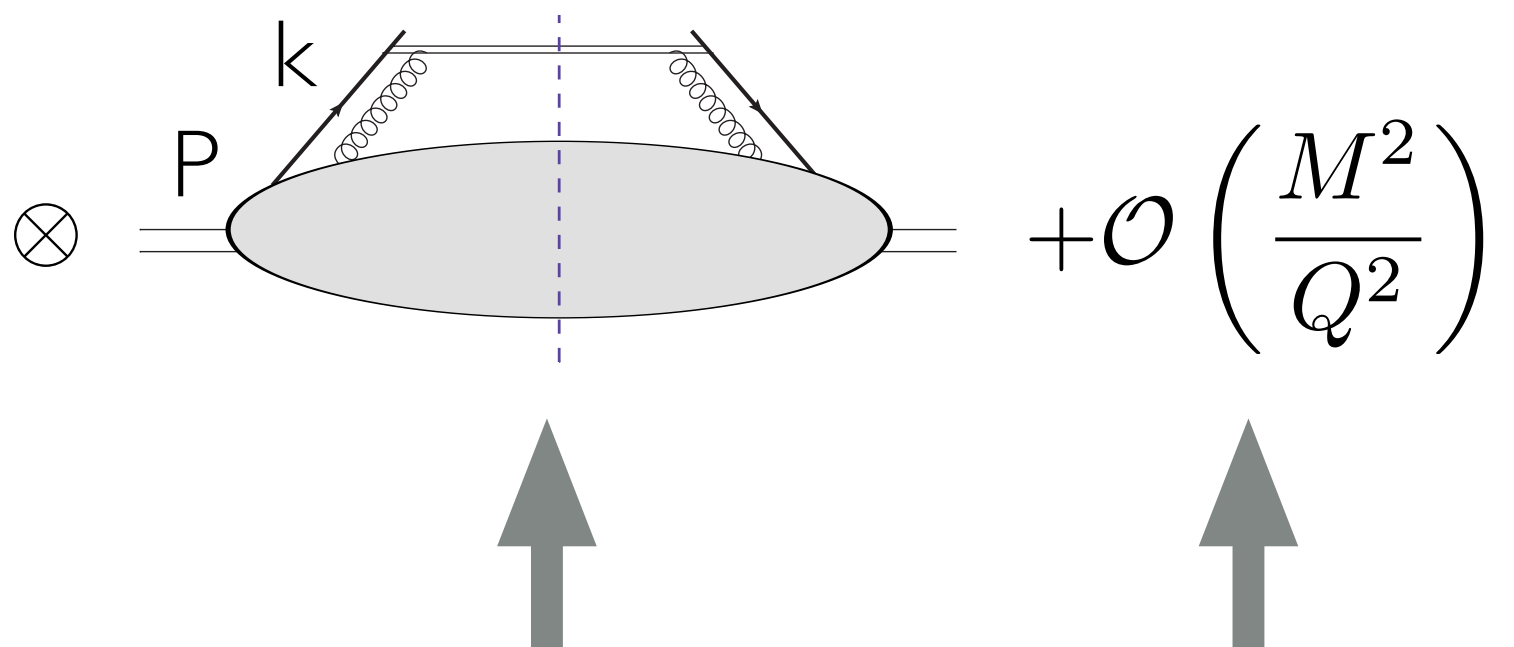
STRUCTURE OF THE NUCLEON

QCD FACTORIZATION IS THE KEY!

We need a probe to “see” quarks and gluons



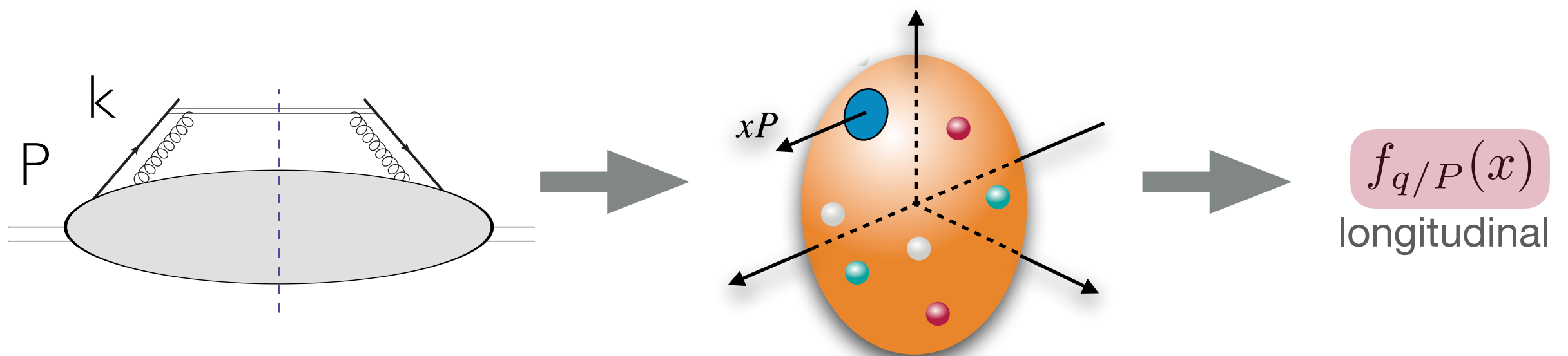
Factorization Probe



Structure Power corrections

HADRON'S PARTONIC STRUCTURE

Collinear Parton Distribution Functions



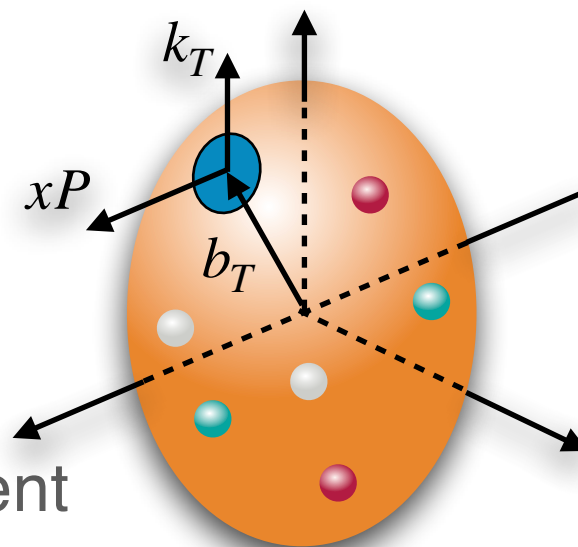
Probability density to find a quark with a momentum fraction x

Hard probe resolves the particle nature of partons, but is not sensitive to hadron's structure at \sim fm distances.

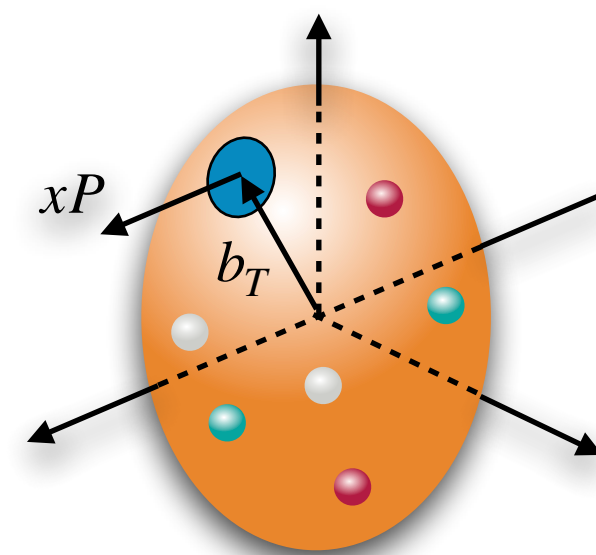
Wigner distributions
(Fourier transform of GTMDs =
Generalized Transverse
Momentum Distributions)

Transverse Momentum Dependent
Distributions TMDs

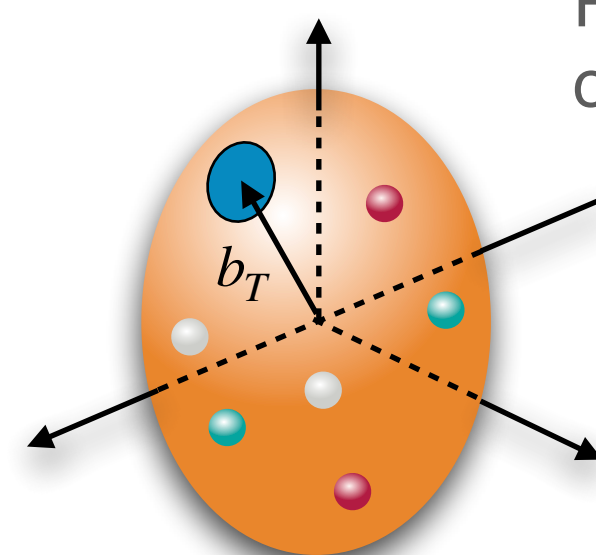
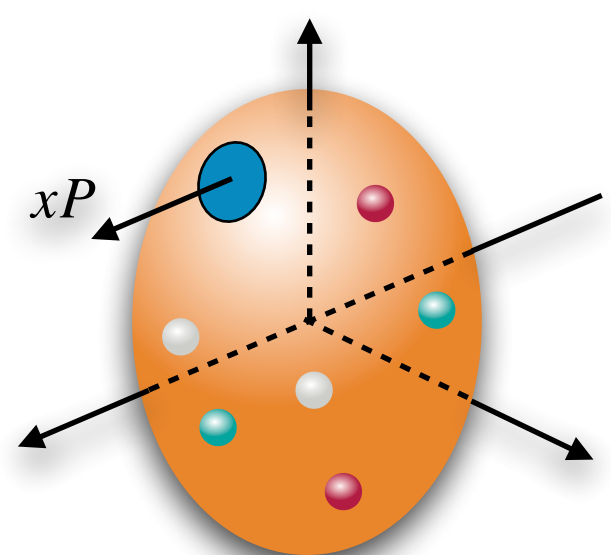
PDFs



Fourier transform
of Generalized Parton Distributions
(GPDs)



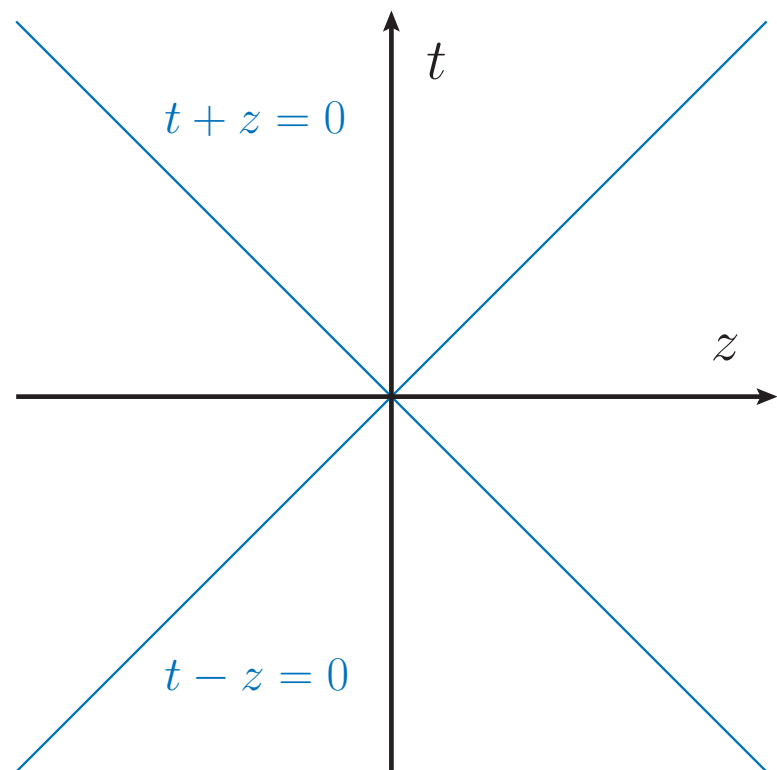
Fourier transform
of Form Factors



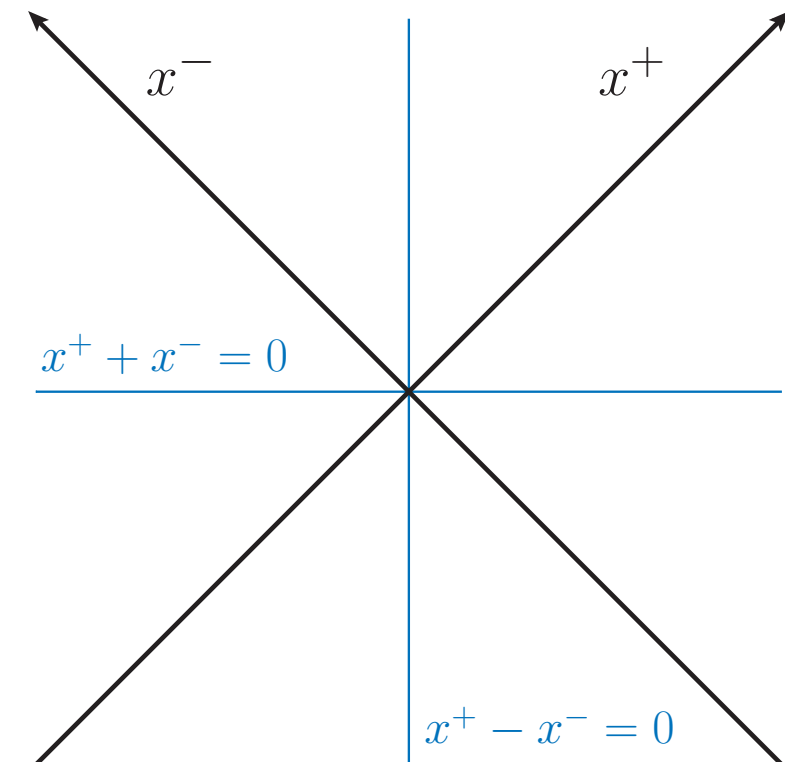
LIGHT FRONT COORDINATES

$$x^\pm = \frac{t \pm z}{\sqrt{2}}$$

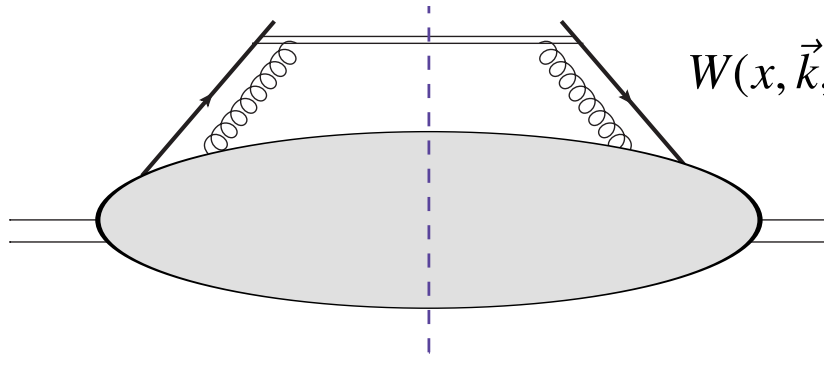
$$\mathbf{x}_\perp = (x, y)$$



Minkowski coordinates



Light front coordinates



Bilocal matrix element of quark fields

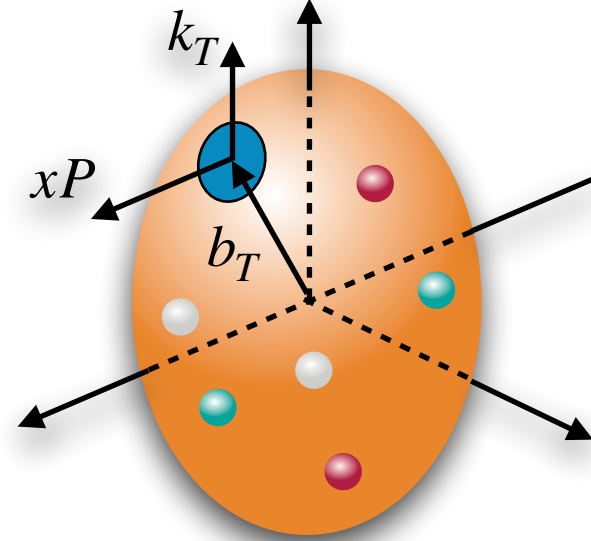
$$\bar{\psi}(k_\perp, z^-) = \int d^2 z_\perp e^{-iz_\perp k_\perp} \psi(z_\perp, z^-)$$

$$\bar{\psi}(k_\perp) \tilde{\psi}(l_\perp) = \int d^2 z_\perp d^2 y_\perp e^{-i(z_\perp k_\perp - y_\perp l_\perp)} \bar{\psi}(z_\perp) \psi(y_\perp)$$

$$z_\perp k_\perp - y_\perp l_\perp = \frac{1}{2}(z_\perp - y_\perp)(k_\perp + l_\perp) + \frac{1}{2}(z_\perp + y_\perp)(k_\perp - l_\perp)$$

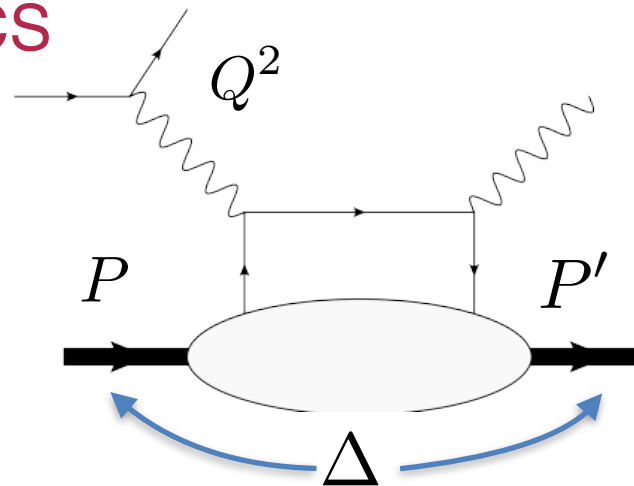
The '**average**' transverse momentum is Fourier conjugate to position difference (TMD)

The momentum transfer is Fourier conjugate to '**average**' position (GPD)



Generalized Parton Distributions

DVCS



Ji (1997)
Radyushkin (1997)

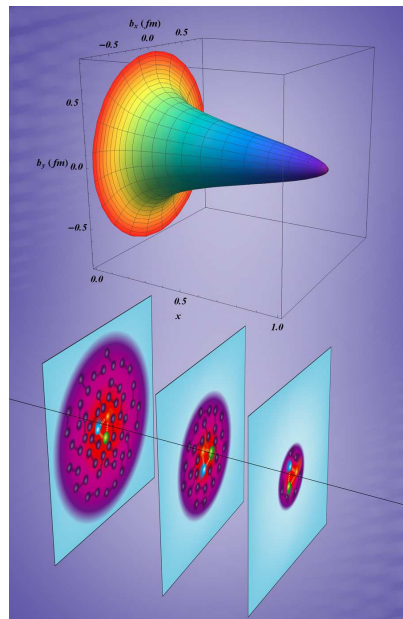
Q^2 ensures hard scale, pointlike interaction

$\Delta = P' - P$ momentum transfer can be varied independently

Connection to 3D structure

$$\rho(x, \vec{b}_\perp) = \int \frac{d^2 \vec{\Delta}_\perp}{(2\pi)^2} e^{-i \vec{\Delta}_\perp \cdot \vec{b}_\perp} H_q(x, \xi = 0, t = -\vec{\Delta}_\perp^2)$$

Burkardt (2000)
Burkardt (2003)

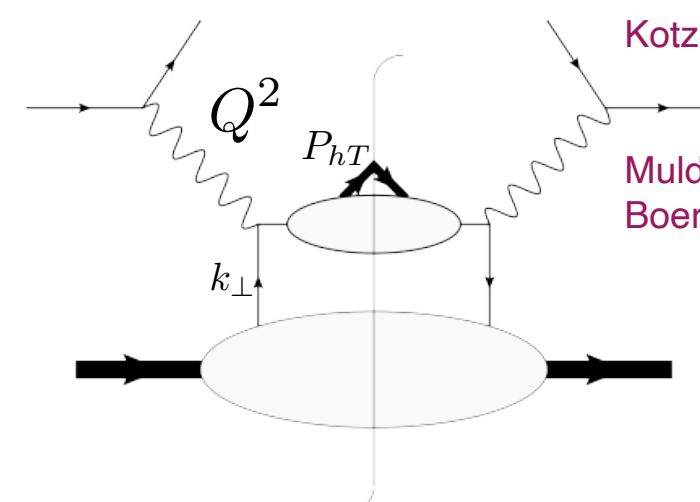


Drell-Yan frame $\Delta^+ = 0$

Dupré, Guidal, Niccolai,
Vanderhaeghen,
arXiv:1704.07330

Transverse Momentum Dependent distributions

SIDIS



Kotzinian (1995)

Mulders, Tangerman (1995)
Boer, Mulders (1998)

Q^2 ensures hard scale, pointlike interaction

P_{hT} final hadron transverse momentum can be varied independently

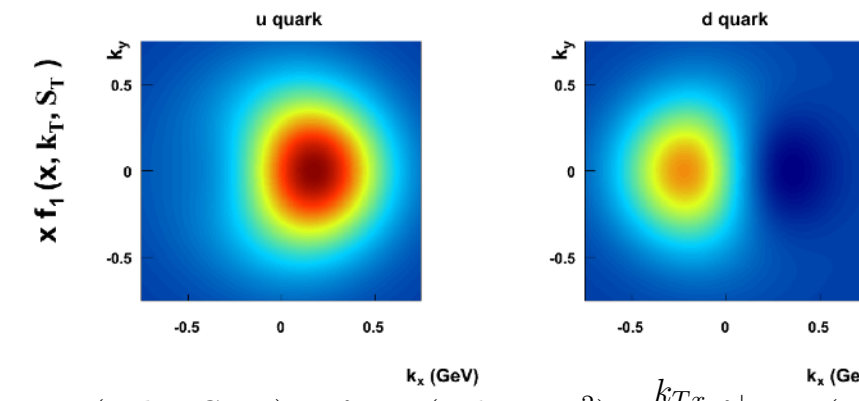
Connection to 3D structure

$$f(x, \vec{k}_T) = \int \frac{d^2 \vec{b}_T}{(2\pi)^2} e^{i \vec{k}_T \cdot \vec{b}_T} \tilde{f}(x, \vec{b}_T)$$

\vec{b}_T is the transverse separation of parton fields in configuration space

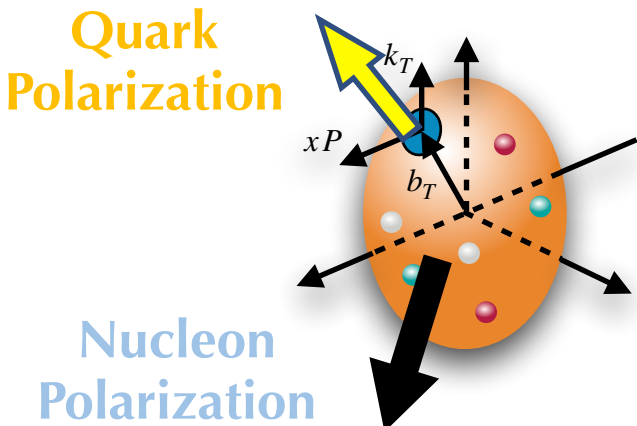
Ji, Ma, Yuan (2004)
Collins (2011)

White Paper (2012) Accardi et al, arXiv:1212:1701



$$\rho_{1;q \leftarrow h^\uparrow}(x, \mathbf{k}_T, \mathbf{S}_T, \mu) = f_{1;q \leftarrow h}(x, k_T; \mu, \mu^2) - \frac{k_{Tx}}{M} f_{1T;q \leftarrow h}^\perp(x, k_T; \mu, \mu^2)$$

Our understanding of the nucleon evolves: SPIN



Nucleon emerges as a strongly interacting, relativistic bound state of quarks and gluons

TMDs

		Quark Polarization		
		Unpolarized (U)	Longitudinally Polarized (L)	Transversely Polarized (T)
Nucleon Polarization	U	$f_1(x, k_T^2)$ Unpolarized		$h_1^\perp(x, k_T^2)$ - Boer-Mulders
	L		$g_1(x, k_T^2)$ - Helicity	$h_{1L}^\perp(x, k_T^2)$ - Kozinian-Mulders, "worm" gear
	T	$f_{1T}^\perp(x, k_T^2)$ - Sivers	$g_{1T}(x, k_T^2)$ - Kozinian-Mulders, "worm" gear	$h_1(x, k_T^2)$ - Transversity $h_{1T}^\perp(x, k_T^2)$ - Pretzelosity

		Quark Polarization		
		Unpolarized (U)	Longitudinally Polarized (L)	Transversely Polarized (T)
Nucleon Polarization	U	H		\mathcal{E}_T
	L			\tilde{H}
	T	E		H_T, \tilde{H}_T

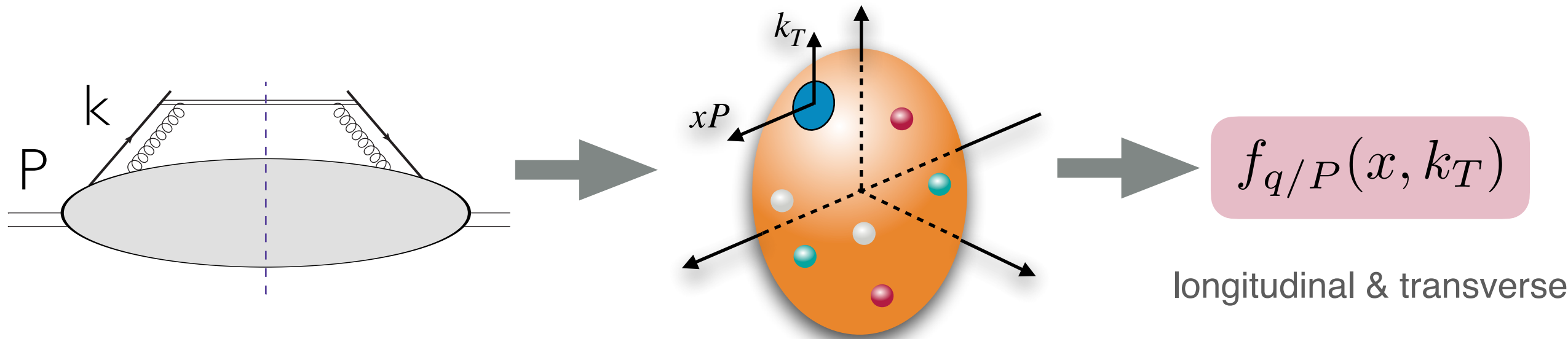
Many TMDs and GPDs cannot exist without OAM.

Examples: TMD Sivers function f_{1T}^\perp and GPD E

HADRON'S PARTONIC STRUCTURE

To study the physics of *confined motion of quarks and gluons* inside of the proton one needs a new type “hard probe” with two scales.

Transverse Momentum Dependent functions



One large scale (Q) sensitive to particle nature of quark and gluons

One small scale (k_T) sensitive to *how QCD bounds partons* and to the detailed structure at \sim fm distances.

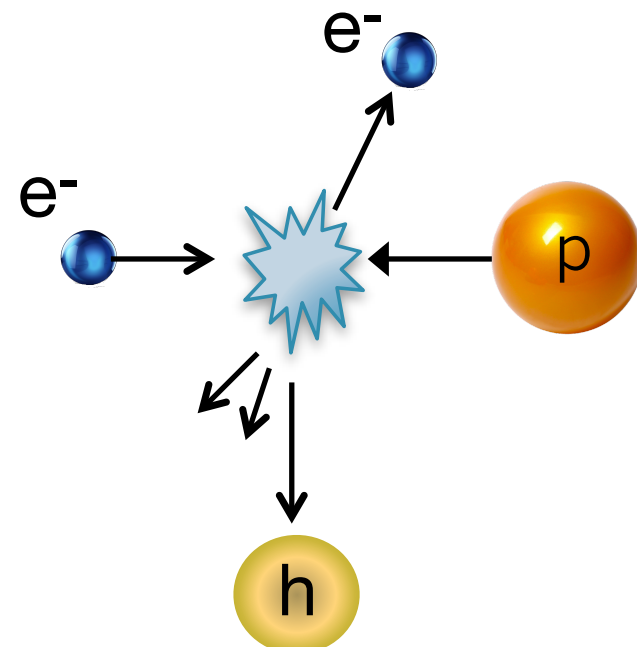
TRANSVERSE MOMENTUM DEPENDENT FACTORIZATION

Small scale $\rightarrow q_T \ll Q \leftarrow$ Large scale

The confined motion (k_T dependence) is encoded in TMDs

Semi-Inclusive DIS

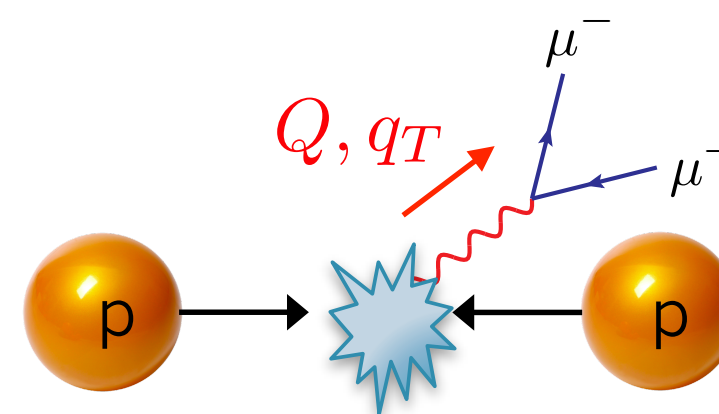
$$\sigma \sim f_{q/P}(x, k_T) D_{h/q}(z, k_T)$$



Meng, Olness, Soper (1992)
Ji, Ma, Yuan (2005)
Idilbi, Ji, Ma, Yuan (2004)
Collins (2011)

Drell-Yan

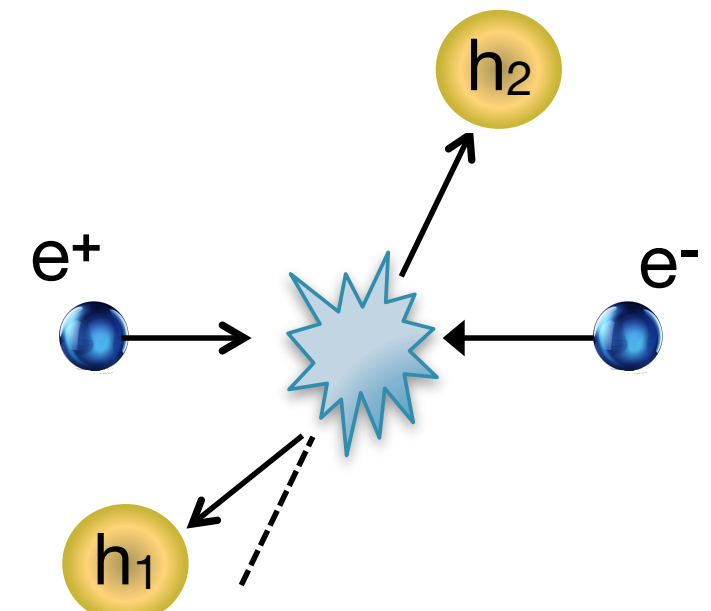
$$\sigma \sim f_{q/P}(x, k_T) f_{q/P}(x, k_T)$$



Collins, Soper, Sterman (1985)
Ji, Ma, Yuan (2004)
Collins (2011)

Dihadron in e^+e^-

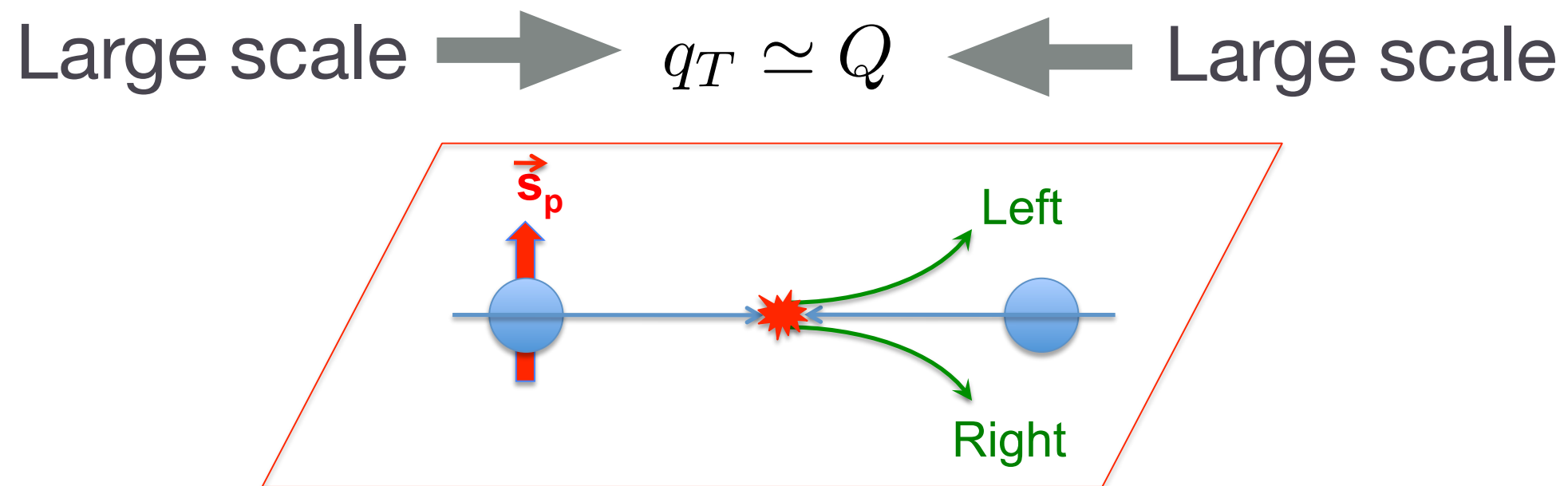
$$\sigma \sim D_{h_1/P}(z, k_T) D_{h_2/q}(z, k_T)$$



Collins, Soper (1983)
Collins (2011)

COLLINEAR TWIST-3 FACTORIZATION

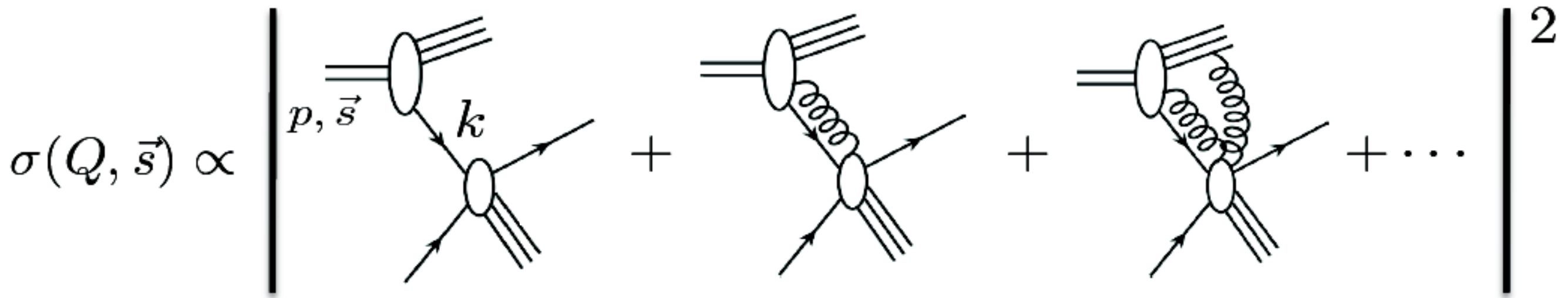
Proton-proton scattering does not have two distinct scales



What factorization is appropriate in this case?

COLLINEAR TWIST-3 FACTORIZATION

Large scale $\rightarrow q_T \simeq Q \leftarrow$ Large scale

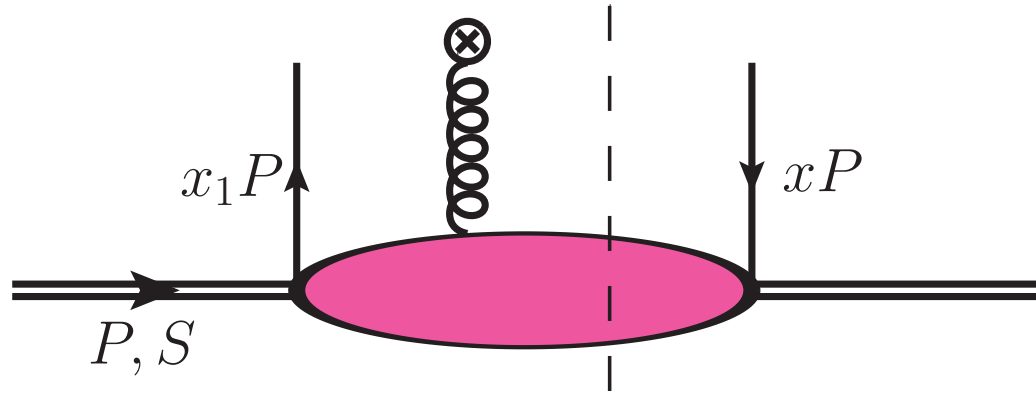


Qiu, Sterman (1991)

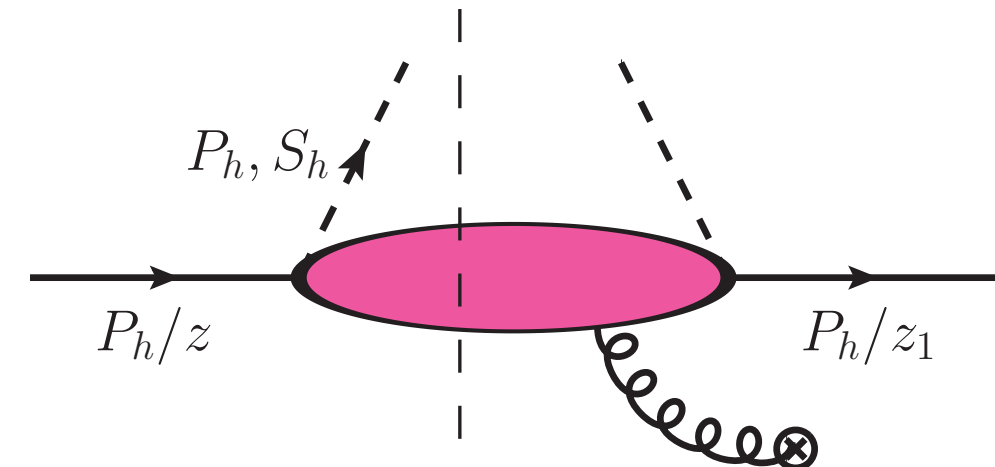
Multi-parton correlations (twist-3 functions) contribute to the cross section and are dominant for asymmetries in PP scattering

COLLINEAR TWIST-3 FACTORIZATION

Large scale $\rightarrow q_T \simeq Q \leftarrow$ Large scale



quark distribution twist-3 function



quark fragmentation twist-3 function

Multi-parton correlations (twist-3 functions) contribute to the cross section and are dominant for asymmetries in PP scattering

QIU-STERMAN MATRIX ELEMENT

$$\int \frac{dy_1^- dy_2^-}{4\pi} e^{ixp^+ y_1^-} \langle p, S | \bar{\psi}(0) F^{+i}(y_2^-) \psi(y_1^-) | p, S \rangle = -\epsilon_T^{ij} S_T^j F_{FT}(x, x)$$

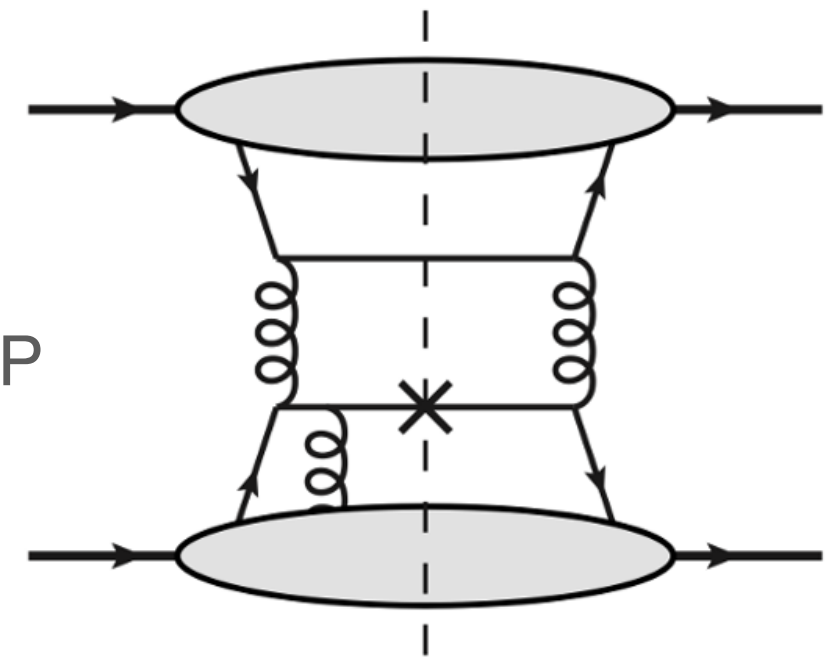
Qiu, Sterman (91)

- Triple-parton correlation (qqg) Qiu-Sterman function:
hard scattering + single-scattering correction
- Intermediate state can produce imaginary phase
necessary for single-spin asymmetries
- Novel evolution equations: generalization of DGLAP

Kang, Qui (09)

Braun, Manachov, Pirna (09)

Vogelsang, Yuan (09)



$$\mu_F^2 \frac{\partial}{\partial \mu_F^2} \mathcal{T}_{q,F}(x, x + x_2, \mu_F) = \frac{1}{2} \left[\mu_F^2 \frac{\partial}{\partial \mu_F^2} \tilde{\mathcal{T}}_{q,F}(x, x + x_2, \mu_F, s_T) + \mu_F^2 \frac{\partial}{\partial \mu_F^2} \tilde{\mathcal{T}}_{q,F}(x + x_2, x, \mu_F, s_T) \right]$$

TMD AND COLLINEAR FACTORIZATIONS ARE RELATED

TMDs and collinear PDFs and FFs are related via Operator Product Expansion in CSS formalism

Collins, Soper, Sterman (1985)

TMD and collinear twist-3 (CT3) formalisms are “unified” in intermediate region of q_T

Ji, Qiu, Vogelsang, Yuan (2006)

TMD and twist-3 (CT3) functions are related by integral relations

Boer, Mulders, Pijlman (2003)

$$\pi F_{FT}(x, x) = \int d^2 \vec{k}_T \frac{k_T^2}{2M^2} f_{1T}^\perp(x, k_T^2) \equiv f_{1T}^{\perp(1)}(x)$$



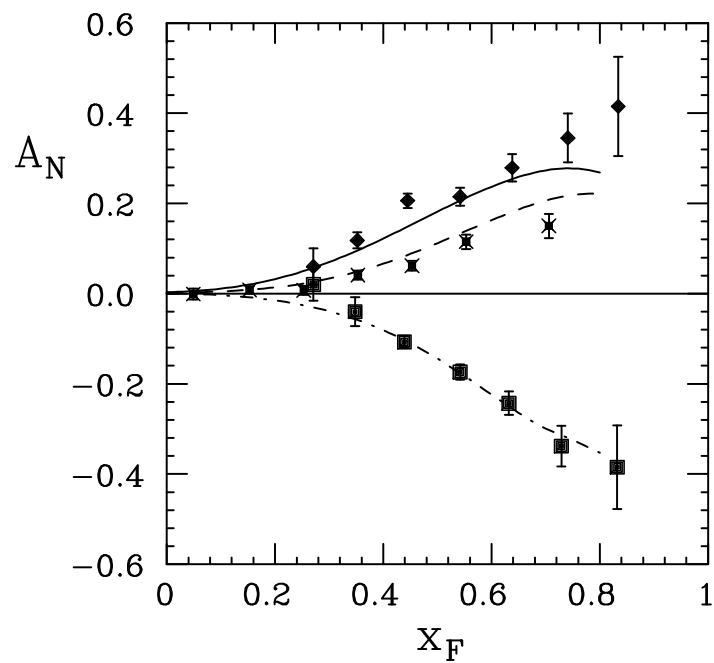
Qiu-Sterman matrix element



The first k_T moment of Sivers function

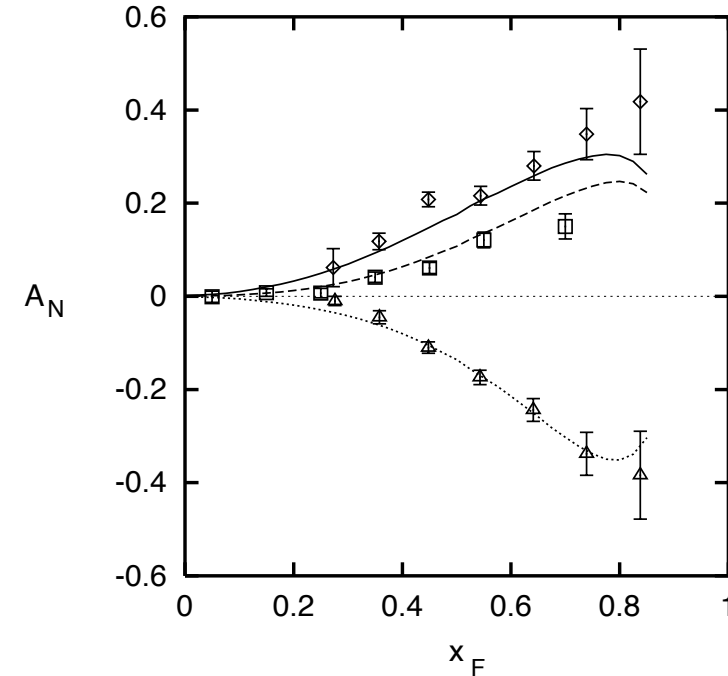
TOWARDS THE SOLUTION OF 40 YEAR OLD PUZZLE

Anselmino, Murgia (1998)



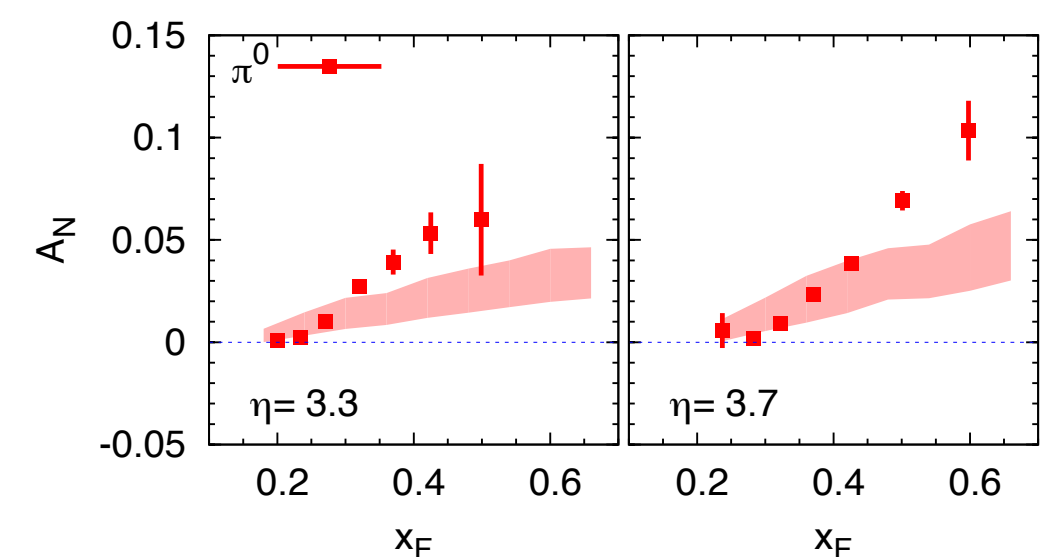
Sivers effect TMD fit

Anselmino, Boglione, Murgia (1999)



Collins effect TMD fit

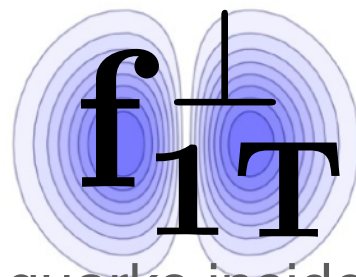
Anselmino, Boglione, D'Alesio, Leader, Melis, Murgia, Prokudin (2013)



TMD Collins effect
only from SIDIS

POLARIZED TMD FUNCTIONS

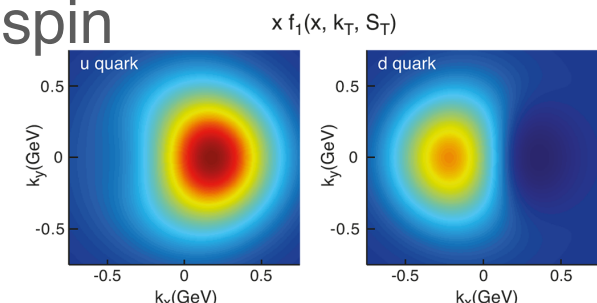
Sivers function



- Describes unpolarized quarks inside of transversely polarized nucleon

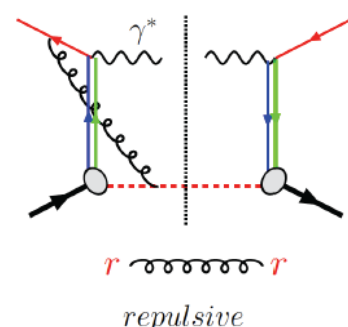
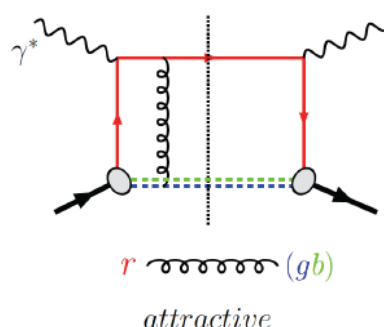
$$\rho_{1;q \leftarrow h^\uparrow}(x, k_T, S_T, \mu) = f_{1;q \leftarrow h}(x, k_T; \mu, \mu^2) - \frac{k_{Tx}}{M} f_{1T;q \leftarrow h}^\perp(x, k_T; \mu, \mu^2)$$

- Encodes the correlation of orbital motion with the spin



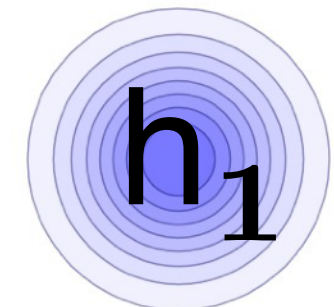
- Sign change of Sivers function is fundamental consequence of QCD

Brodsky, Hwang, Schmidt (2002), Collins (2002)



$$f_{1T}^{\perp SIDIS} = -f_{1T}^{\perp DY}$$

Transversity

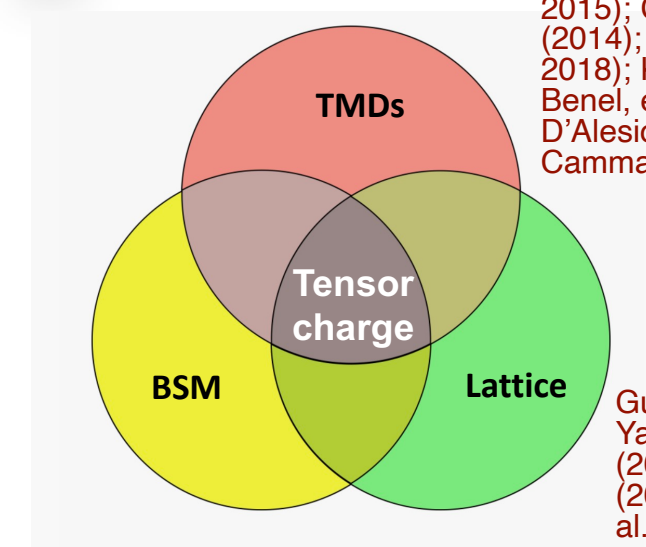


- The only source of information on tensor charge of the nucleon

- Couples to Collins fragmentation function or di-hadron interference fragmentation functions in SIDIS

$$\delta q \equiv g_T^q = \int_0^1 dx \ [h_1^q(x, Q^2) - h_1^{\bar{q}}(x, Q^2)]$$

Anselmino, et al. (2013, 2015); Goldstein, et al. (2014); Radici, et al. (2013, 2018); Kang, et al. (2016); Benel, et al. (2019); D'Alesio, et al. (2020); Cammarota, et al. (2020)



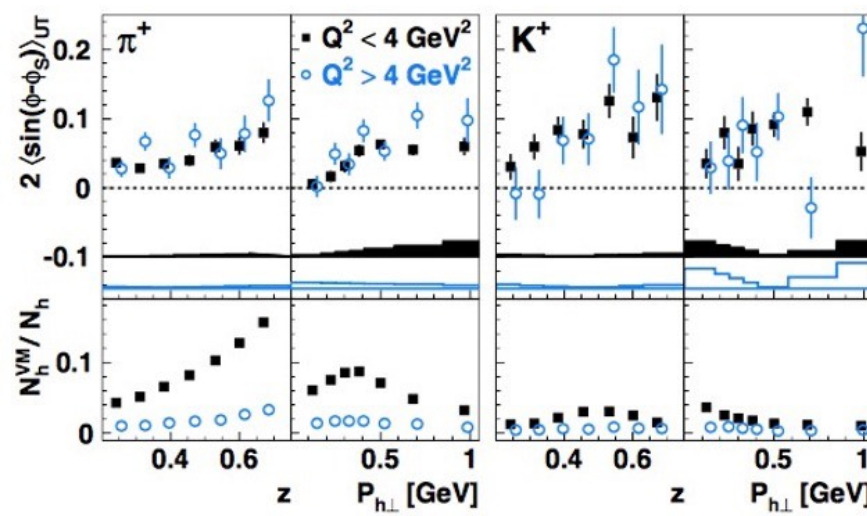
Courtoy, et al. (2015); Yamanaka, et al. (2017); Liu, et al. (2018); Gonzalez-Alonso, et al. (2019)

Gupta, et al. (2018); Yamanaka, et al. (2018); Hasan, et al. (2019); Alexandrou, et al. (2019)

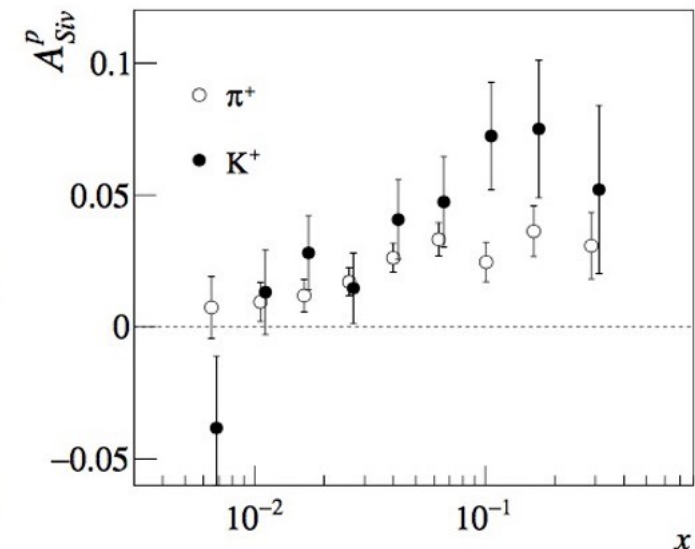
TRANSVERSE SPIN ASYMMETRIES

Transverse Single Spin Asymmetries (SSAs) have been observed in a variety of processes

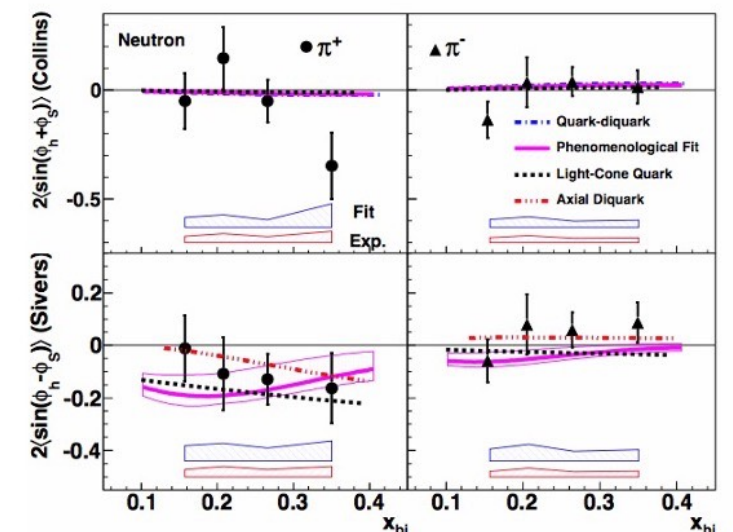
Sivers asymmetry in SIDIS



HERMES (09)



COMPASS (15)



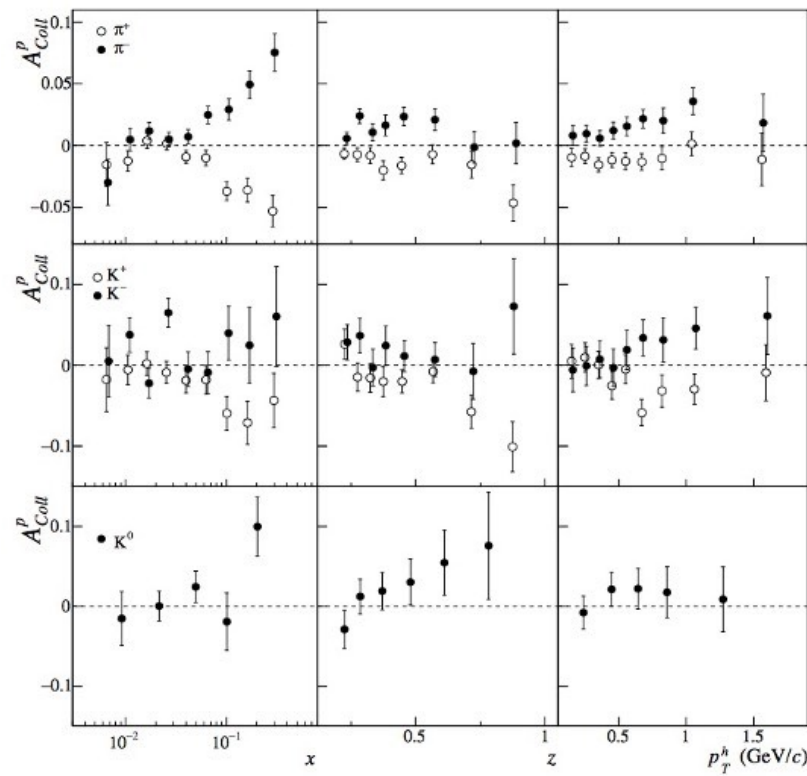
JLAB (11)

$$F_{UT}^{\sin(\phi_h - \phi_S)} = \mathcal{C} \left[-\frac{\hat{h} \cdot \vec{k}_T}{M} \mathbf{f}_{1T}^\perp D_1 \right]$$

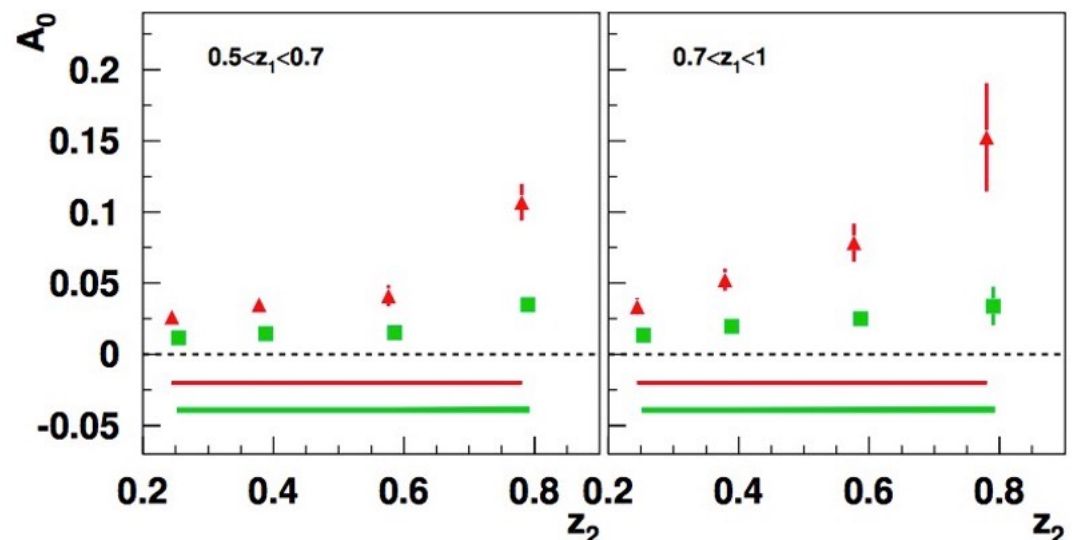
TRANSVERSE SPIN ASYMMETRIES

Transverse Single Spin Asymmetries (SSAs) have been observed in a variety of processes

Collins asymmetry in SIDIS and e^+e^-



COMPASS (15),
also HERMES (05,10, 20), JLab (11,14)



BELLE (08),
also BaBar (14), BESIII (16)

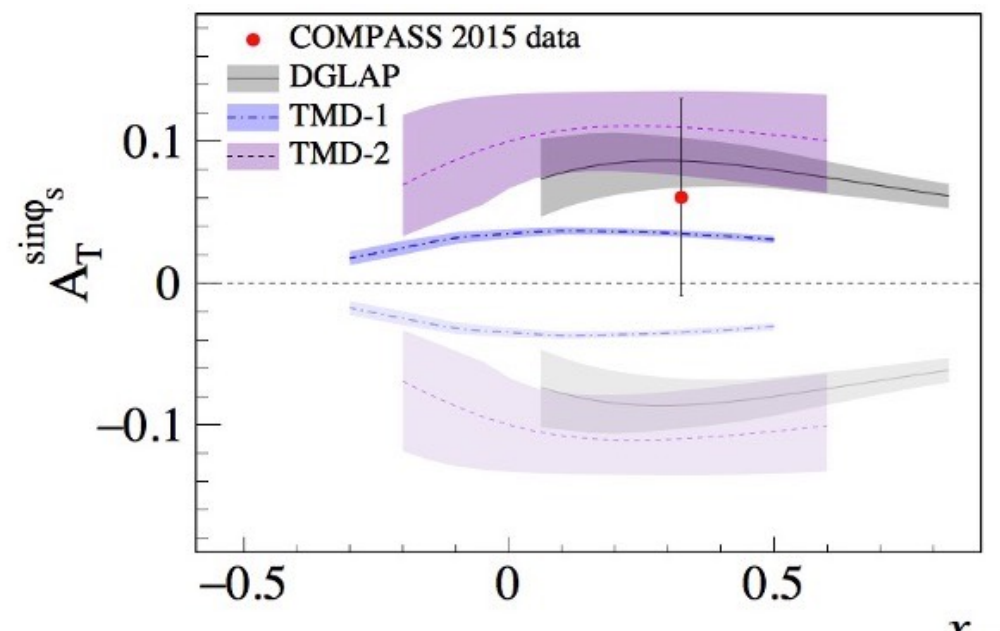
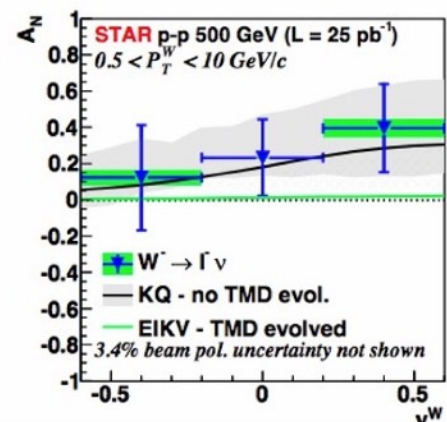
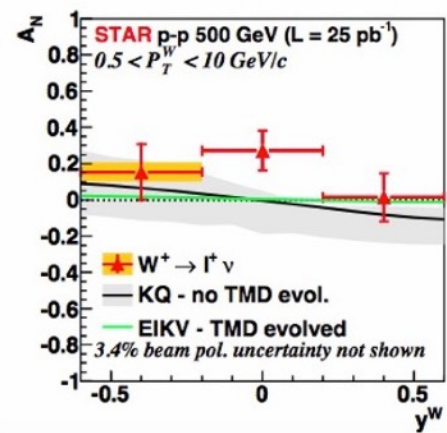
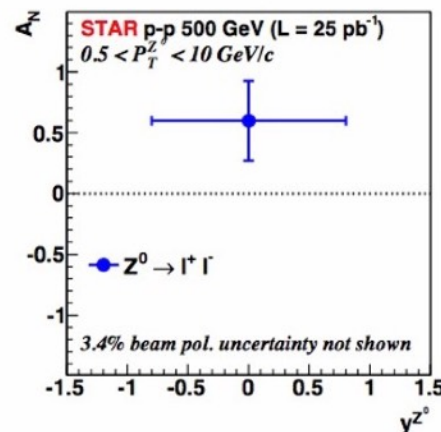
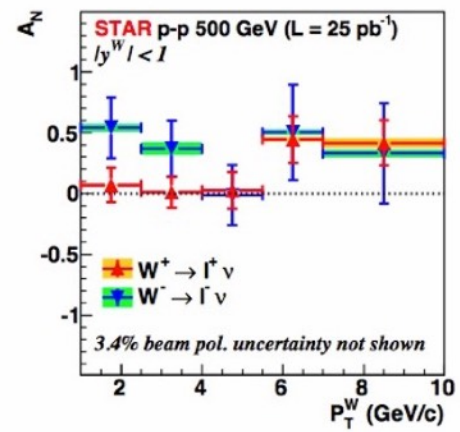
$$F_{UT}^{\sin(\phi_h + \phi_S)} = \mathcal{C} \left[-\frac{\hat{h} \cdot \vec{p}_\perp}{M_h} \boldsymbol{h}_1 \boldsymbol{H}_1^\perp \right]$$

$$F_{UU}^{\cos(2\phi_0)} = \mathcal{C} \left[\frac{2\hat{h} \cdot \vec{p}_{a\perp} \hat{h} \cdot \vec{p}_{b\perp} - \vec{p}_{a\perp} \cdot \vec{p}_{b\perp}}{M_a M_b} \boldsymbol{H}_1^\perp \bar{\boldsymbol{H}}_1^\perp \right]$$

TRANSVERSE SPIN ASYMMETRIES

Transverse Single Spin Asymmetries (SSAs) have been observed in a variety of processes

Sivers effect in Drell-Yan



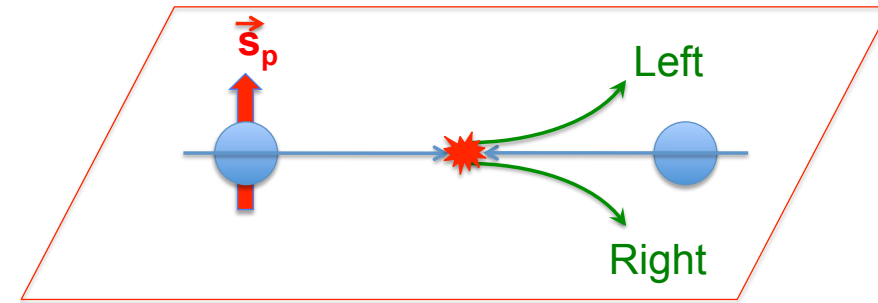
COMPASS (17)

STAR (15)

$$F_{TU}^1 = \mathcal{C} \left[-\frac{\vec{h} \cdot \vec{k}_{aT}}{M_a} \mathbf{f}_{1T}^\perp \bar{f}_1 \right]$$

TRANSVERSE SPIN ASYMMETRIES

A_N in pp scattering is related to
collinear twist-3 (CT3) factorization



$$d\Delta\sigma(S_T) \sim H_{QS} \otimes f_1 \otimes \mathbf{F}_{FT} \otimes D_1 + H_F \otimes f_1 \otimes \mathbf{h}_1 \otimes (\mathbf{H}_1^{\perp(1)}, \tilde{\mathbf{H}})$$

Qiu-Sterman term

$$\mathbf{F}_{FT} \sim \text{quark-gluon-quark correlator}$$

Qiu, Sterman (91), Kouvaris, et al (06)

$$\pi \mathbf{F}_{FT}(x, x) = \int d^2 \vec{k}_T \frac{k_T^2}{2M^2} \mathbf{f}_{1T}^{\perp}(x, \mathbf{k}_T^2) \equiv f_{1T}^{\perp(1)}(x) \text{ the first moment of Sivers function}$$

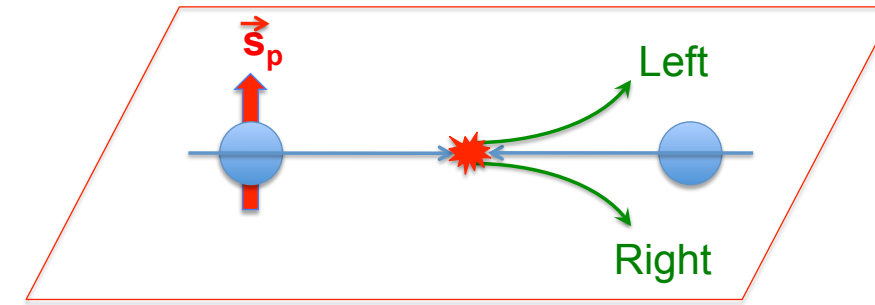
Boer, et al (03)

TMD and CT3 factorization agree in their overlapping region of applicability

Ji, et al (06); Koike, et al. (08); Zhou, et al (08, 10); Yuan and Zhou (09)

TRANSVERSE SPIN ASYMMETRIES

A_N in pp scattering is related to
collinear twist-3 (CT3) factorization

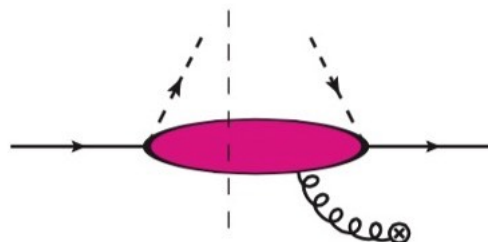


$$d\Delta\sigma(S_T) \sim H_{QS} \otimes f_1 \otimes \mathbf{F}_{FT} \otimes D_1 + H_F \otimes f_1 \otimes \mathbf{h}_1 \otimes \left(\mathbf{H}_1^{\perp(1)}, \tilde{\mathbf{H}} \right)$$

Fragmentation term

\mathbf{h}_1 collinear transversity

$$\mathbf{H}_1^{\perp(1)} \quad \tilde{\mathbf{H}}$$



Kanazawa, Koike, Metz, Pitonyak, Schlegel, (14)

quark-gluon-quark fragmentation functions

$$\mathbf{H}_1^{\perp(1)}(z) \equiv z^2 \int d^2 \vec{p}_\perp \frac{p_\perp^2}{2M_h^2} \mathbf{H}_1^\perp(z, z^2 p_\perp^2) \quad \text{the first moment of Collins FF}$$

$$F_{UT}^{\sin \phi_S} \sim \sum_a e_a^2 \frac{2M_h}{Q} h_1^a(x) \frac{\tilde{\mathbf{H}}(z)}{z}$$

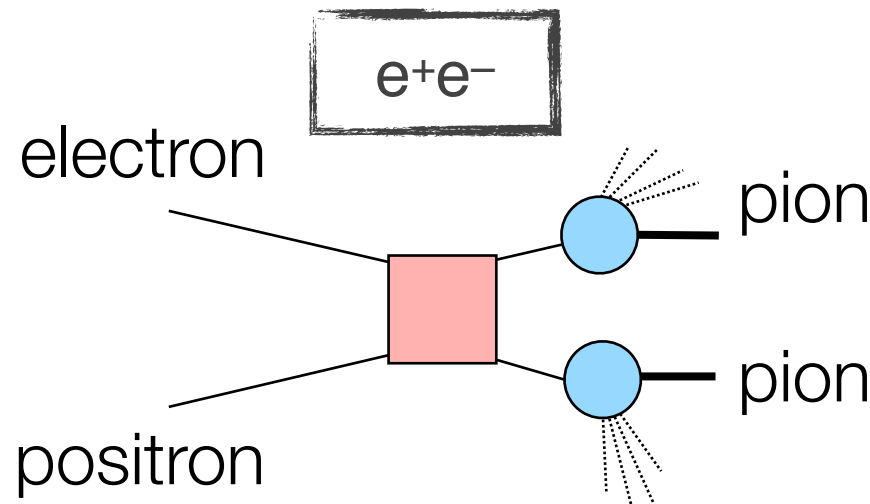
Mulders, Tangerman (96); Bacchetta, et al (07)

Cammarota, Gamberg, Kang, Miller, Pitonyak, Prokudin, Rogers, Sato Phys.Rev.D 102 (2020) 5, 05400 (2020)

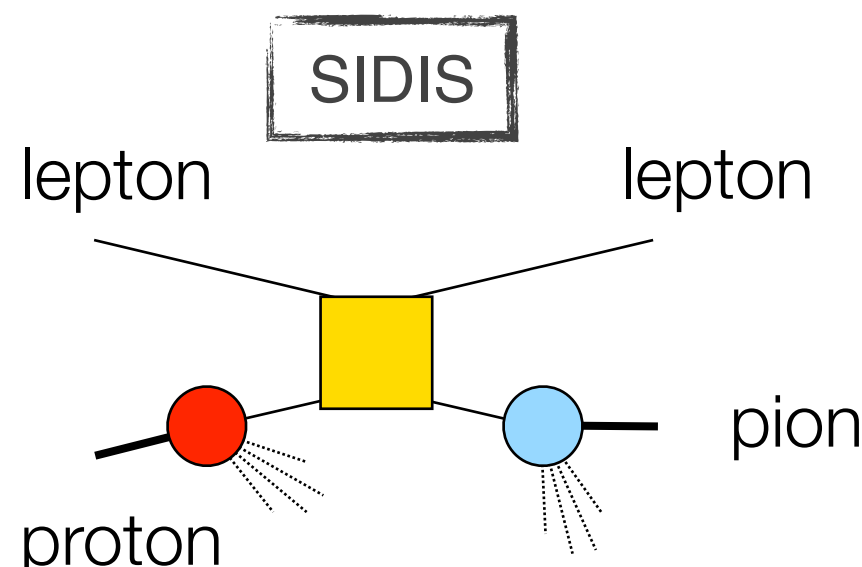
JAM20 ANALYSIS

UNIVERSAL GLOBAL ANALYSIS 2020

Cammarota, Gamberg, Kang, Miller, Pitonyak, Prokudin, Rogers, Sato Phys.Rev.D 102 (2020) 5, 05400 (2020)

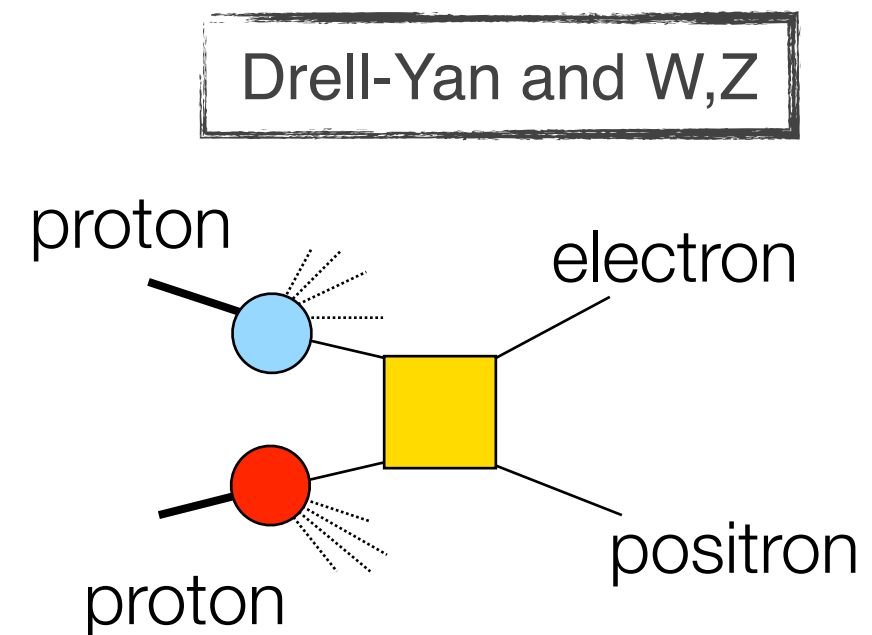


*Collins asymmetries
BELLE, BaBar, BESIII data*

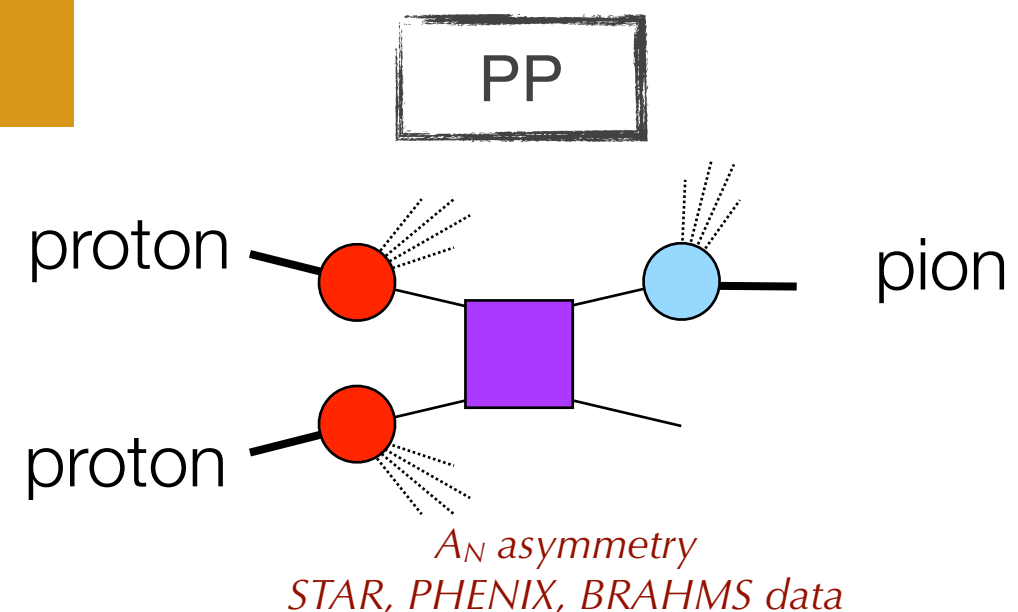


*Sivers, Collins asymmetries
COMPASS, HERMES, JLab data*

To demonstrate the common origin of SSAs in various processes, we combined all available data and extracted a universal set of non perturbative functions that describes all of them



*Sivers asymmetries
COMPASS, STAR data*



*A_N asymmetry
STAR, PHENIX, BRAHMS data*

UNIVERSAL GLOBAL ANALYSIS 2020

Jefferson Lab Angular Momentum Collaboration

<https://www.jlab.org/theory/jam>

Observable	Reactions	Non-Perturbative Function(s)	$\chi^2/N_{\text{pts.}}$
$A_{\text{SIDIS}}^{\text{Siv}}$	$e + (p, d)^\uparrow \rightarrow e + (\pi^+, \pi^-, \pi^0) + X$	$f_{1T}^\perp(x, k_T^2)$	$150.0/126 = 1.19$
$A_{\text{SIDIS}}^{\text{Col}}$	$e + (p, d)^\uparrow \rightarrow e + (\pi^+, \pi^-, \pi^0) + X$	$h_1(x, k_T^2), H_1^\perp(z, z^2 p_\perp^2)$	$111.3/126 = 0.88$
$A_{\text{SIA}}^{\text{Col}}$	$e^+ + e^- \rightarrow \pi^+ \pi^- (\text{UC}, \text{UL}) + X$	$H_1^\perp(z, z^2 p_\perp^2)$	$154.5/176 = 0.88$
$A_{\text{DY}}^{\text{Siv}}$	$\pi^- + p^\uparrow \rightarrow \mu^+ \mu^- + X$	$f_{1T}^\perp(x, k_T^2)$	$5.96/12 = 0.50$
$A_{\text{DY}}^{\text{Siv}}$	$p^\uparrow + p \rightarrow (W^+, W^-, Z) + X$	$f_{1T}^\perp(x, k_T^2)$	$31.8/17 = 1.87$
A_N^h	$p^\uparrow + p \rightarrow (\pi^+, \pi^-, \pi^0) + X$	$h_1(x), F_{FT}(x, x) = \frac{1}{\pi} f_{1T}^{\perp(1)}(x), H_1^{\perp(1)}(z)$	$66.5/60 = 1.11$

Cammarota, Gamberg, Kang, Miller, Pitonyak, Prokudin, Rogers, Sato Phys.Rev.D 102 (2020) 5, 05400 (2020)

► 18 observables and 6 non-perturbative functions (Sivers up/down; transversity up/down; Collins favored/unfavored)

$$h_1(x), F_{FT}(x, x), H_1^{\perp(1)}(z), \tilde{H}(z)$$

► Broad kinematical coverage to test universality

► The analysis is performed at parton level leading order, gaussian model is used for TMDs, and DGLAP-type evolution is implemented

$$F^q(x) = \frac{N_q x^{a_q} (1-x)^{b_q} (1 + \gamma_q x^{\alpha_q} (1-x)^{\beta_q})}{B[a_q+2, b_q+1] + \gamma_q B[a_q+\alpha_q+2, b_q+\beta_q+1]}$$

UNIVERSAL GLOBAL FIT 2020

Cammarota, Gamberg, Kang, Miller, Pitonyak, Prokudin, Rogers, Sato Phys.Rev.D 102 (2020) 5, 05400 (2020)

The relevant set of TMD functions to extract

$$h_1(x, k_T) = h_1(x) \mathcal{G}_h(k_T^2) \quad \text{transversity}$$

$$f_{1T}^\perp(x, k_T) = \frac{2M^2}{\langle k_T^2 \rangle_{f_{1T}^\perp}} \pi F_{FT}(x, x) \mathcal{G}_{f_{1T}^\perp}(k_T^2)$$

Sivers function

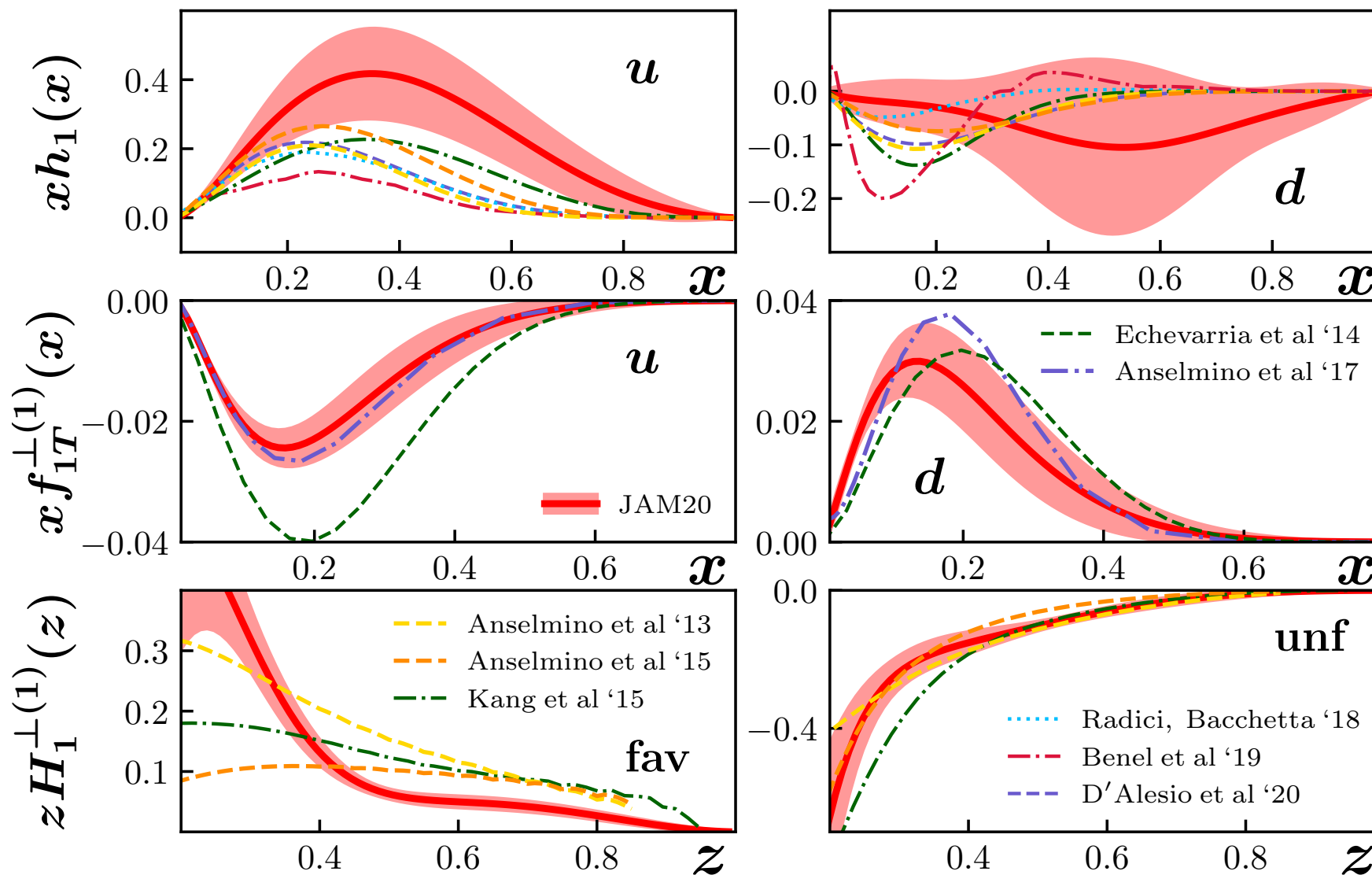
$$H_1^\perp(z, z p_T) = \frac{2z^2 M^2}{\langle p_T^2 \rangle_{H_1^\perp}} H_1^{\perp(1)}(z) \mathcal{G}_{H_1^\perp}(z^2 p_T^2)$$

Collins function

$$\mathcal{G}_f(k_T^2) = \frac{1}{\pi \langle k_T^2 \rangle_f} e^{-\frac{k_T^2}{\langle k_T^2 \rangle_f}}$$

UNIVERSAL GLOBAL ANALYSIS 2020

Cammarota, Gamberg, Kang, Miller, Pitonyak, Prokudin, Rogers, Sato Phys.Rev.D 102 (2020) 5, 05400 (2020)



Transversity

$$h_1(x)$$

Sivers

$$f_{1T}^{\perp(1)}(x)$$

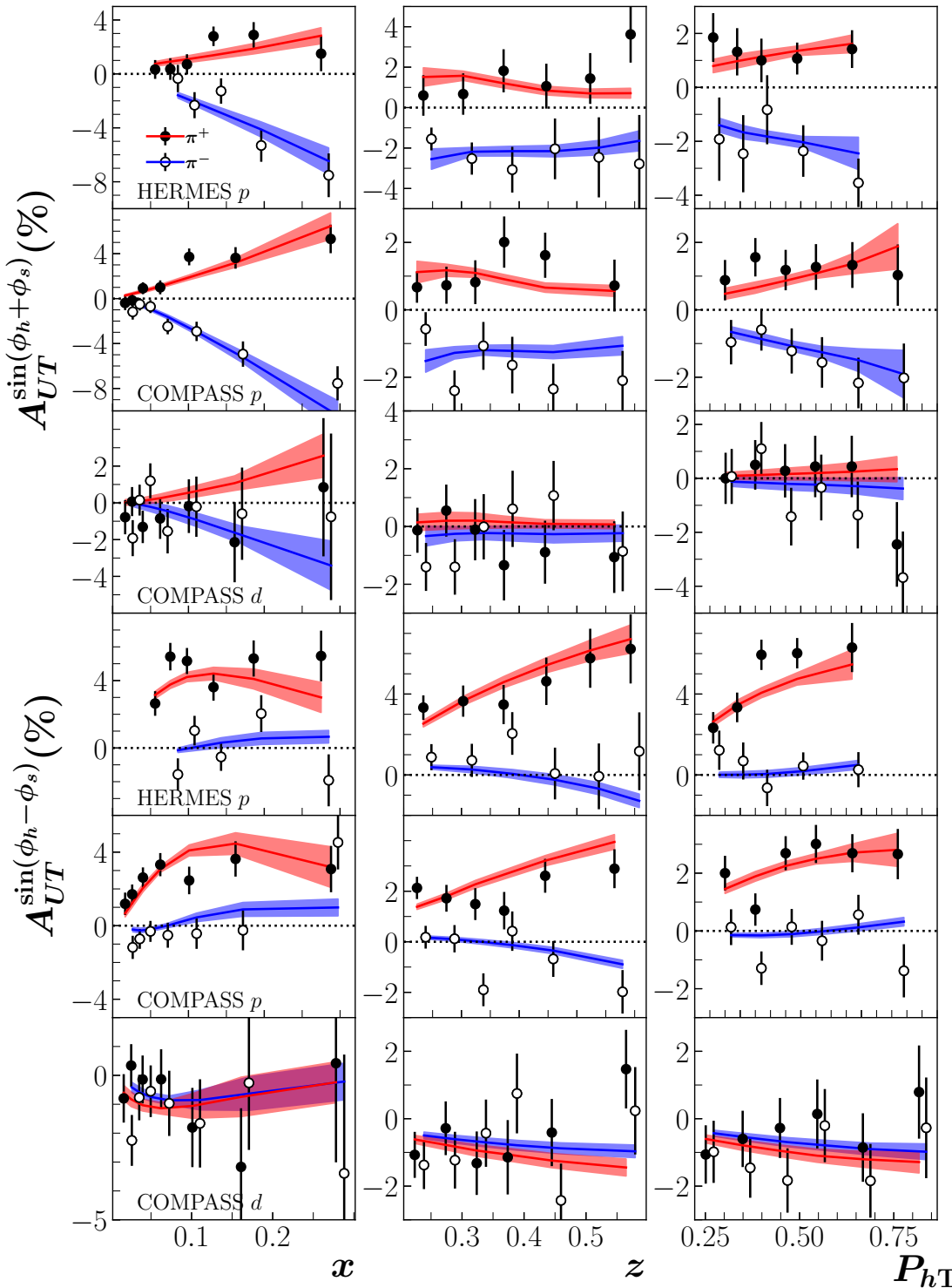
Collins FF

$$H_1^{\perp(1)}(z)$$

UNIVERSAL GLOBAL ANALYSIS 2020

Cammarota, Gamberg, Kang, Miller, Pitonyak, Prokudin, Rogers, Sato Phys.Rev.D 102 (2020) 5, 05400 (2020)

SIDIS



Collins asymmetry

$$\frac{\chi^2}{npoints} = \frac{111.3}{126} = 0.88$$

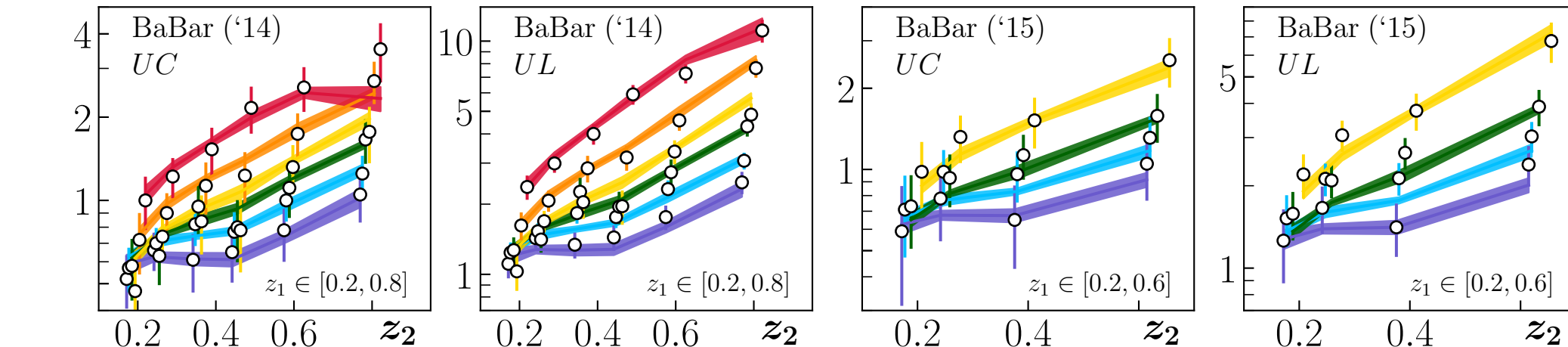
Sivers asymmetry

$$\frac{\chi^2}{npoints} = \frac{150.0}{126} = 1.19$$

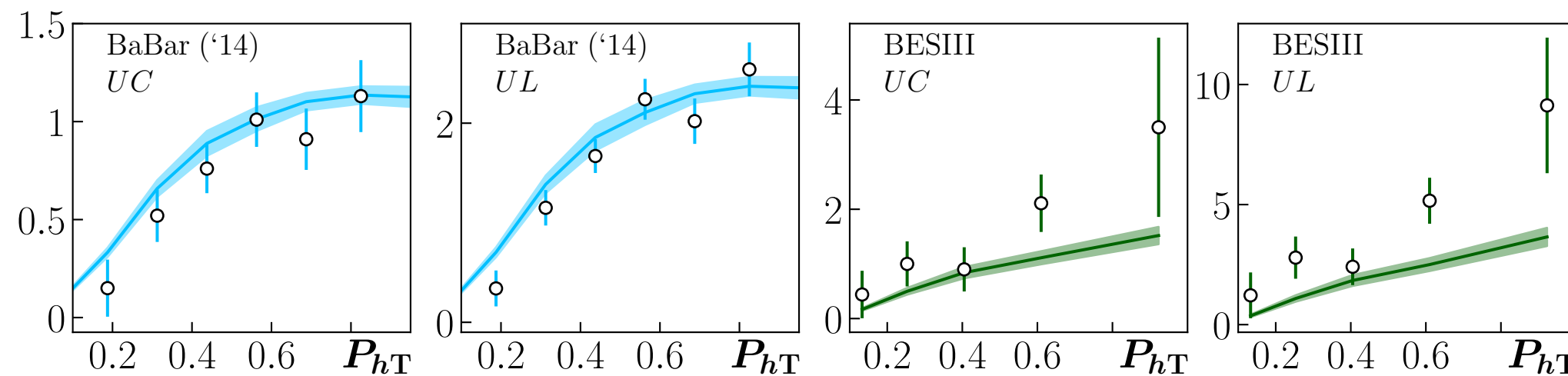
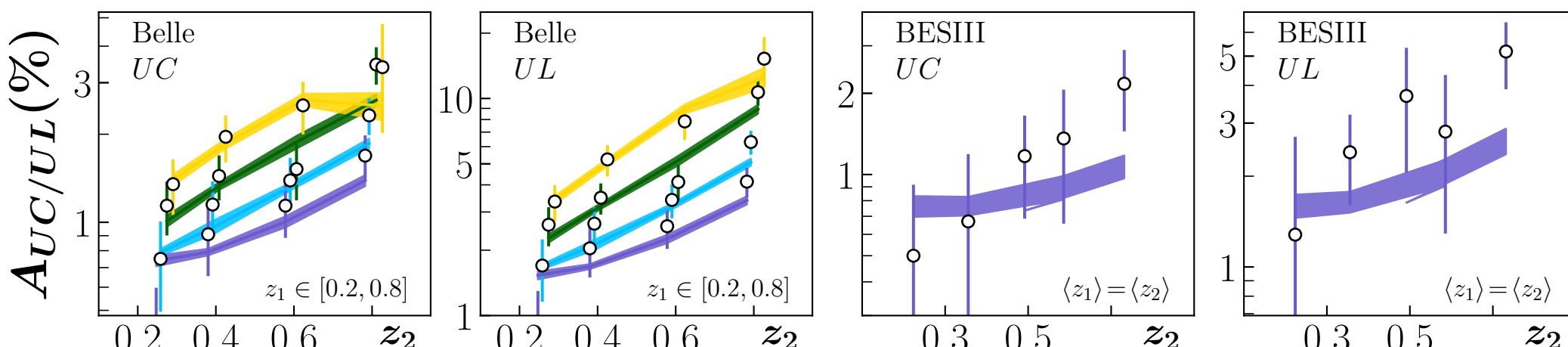
UNIVERSAL GLOBAL ANALYSIS 2020

Cammarota, Gamberg, Kang, Miller, Pitonyak, Prokudin, Rogers, Sato Phys.Rev.D 102 (2020) 5, 05400 (2020)

e^+e^-



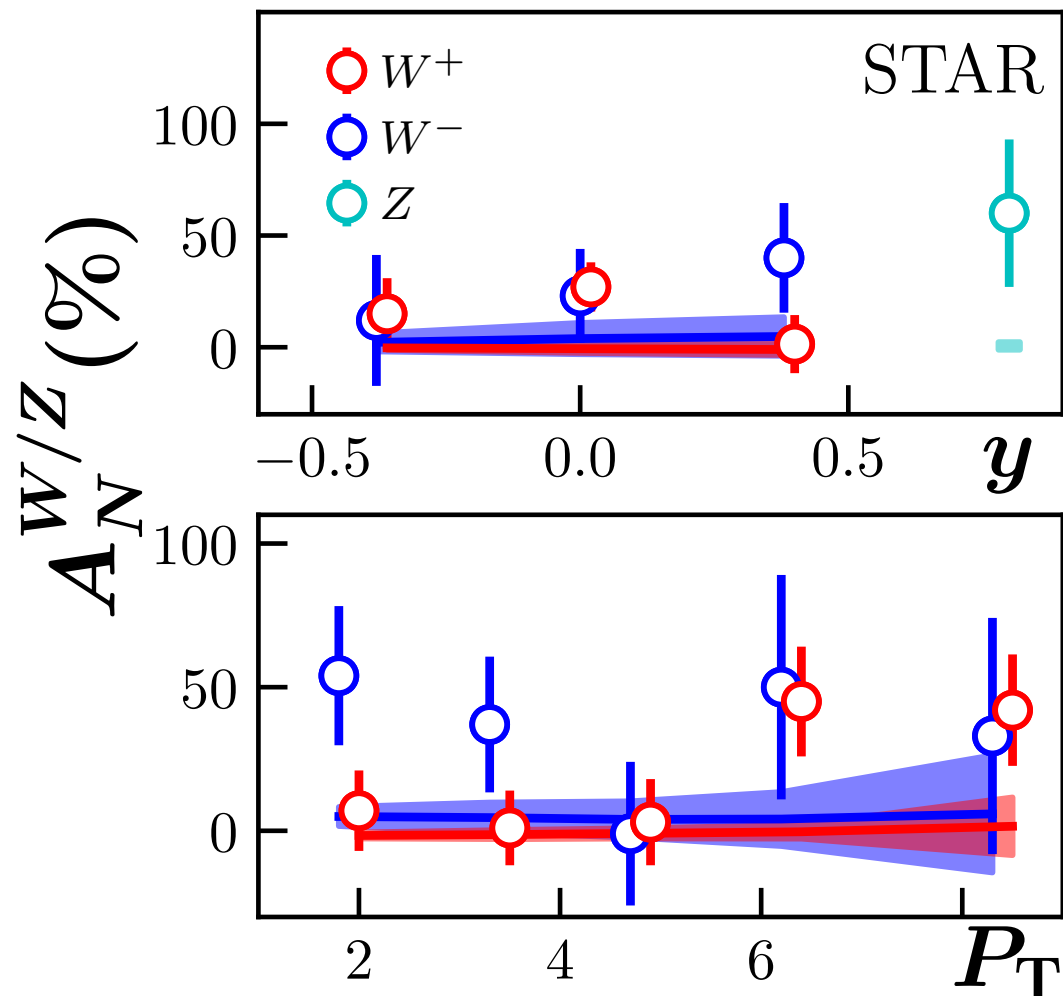
$$\frac{\chi^2}{n\text{points}} = \frac{154.5}{176} = 0.88$$



UNIVERSAL GLOBAL ANALYSIS 2020

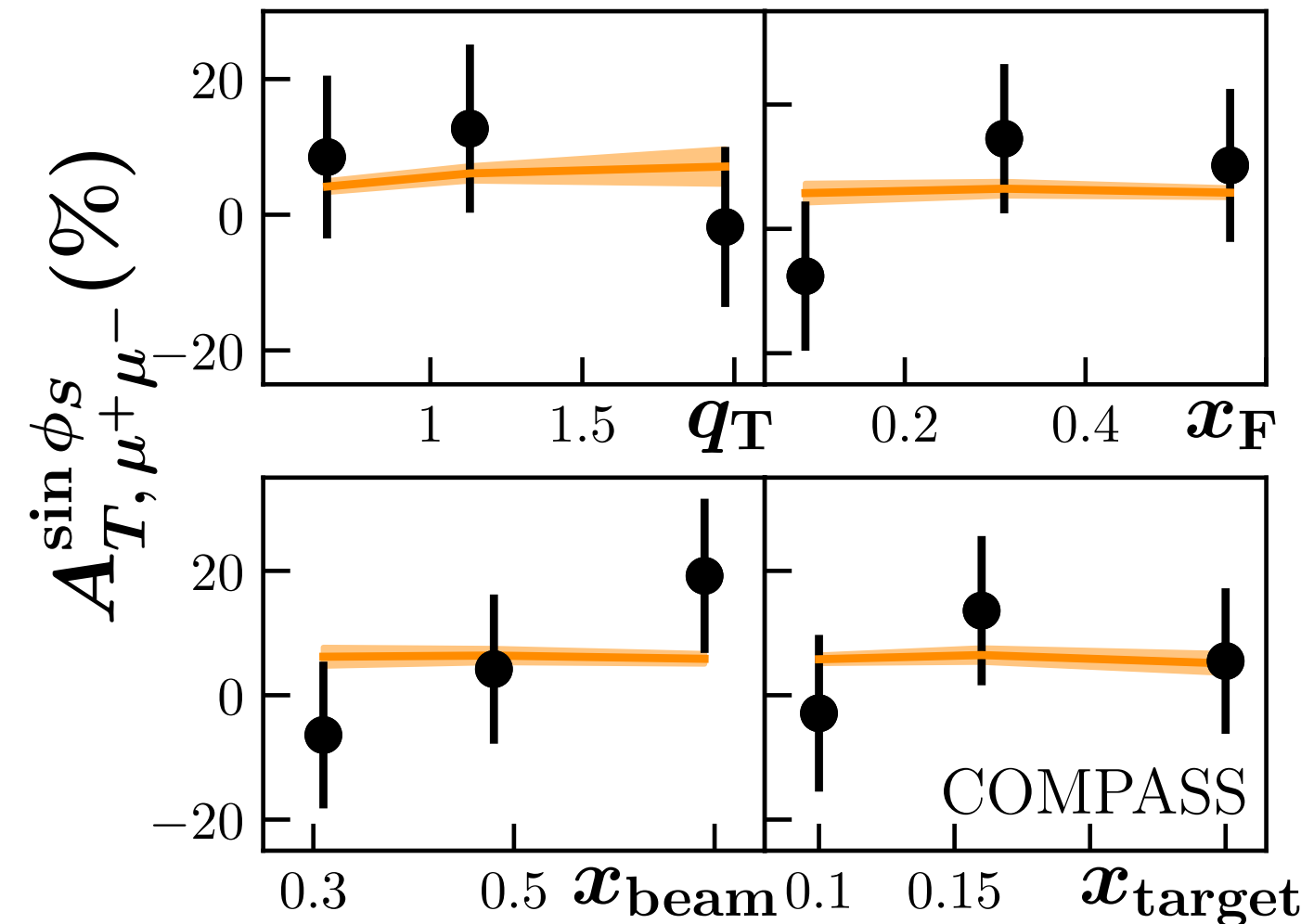
Cammarota, Gamberg, Kang, Miller, Pitonyak, Prokudin, Rogers, Sato Phys.Rev.D 102 (2020) 5, 05400 (2020)

Drell-Yan



STAR

$$\frac{\chi^2}{npoints} = \frac{31.8}{17} = 1.87$$



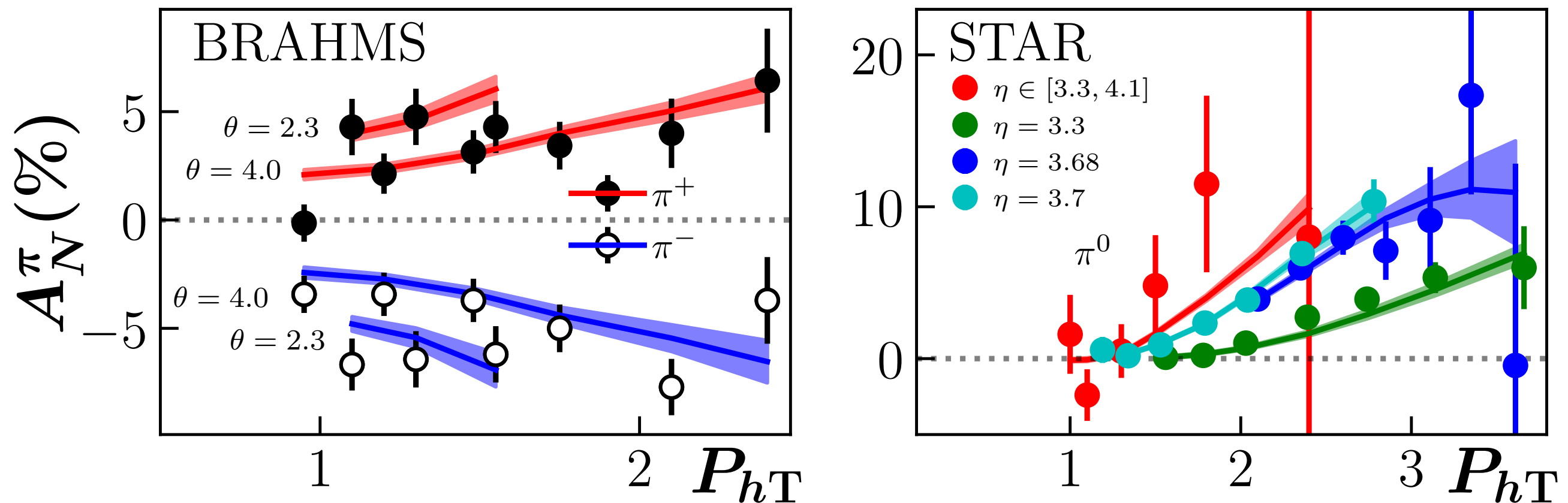
COMPASS DY

$$\frac{\chi^2}{npoints} = \frac{5.96}{12} = 0.5$$

UNIVERSAL GLOBAL ANALYSIS 2020

Cammarota, Gamberg, Kang, Miller, Pitonyak, Prokudin, Rogers, Sato Phys.Rev.D 102 (2020) 5, 05400 (2020)

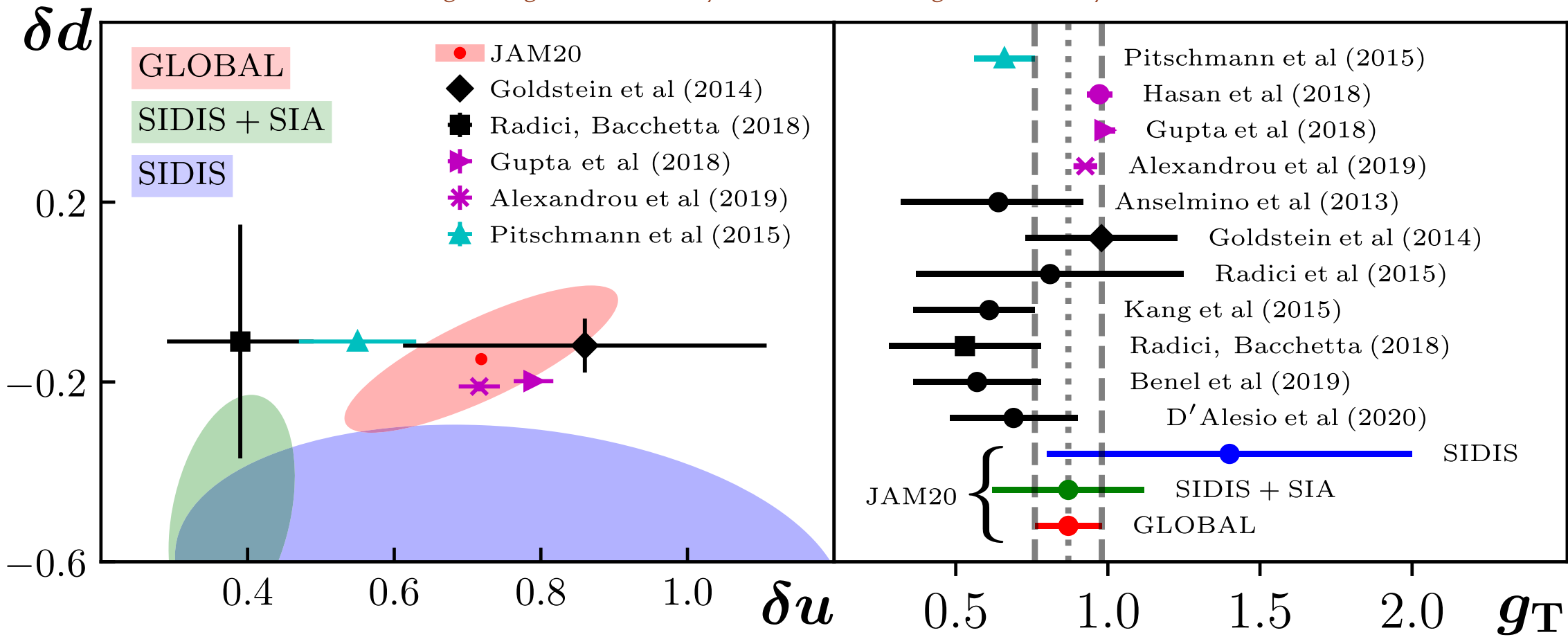
proton-proton A_N



$$\frac{\chi^2}{npoints} = \frac{66.5}{60} = 1.11$$

UNIVERSAL GLOBAL ANALYSIS 2020

Cammarota, Gamberg, Kang, Miller, Pitonyak, Prokudin, Rogers, Sato Phys.Rev.D 102 (2020) 5, 05400 (2020)



- Tensor charge from up and down quarks is constrained and compatible with lattice results
- Isovector tensor charge $g_T = \delta u - \delta d$
 $g_T = 0.87 \pm 0.11$ compatible with lattice results

δu and δd $Q^2=4$ GeV 2

$\delta u = 0.72 \pm 0.19$

$\delta d = -0.15 \pm 0.16$

JAM22 ANALYSIS

JAM22: SET UP

JAM22: Gamberg, Malda, Miller,
Pitonyak, Prokudin, Sato,
arXiv:2205.00999

- Collins and Sivers (3D binned) SIDIS data from HERMES (2020)

HERMES Collaboration, A. Airapetian et al. JHEP 12 (2020) 010



- $A_{UT}^{\sin \phi_S}$ (x and z projections only) from HERMES (2020)

- All other data sets are the same as in JAM20, except for the new HERMES data that supersedes previous sets
- 19 observables and 8 non-perturbative functions (Sivers up/down; transversity up/down; Collins fav/unf, \tilde{H} fav/unf)

$$h_1(x), F_{FT}(x, x), H_1^{\perp(1)}(z), \tilde{H}(z) \quad \checkmark$$

- Lattice data on g_T at the physical pion mass from Alexandrou, et al. (2020)

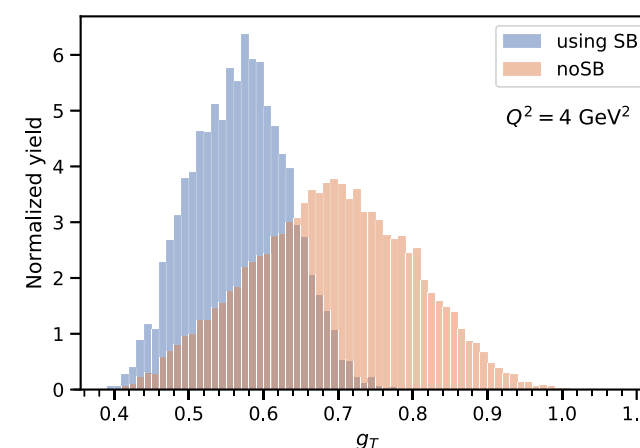
C. Alexandrou et al, Phys.Rev.D 102 (2020)

- Imposing the Soffer bound on transversity $|h_1^q(x)| \leq \frac{1}{2}(f_1^q(x) + g_1^q(x))$

J. Soffer, Phys.Rev.Lett. 74 (1995)

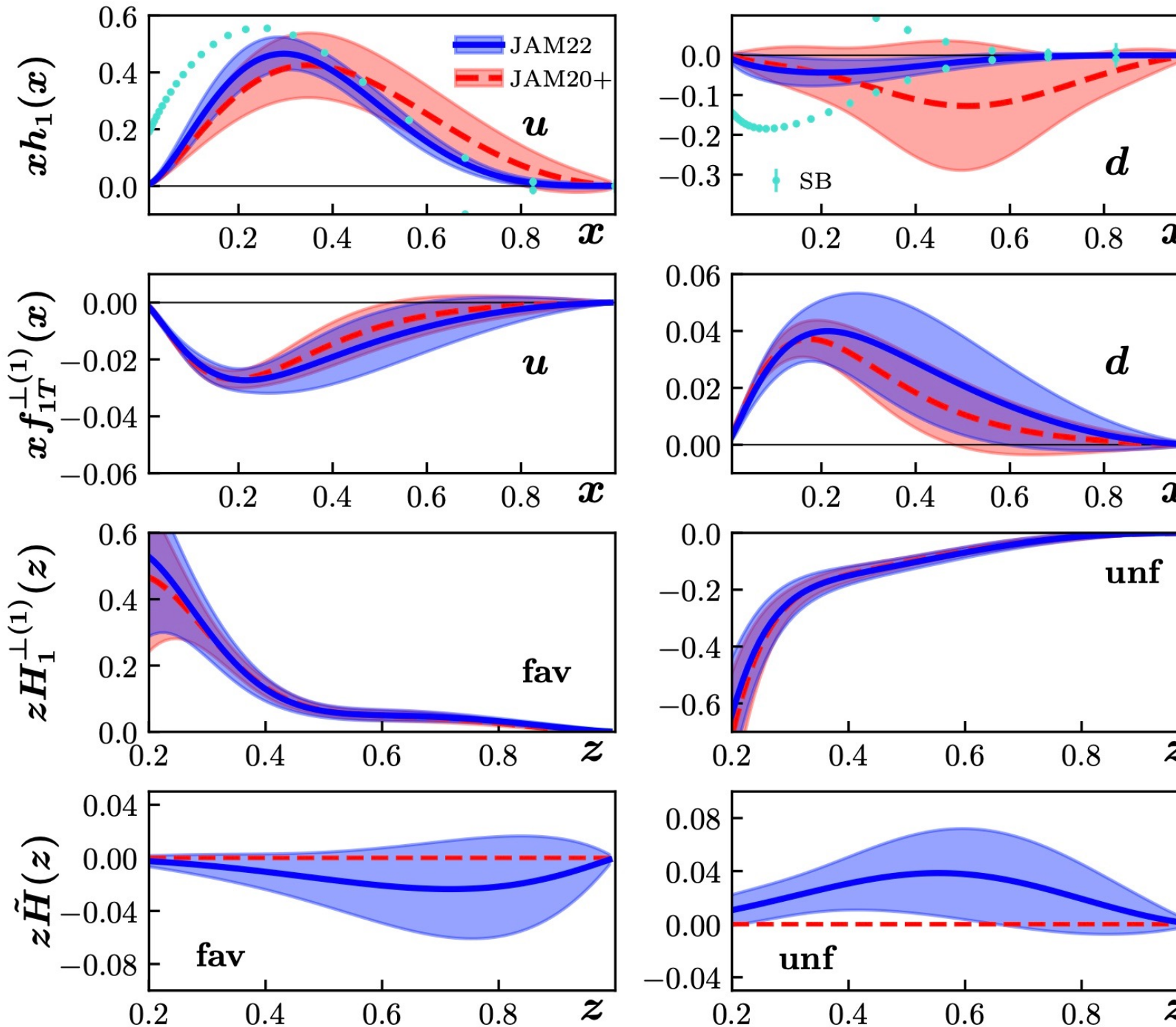
Recent phenomenology indicates substantial influence of imposing the Soffer bounds

*U. D'Alesio, C. Flore, A. Prokudin
Phys.Lett.B 803 (2020) 135347*



UNIVERSAL GLOBAL ANALYSIS 2022

JAM22: Gumberg, Malda, Miller,
Pitonyak, Prokudin, Sato,
arXiv:2205.00999



Transversity

$h_1(x)$

Sivers

$f_{1T}^{\perp(1)}(x)$

Collins FF

$H_1^{\perp(1)}(z)$

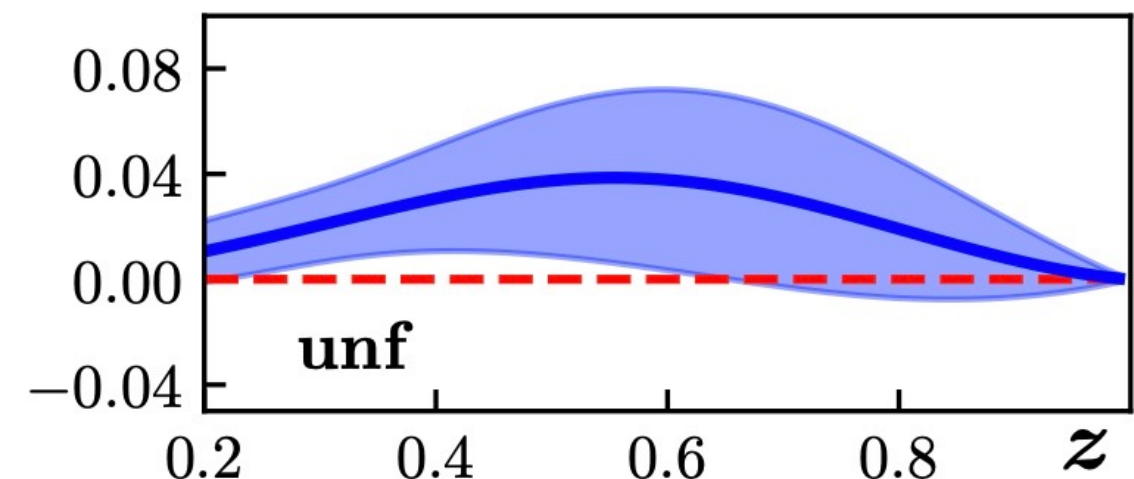
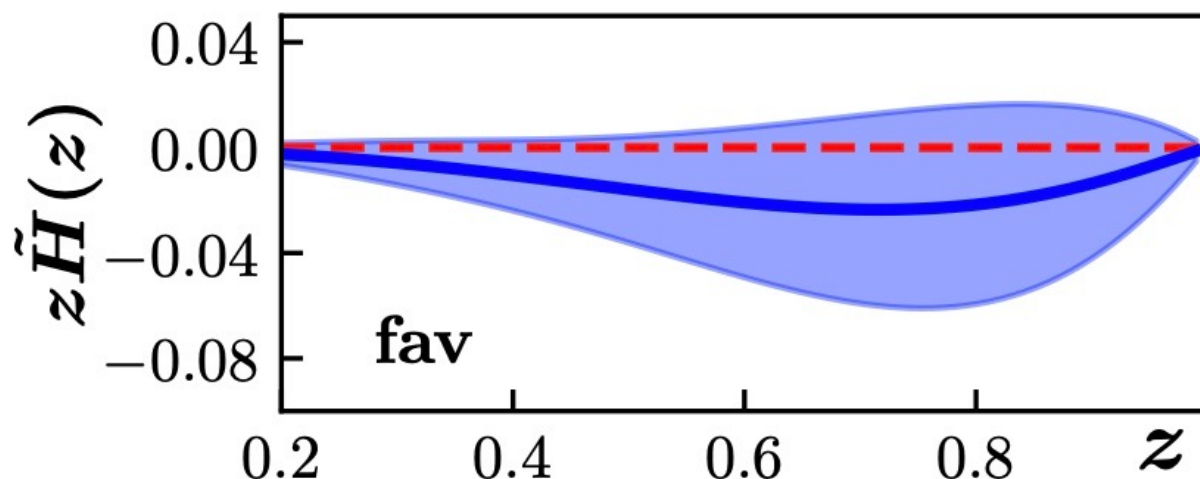
Twist-3 FF

$\tilde{H}(z)$

JAM22: TWIST-3 FF \tilde{H}

JAM22: Gumberg, Malda, Miller,
Pitonyak, Prokudin, Sato,
arXiv:2205.00999

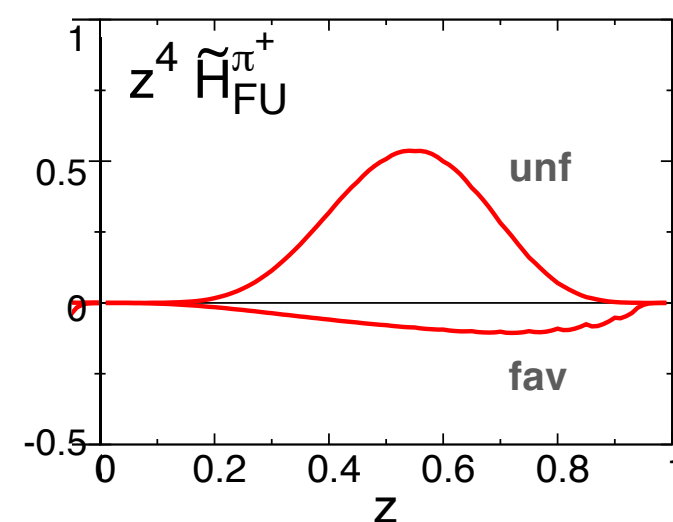
The first insight to the twist-3 fragmentation function \tilde{H}



Compatible with signs to the model calculation
and previous phenomenology

Z. Lu and I. Schmidt Phys.Lett.B 747 (2015)

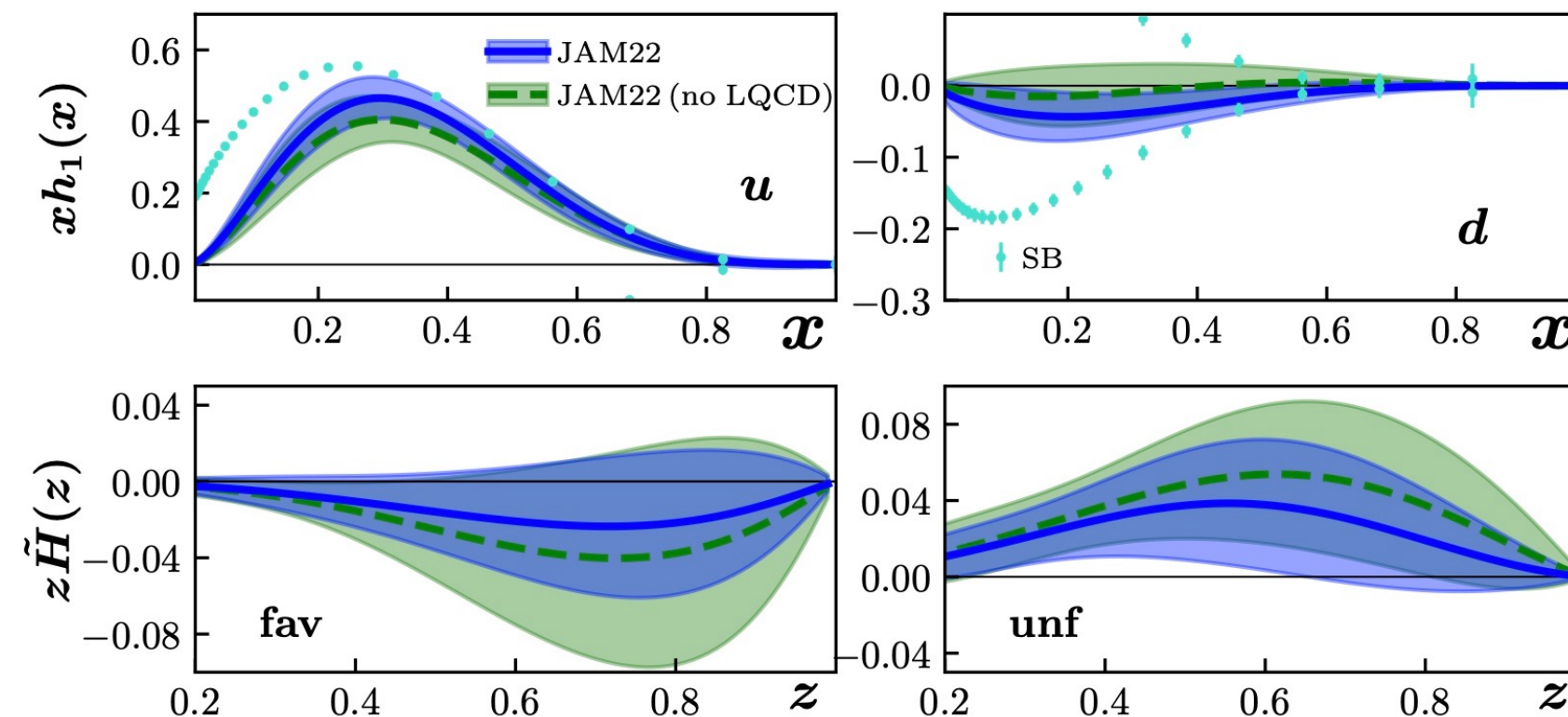
K. Kanazawa, Y. Koike, A. Metz, D. Pitonyak,
Phys.Rev.D 89 (2014) 11, 111501



JAM22: TRANSVERSITY

JAM22: Gamberg, Malda, Miller,
Pitonyak, Prokudin, Sato,
arXiv:2205.00999

Transversity becomes much more tightly constrained by now imposing the SB and including the lattice g_T data point

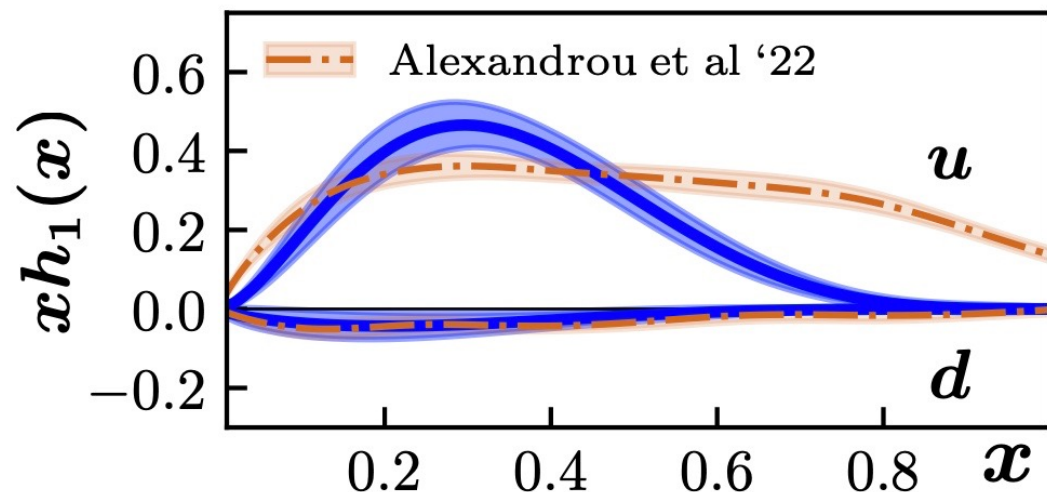
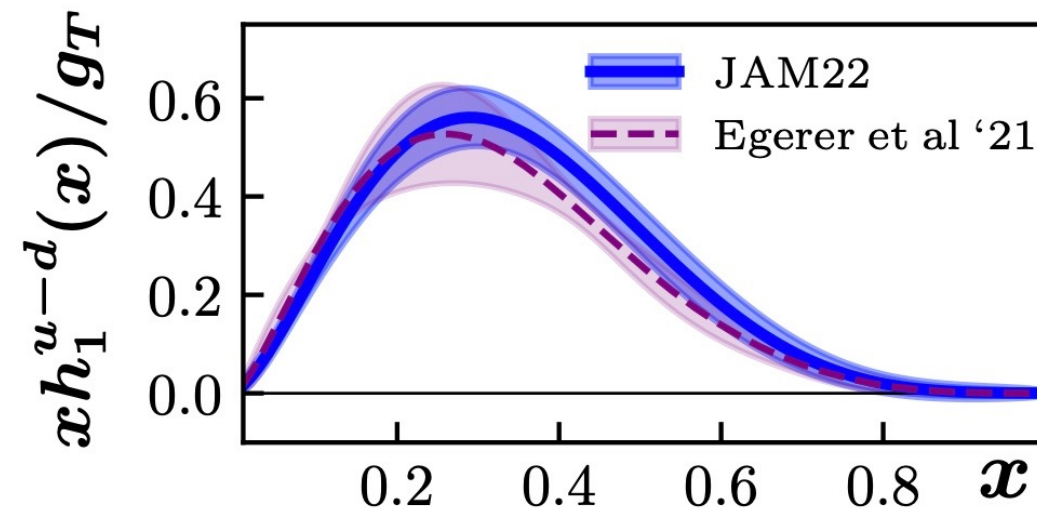


Extracted Collins FFs are compatible within the errors with JAM20, e^+e^- data constrains those functions well.

\tilde{H} behaves similar to the Collins function (favored and unfavored roughly equal in magnitude but opposite in sign) - expected since both are derived from the same underlying quark-gluon-quark FF

JAM22: TRANSVERSITY AND LATTICE

JAM22: Gamberg, Malda, Miller,
Pitonyak, Prokudin, Sato,
arXiv:2205.00999



The raw lattice data for Egerer, et al. and Alexandrou, et al. are compatible, but the former uses pseudo-PDFs and the latter quasi-PDFs

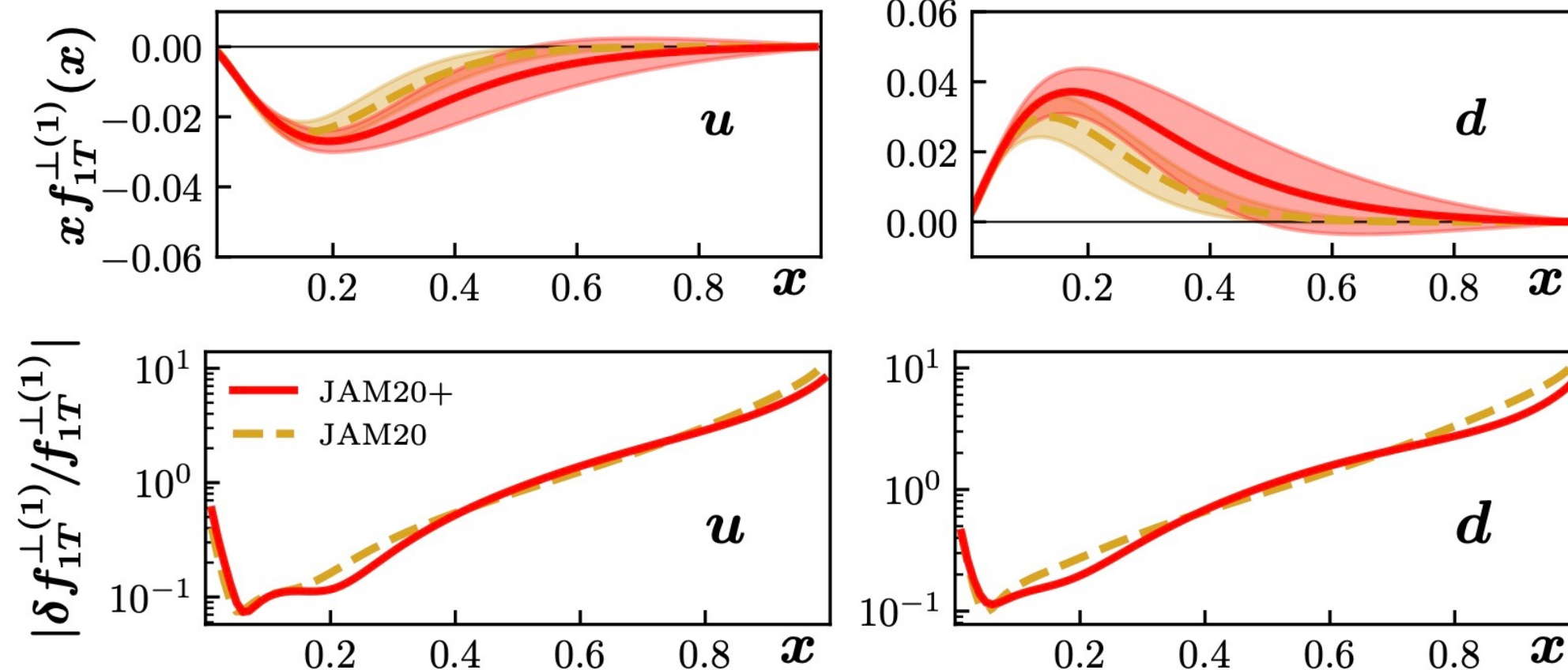
The behavior at large x for the up quark in Alexandrou, et al. is due to systematics in the reconstruction of the x dependence in the quasi-PDF approach

We find good agreement with lattice calculations of transversity

Now that the lattice g_T data point is included in JAM3D-22, the uncertainties in the phenomenological extraction of transversity are compatible with lattice

JAM22: SIVERS FUNCTIONS, THE QIU-STERMAN MATRIX ELEMENT

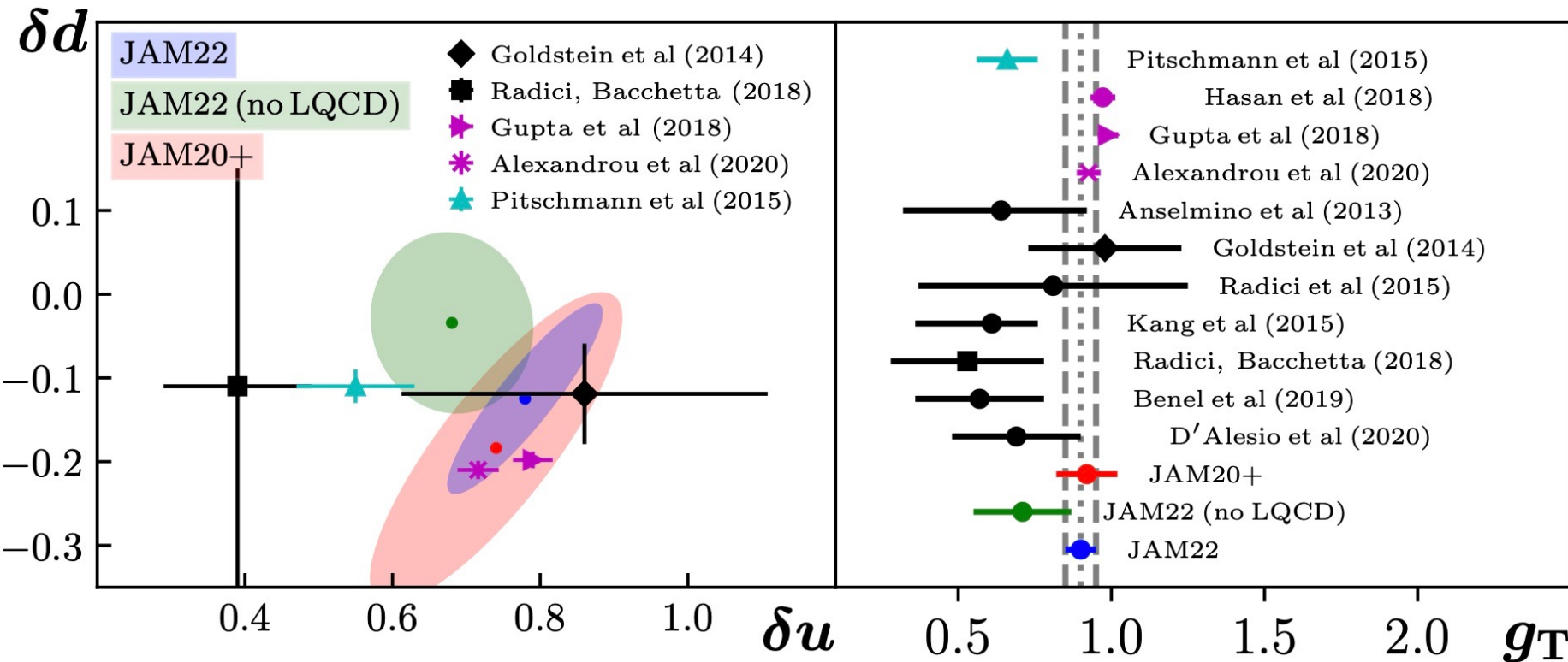
JAM22: Gamberg, Malda, Miller,
Pitonyak, Prokudin, Sato,
arXiv:2205.00999



Extracted Sivers functions are compatible within the errors with JAM20, the increase in magnitude and the error is due to the new HERMES 3D data.

UNIVERSAL GLOBAL ANALYSIS 2022

JAM22: Gamberg, Malda, Miller,
Pitonyak, Prokudin, Sato,
arXiv:2205.00999



- Tensor charge from up and down quarks and $g_T = \delta u - \delta d$ are well constrained and compatible with both lattice results and the Soffer bound
- The tension with diFF method, Radici, Bacchetta (2018) becomes more pronounced: is it due to the data, theory, methodology? Both methods should be scrutinized.

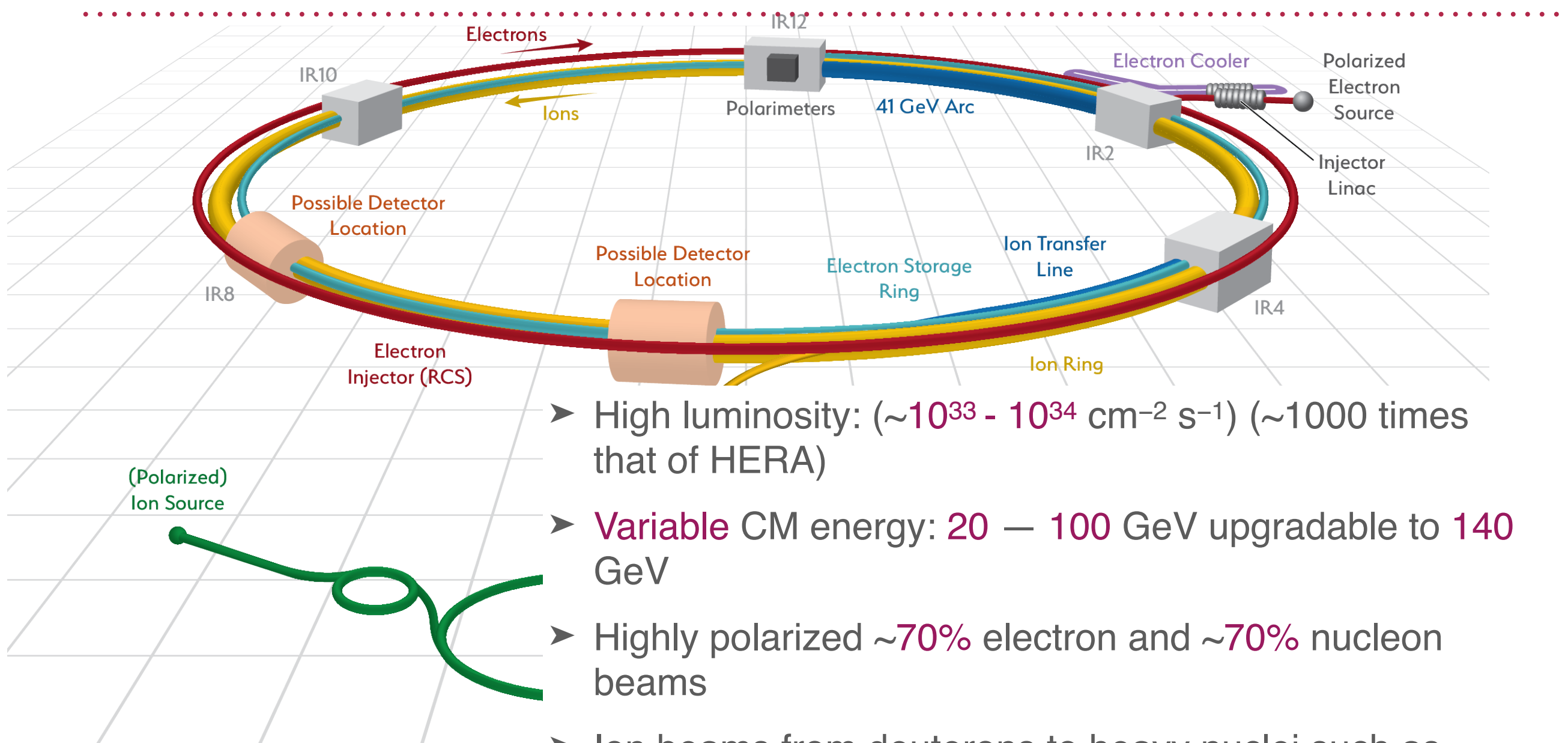
δu and δd $Q^2=4$ GeV 2

$\delta u = 0.74 \pm 0.11$

$\delta d = -0.15 \pm 0.12$

$g_T = 0.89 \pm 0.06$

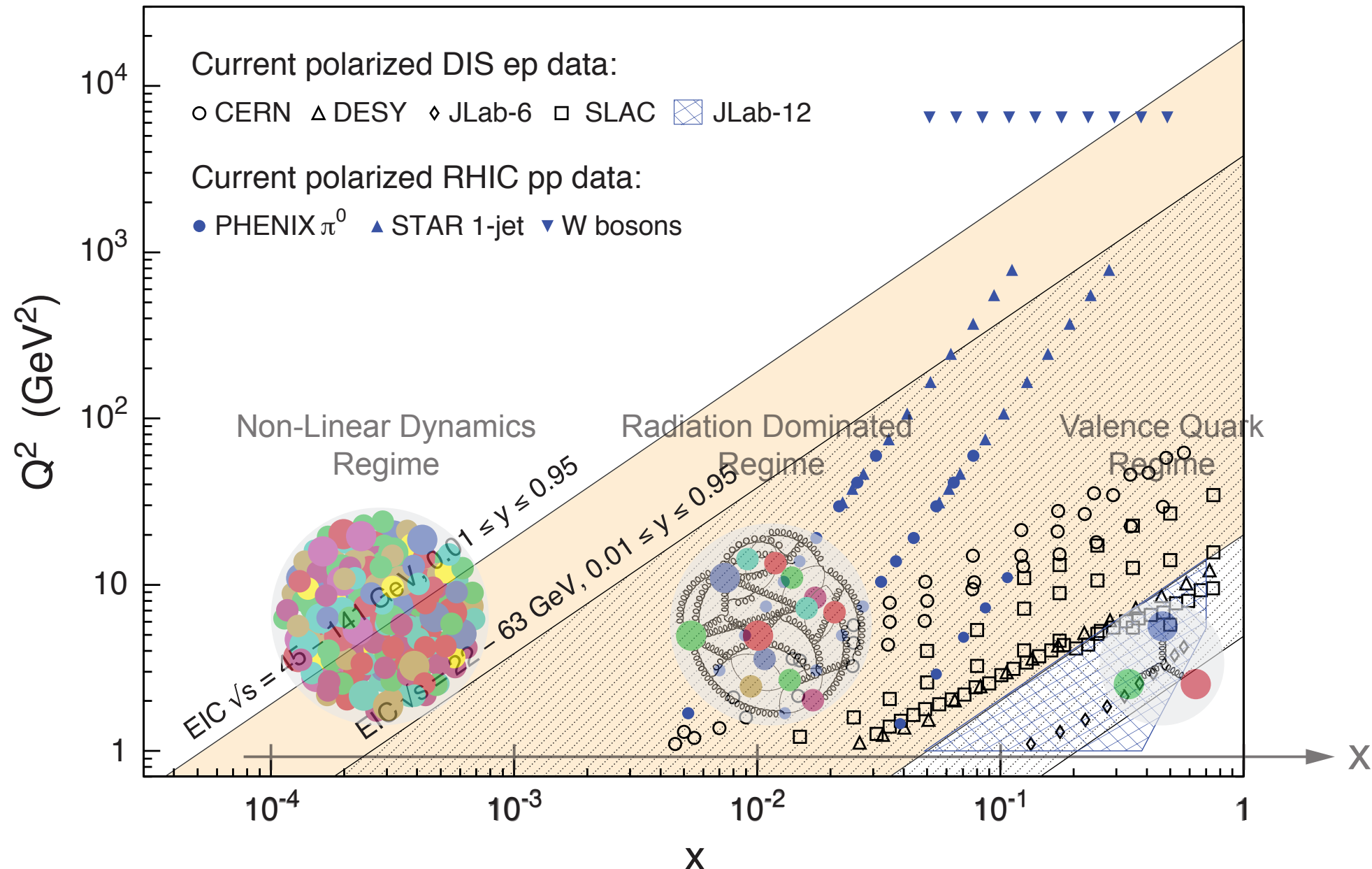
THE ELECTRON-ION COLLIDER @ BNL



White Paper (2012)
Accardi et al, arXiv:1212:1701

- High luminosity: ($\sim 10^{33} - 10^{34} \text{ cm}^{-2} \text{ s}^{-1}$) (~ 1000 times that of HERA)
- Variable CM energy: 20 – 100 GeV upgradable to 140 GeV
- Highly polarized ~70% electron and ~70% nucleon beams
- Ion beams from deuterons to heavy nuclei such as gold, lead, or uranium
- Possibility of more than one interaction region (none of the major facilities operates with one detector only - important for discovery potential)

THE ELECTRON-ION COLLIDER: KINEMATICS



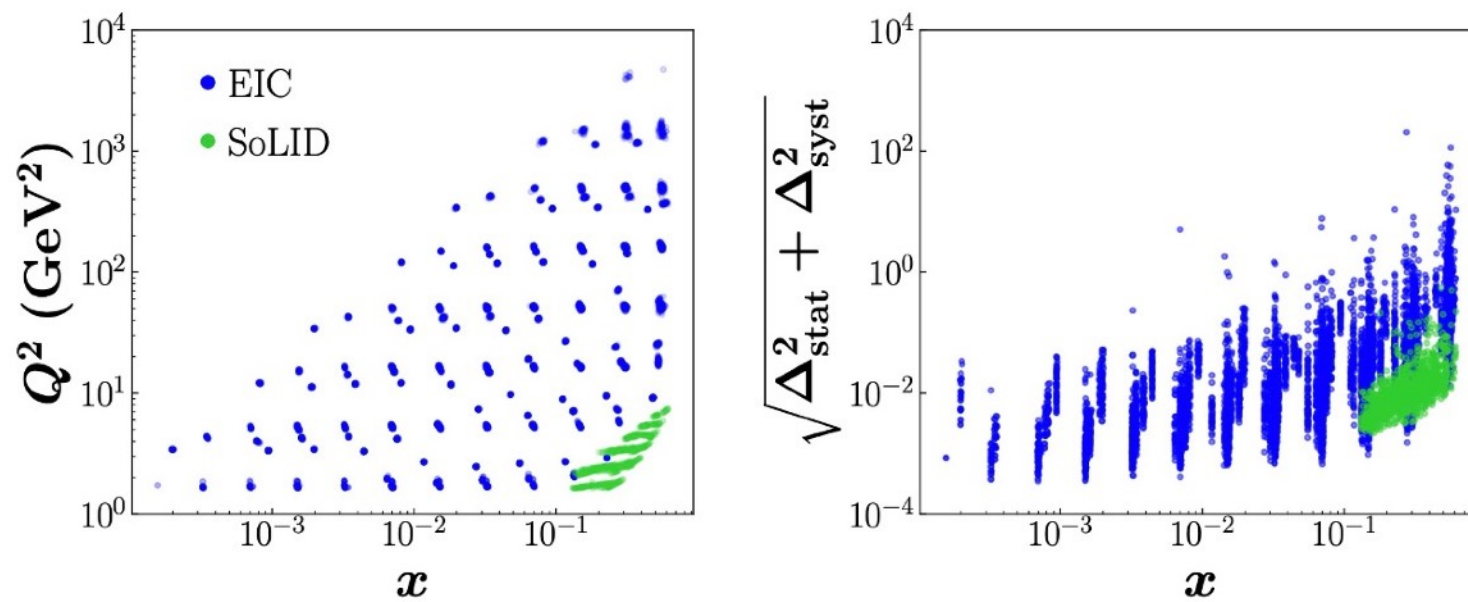
BNL Report (2017)
Aschenauer et al, arXiv:1708.01527

TENSOR CHARGE AND FUTURE FACILITIES

L. Gamberg, Z. Kang, D. Pitonyak, A. Prokudin, N. Sato Phys.Lett.B 816 (2021)

EIC Pseudo-data			
Observable	Reactions	CM Energy (\sqrt{S})	$N_{\text{pts.}}$
Collins (SIDIS)	$e + p^\uparrow \rightarrow e + \pi^\pm + X$	141 GeV	756 (π^+) 744 (π^-)
		63 GeV	634 (π^+) 619 (π^-)
		45 GeV	537 (π^+) 556 (π^-)
		29 GeV	464 (π^+) 453 (π^-)
	$e + {}^3He^\uparrow \rightarrow e + \pi^\pm + X$	85 GeV	647 (π^+) 650 (π^-)
		63 GeV	622 (π^+) 621 (π^-)
		29 GeV	461 (π^+) 459 (π^-)
		Total EIC $N_{\text{pts.}}$	8223

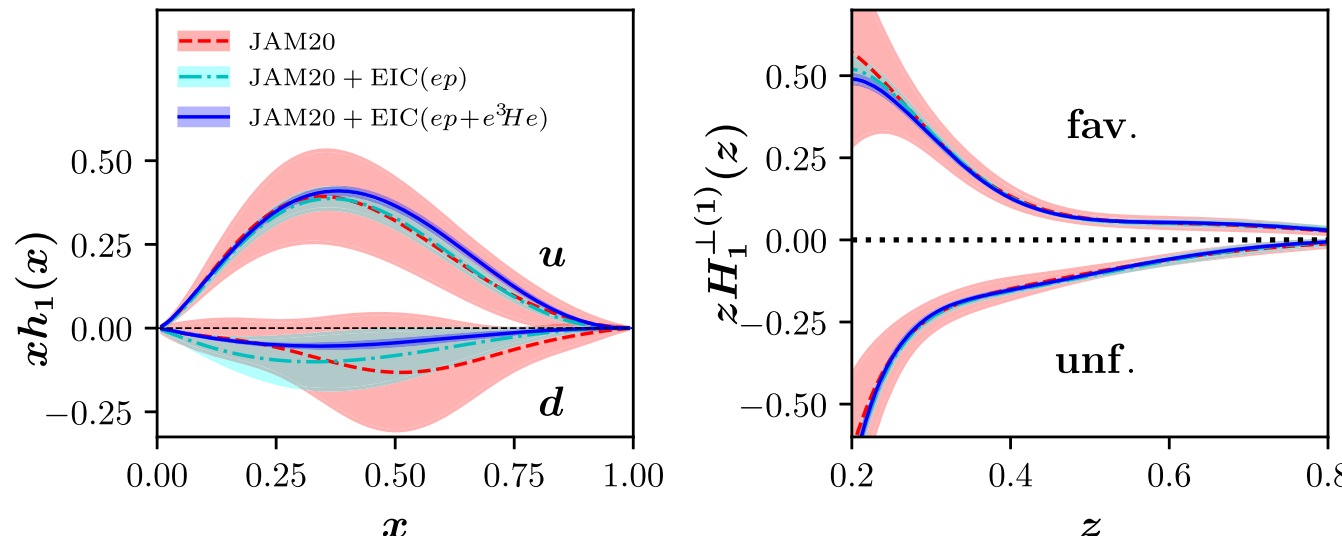
Assumed accumulated luminosities of 10 fb⁻¹, 70% polarization, conservatively accounted for detector smearing and acceptance effects



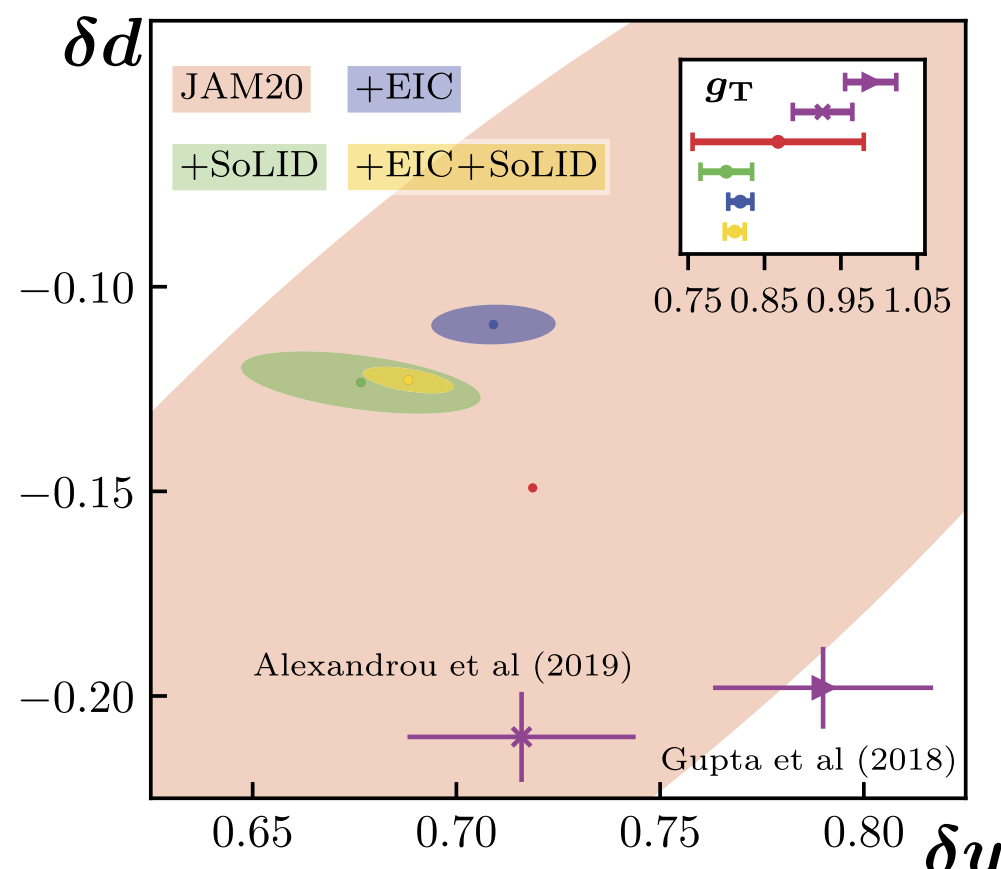
SoLID at JLab covers a complimentary region at higher x and lower Q^2 with much greater luminosity – important to explore the effect of multiple measurements in different kinematic regions

TENSOR CHARGE AT THE EIC AND JLAB

L. Gumberg, Z. Kang, D. Pitonyak, A. Prokudin, N. Sato Phys.Lett.B 816 (2021)



JAM20: Cammarota, Gumberg, Kang, Miller, Pitonyak, Prokudin, Rogers, Sato, Phys.Rev.D 102 (2020)



- EIC data will allow to have g_T extraction at the precision at the level of lattice QCD calculations

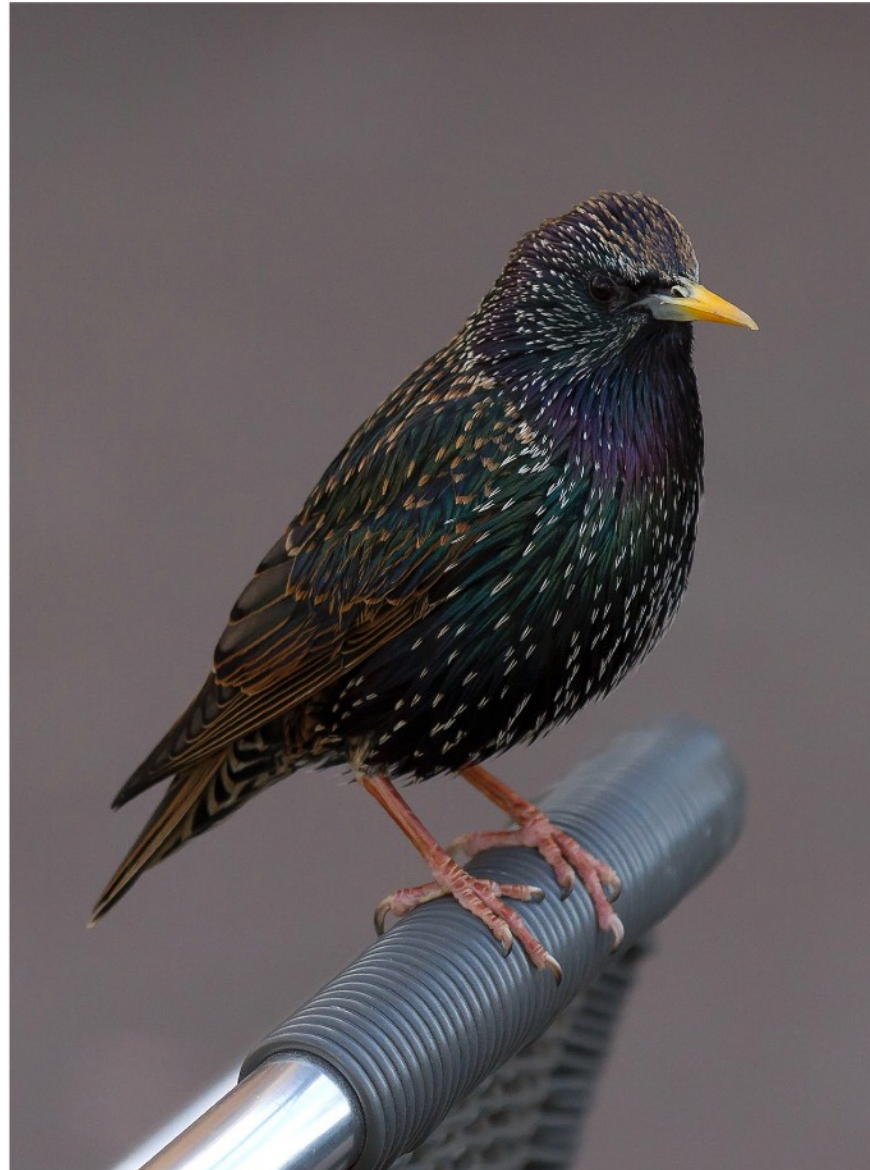
- JLab 12 data will allow to have complementary information on tensor charge to test the consistency of the extraction and expand the kinematical region

CONCLUSIONS

<https://github.com/JeffersonLab/jam3dlib>

- Shown for the first time that transverse spin asymmetries in a variety of processes SIDIS, Drell-Yan, e^+e^- , and proton proton scattering have the same origin: (multi) parton correlation functions
- Extracted a universal set of non perturbative functions responsible for spin asymmetries
- Shown consistency of phenomenological results with lattice QCD in extraction of isovector tensor charge and individual contributions from up and down quark

HADRONS ARE EMERGENT PHENOMENA IN QCD

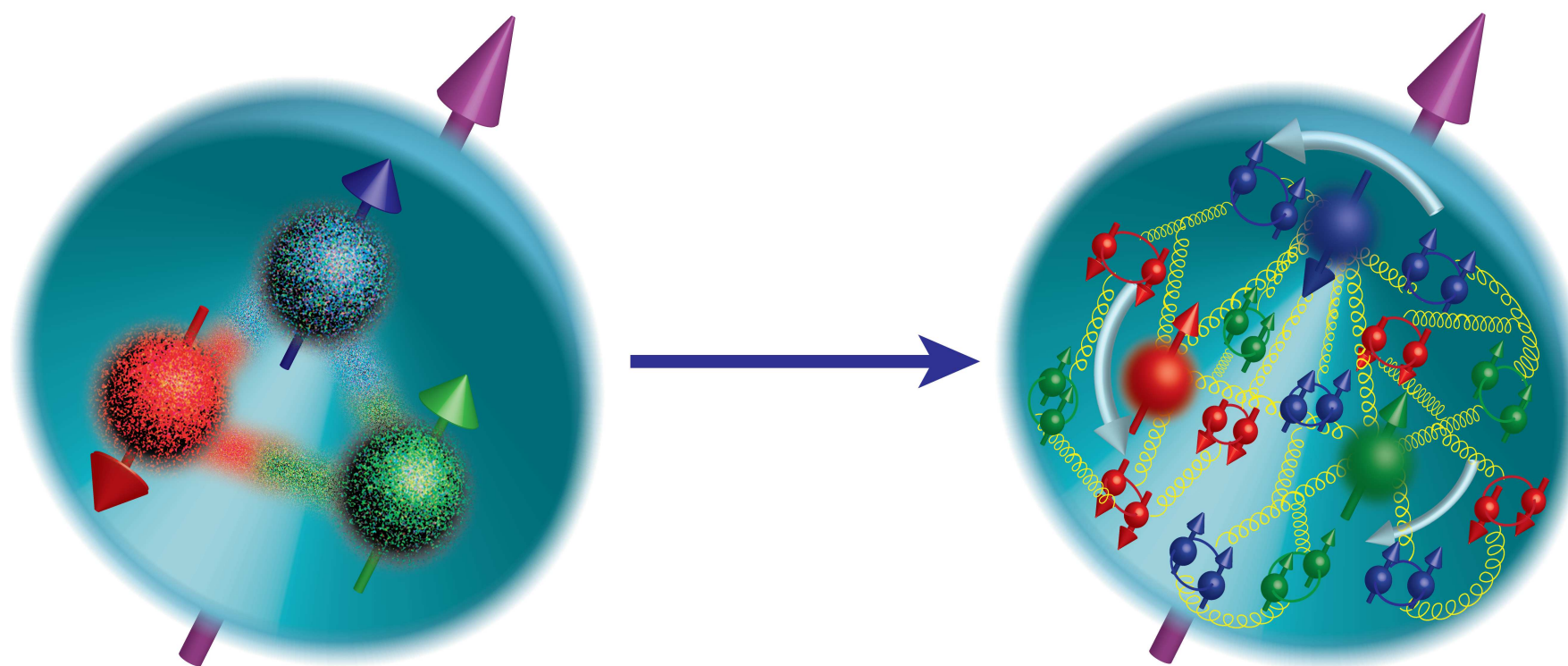


Individual starling



Murmuration of starlings

EVOLUTION OF OUR UNDERSTANDING OF THE SPIN STRUCTURE



1980' - the spin of the nucleon
is due to the valence quarks

Modern concept: valence quarks, sea quarks,
and gluons together with orbital angular
momentum are contributing

BACKUP SLIDES

UNIVERSAL GLOBAL FIT 2020

..... Cammarota, Gamberg, Kang, Miller, Pitonyak, Prokudin, Rogers, Sato (2020)

The relevant set of TMD functions to extract

$$h_1(x, k_T) = h_1(x) \mathcal{G}_h(k_T^2) \quad \text{transversity}$$

$$f_{1T}^\perp(x, k_T) = \frac{2M^2}{\langle k_T^2 \rangle_{f_{1T}^\perp}} \pi F_{FT}(x, x) \mathcal{G}_{f_{1T}^\perp}(k_T^2)$$

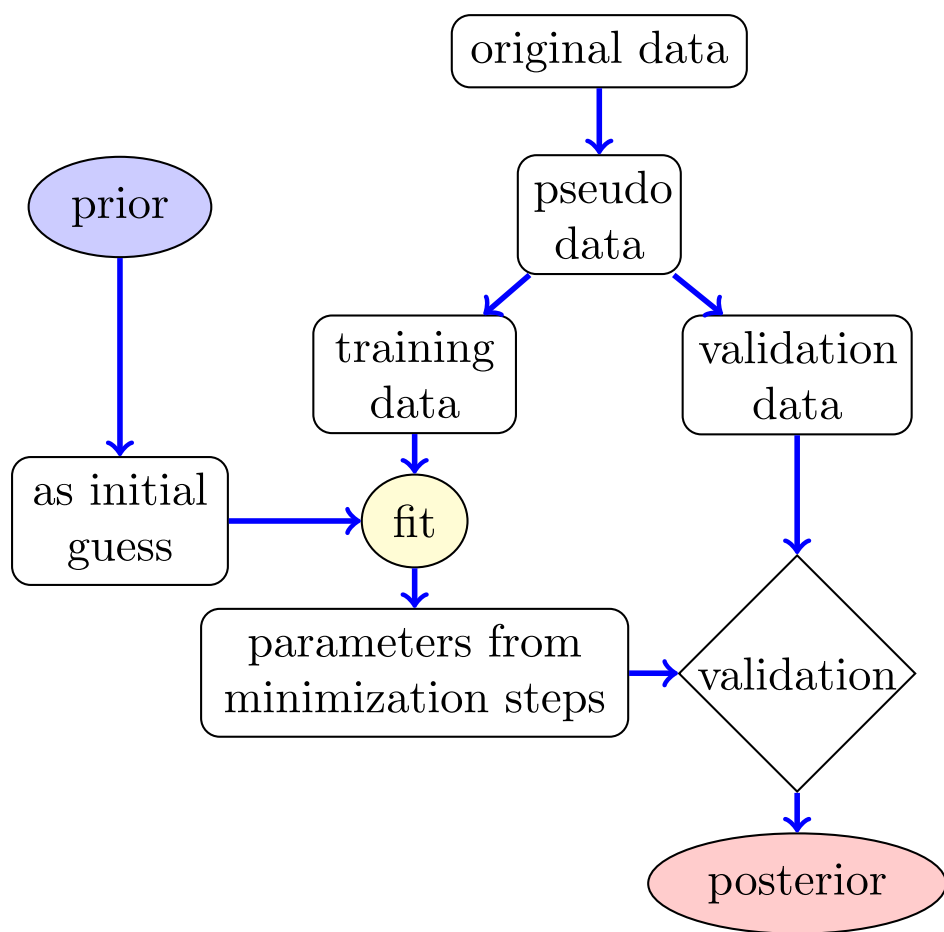
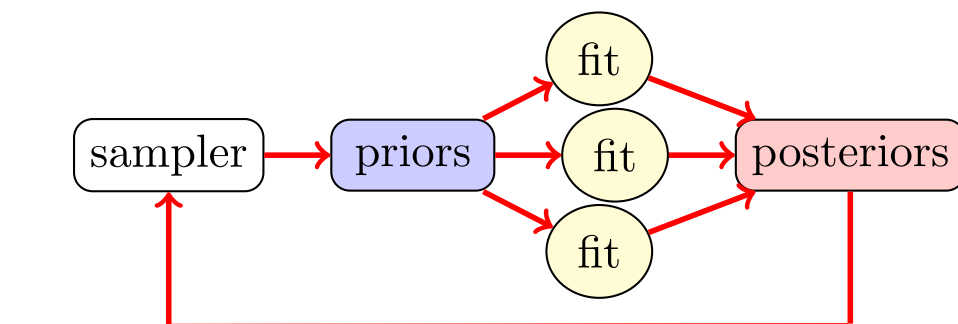
Sivers function

$$H_1^\perp(z, z p_T) = \frac{2z^2 M^2}{\langle p_T^2 \rangle_{H_1^\perp}} H_1^{\perp(1)}(z) \mathcal{G}_{H_1^\perp}(z^2 p_T^2)$$

Collins function

$$\mathcal{G}_f(k_T^2) = \frac{1}{\pi \langle k_T^2 \rangle_f} e^{-\frac{k_T^2}{\langle k_T^2 \rangle_f}}$$

JAM FITTING METHODOLOGY



- Bayesian inference is used

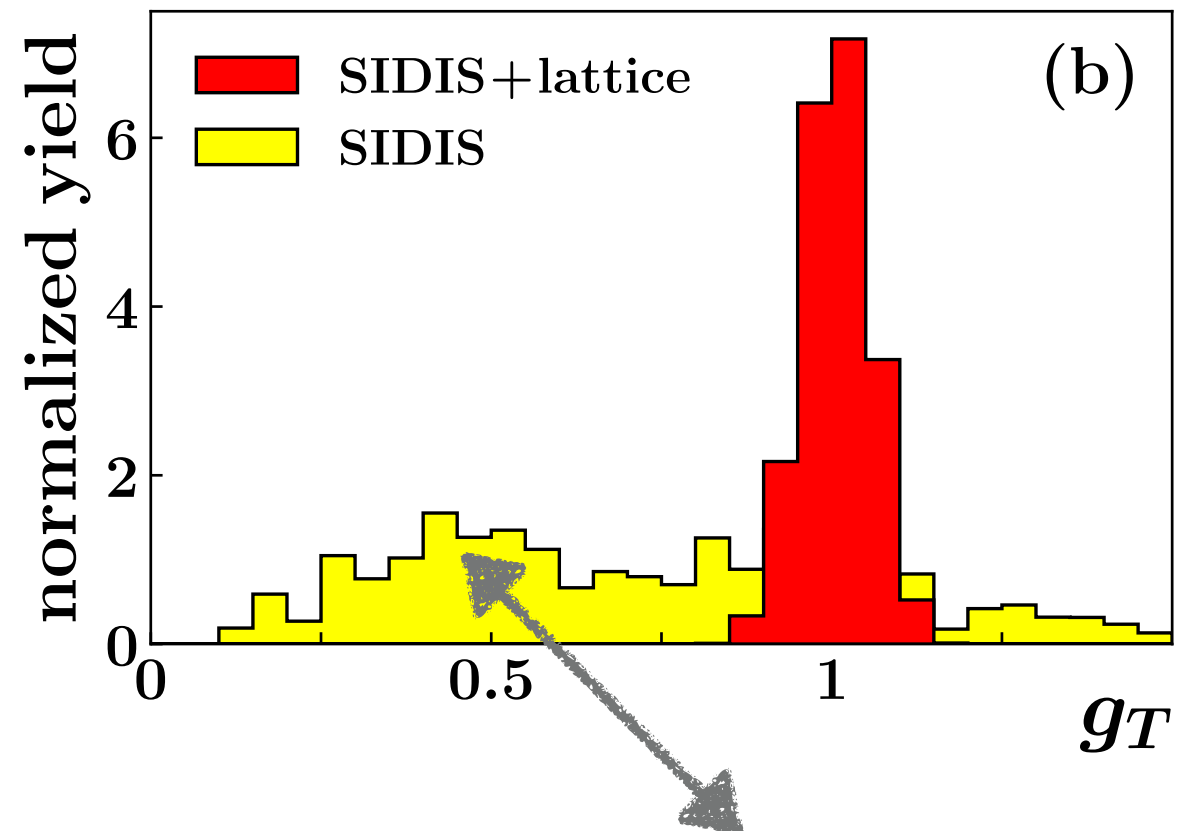
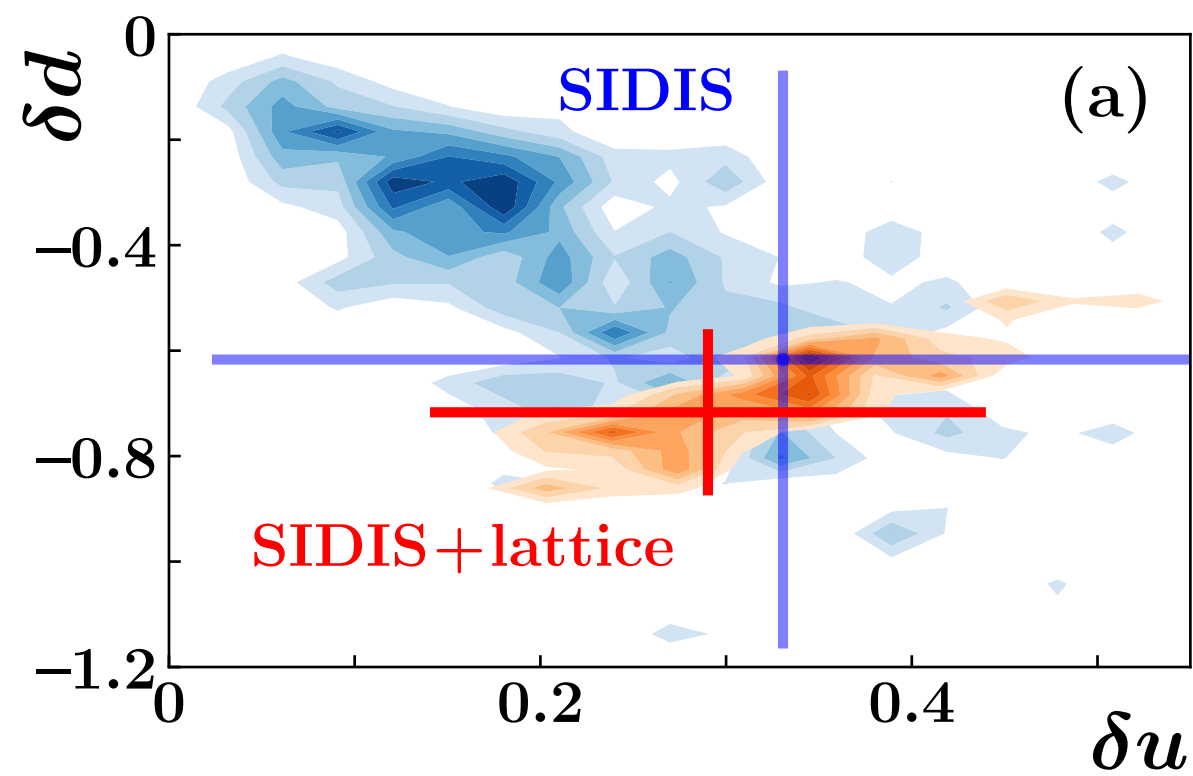
$$E[\mathcal{O}] = \int d^n a \mathcal{P}(\vec{a} | \text{data}) \mathcal{O}(\vec{a})$$

- Iterative Monte Carlo is then used to perform the fit
- Large parameter space is sampled
- Data is partitioned in validation and training sets
- Training set is fitted via chi-square minimization
- Posteriors are used to feed the next iterations

TMD AND LATTICE

Lin, Melnitchouk, Prokudin, Sato, Shows PRL 2018

First JAM analysis of SIDIS data including lattice QCD constraints on g_T

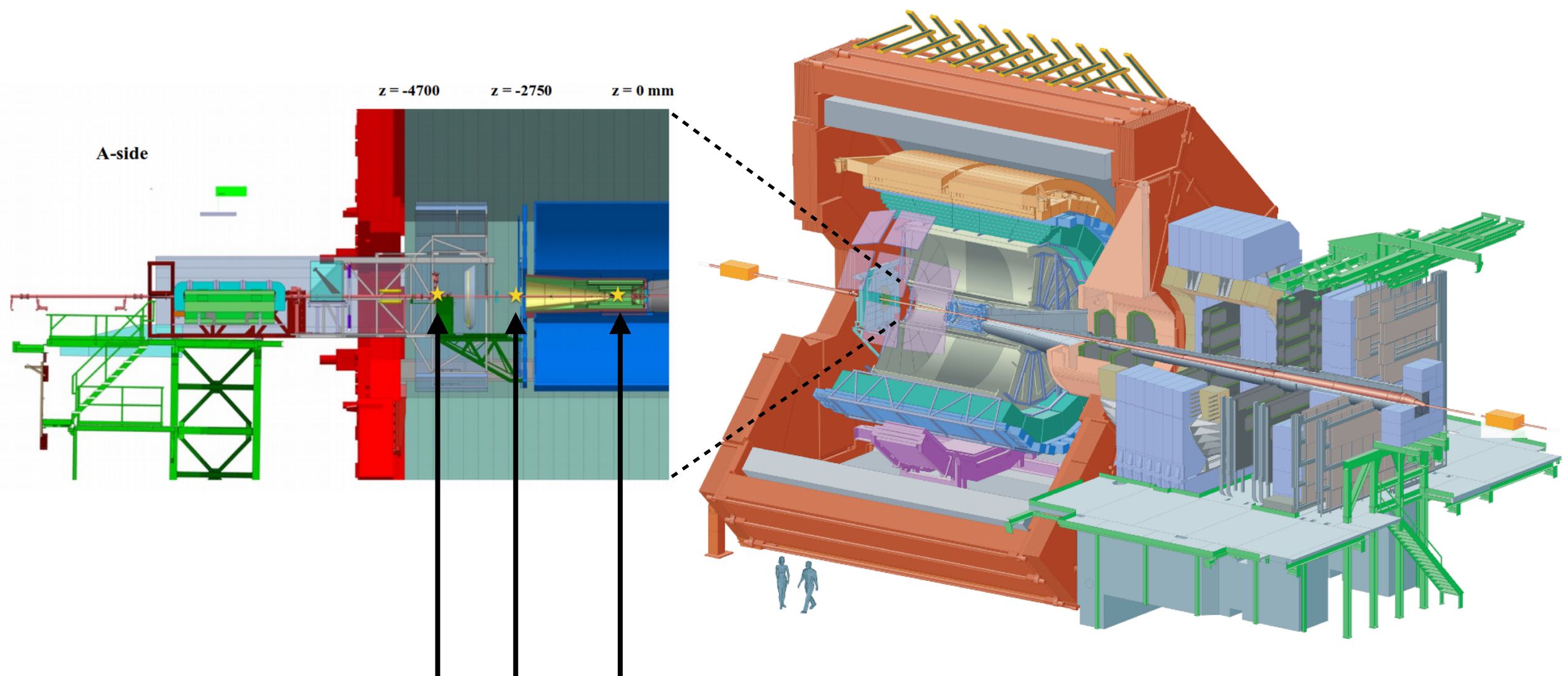


Any analysis based on a single fit would have given a wrong result on g_T

Analysis of probability density distribution of results used in JAM is crucial in obtaining correct results

ALICE FIXED TARGET

<https://indico.cern.ch/event/755856/>



Possible fixed-target positioning

JAM FITTING METHODOLOGY

Sato et al., P.R. D94 (16) 114004

- Jefferson Lab Angular Momentum Collaboration has developed a robust fitting methodology based on Bayesian statistical methods and machine learning algorithms
- Such methodology may prove crucial and essential for our future endeavors in studies of the structure of the nucleon and beyond.
- Expectation value and variance estimates:

$$E[\mathcal{O}] = \int d^n a \mathcal{P}(\vec{a}|data) \mathcal{O}(\vec{a}) \quad V[\mathcal{O}] = \int d^n a \mathcal{P}(\vec{a}|data) [\mathcal{O}(\vec{a}) - E[\mathcal{O}]]^2$$

- Bayes' theorem defines probability density \mathcal{P} as

$$\mathcal{P}(\vec{a}|data) = \frac{1}{Z} \mathcal{L}(\vec{a}|data) \pi(\vec{a})$$

↑

Evidence Likelihood function Prior

$$Z = \int d^n a \mathcal{L}(\vec{a}|data) \pi(\vec{a}) \quad \mathcal{L}(\vec{a}|data) = \exp\left(-\frac{1}{2}\chi^2(\vec{a})\right)$$

TREATMENT OF EVOLUTION

TMDs are parametrized with gaussian k_T dependence (no widening with Q^2) and x,z - dependent collinear functions evolved in Q^2

Evolution in collinear functions are done by Q^2 parametrization using Duke, Ownen method Phys. Rev. D 30, 49 (1984)

$$N_0 + N_1 \log \left(\frac{\log(Q^2/\Lambda^2)}{\log(Q_0^2/\Lambda^2)} \right)$$

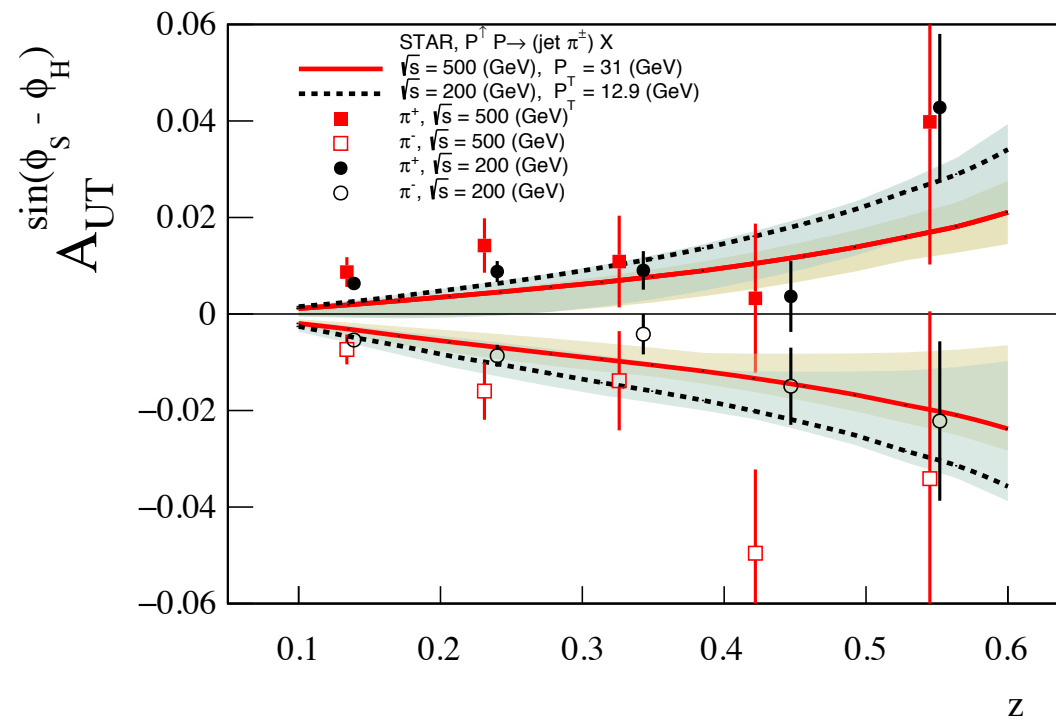
Success is achieved with Gaussian shapes for the transverse momentum dependence further implies that the effects are dominantly non-perturbative and intrinsic to the hadron wavefunctions.

TREATMENT OF EVOLUTION

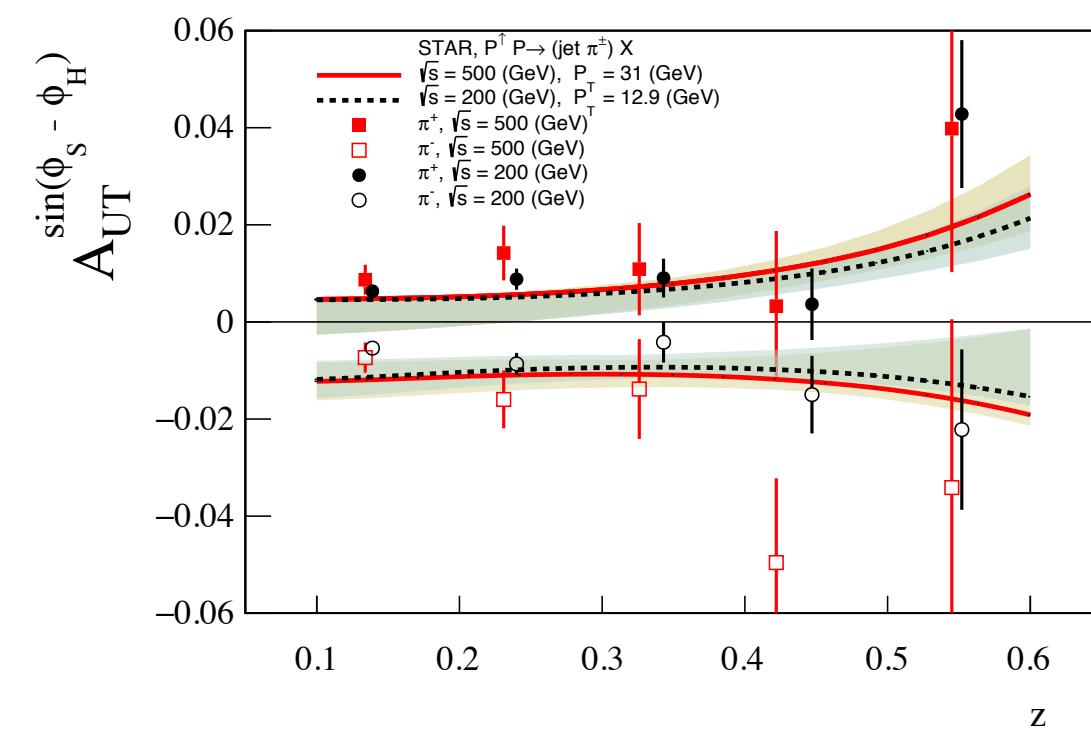
Results of this approach are consistent with resummation for asymmetries

Kang, Prokudin, Ringer, Yuan (2017)

NLL TMD evolution



Gaussian Torino model



functions: Kang, Prokudin, Sun, Yuan (2015)

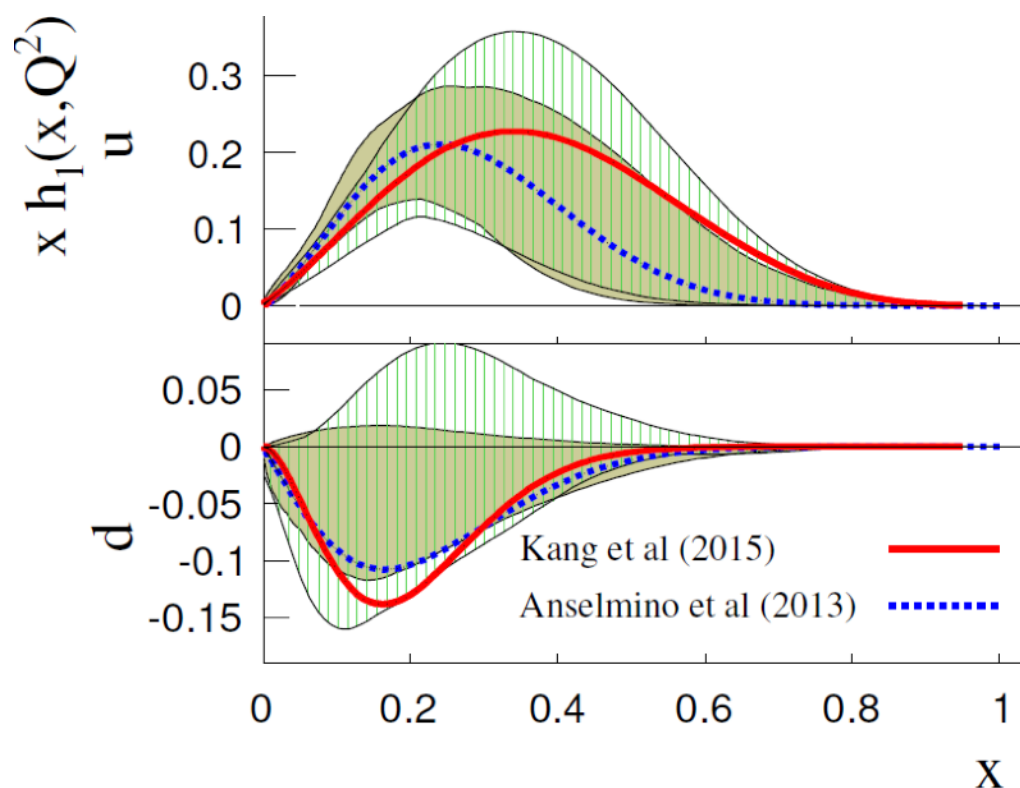
functions: Anselmino et al (2015)

TREATMENT OF EVOLUTION

Results of this approach are consistent with resummation for asymmetries

Kang, Prokudin, Ringer, Yuan (2017)

NLL TMD evolution



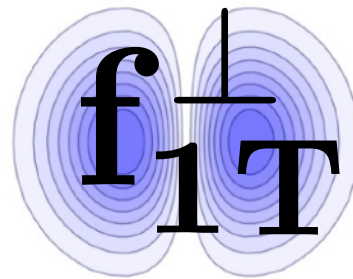
functions: Kang, Prokudin, Sun, Yuan (2015)

Gaussian Torino model

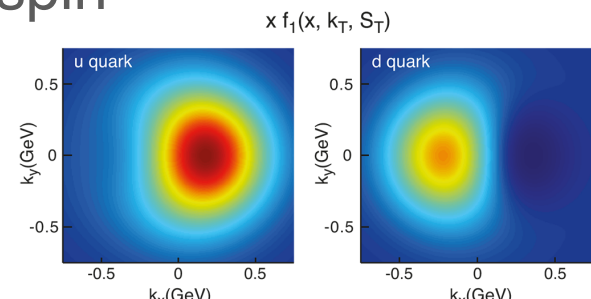
functions: Anselmino et al (2013)

POLARIZED TMD FUNCTIONS

Sivers function

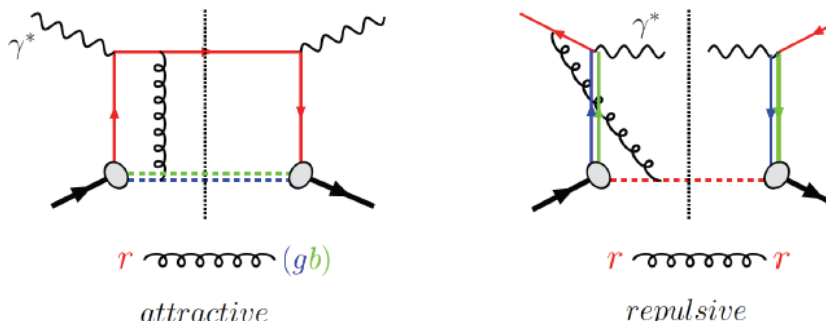


- Describes unpolarized quarks inside of transversely polarized nucleon
- Encodes the correlation of orbital motion with the spin

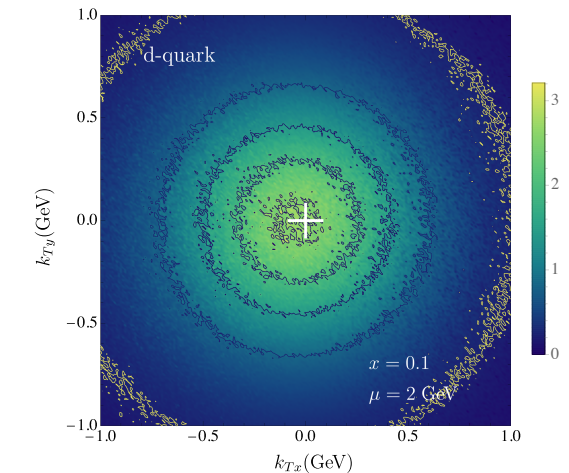
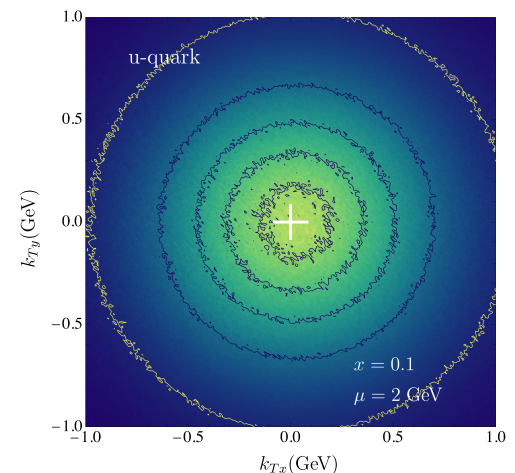


- Sign change of Sivers function is fundamental consequence of QCD

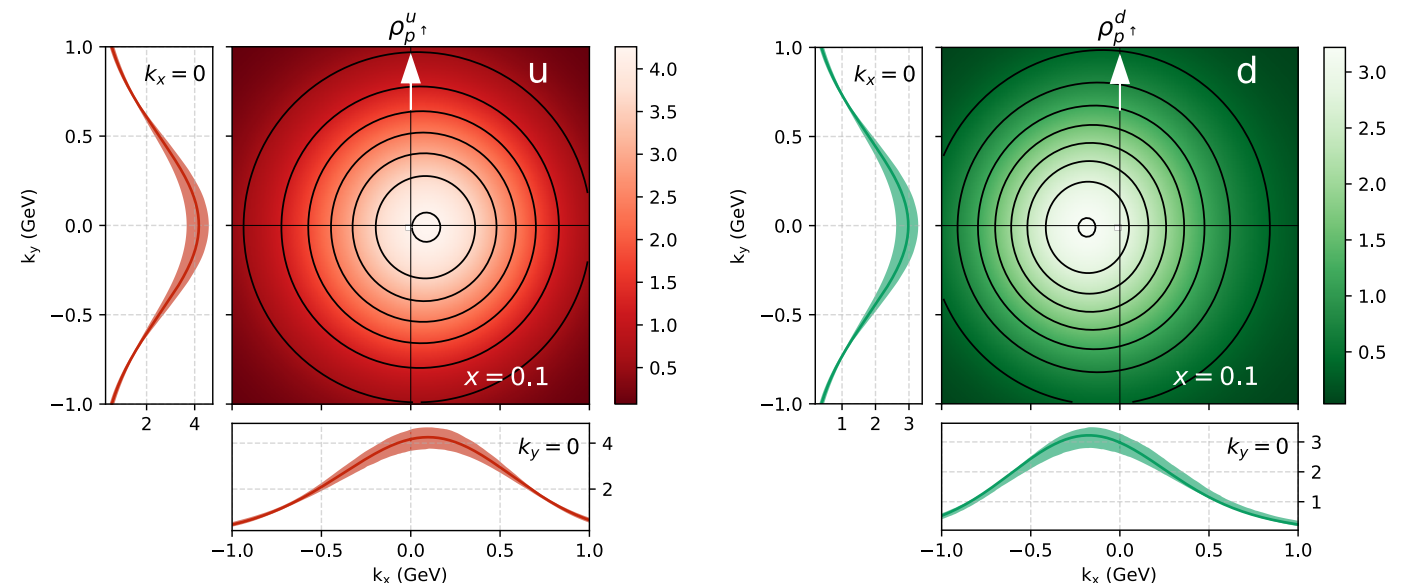
Brodsky, Hwang, Schmidt (2002), Collins (2002)



$$f_{1T}^{\perp SIDIS} = -f_{1T}^{\perp DY}$$



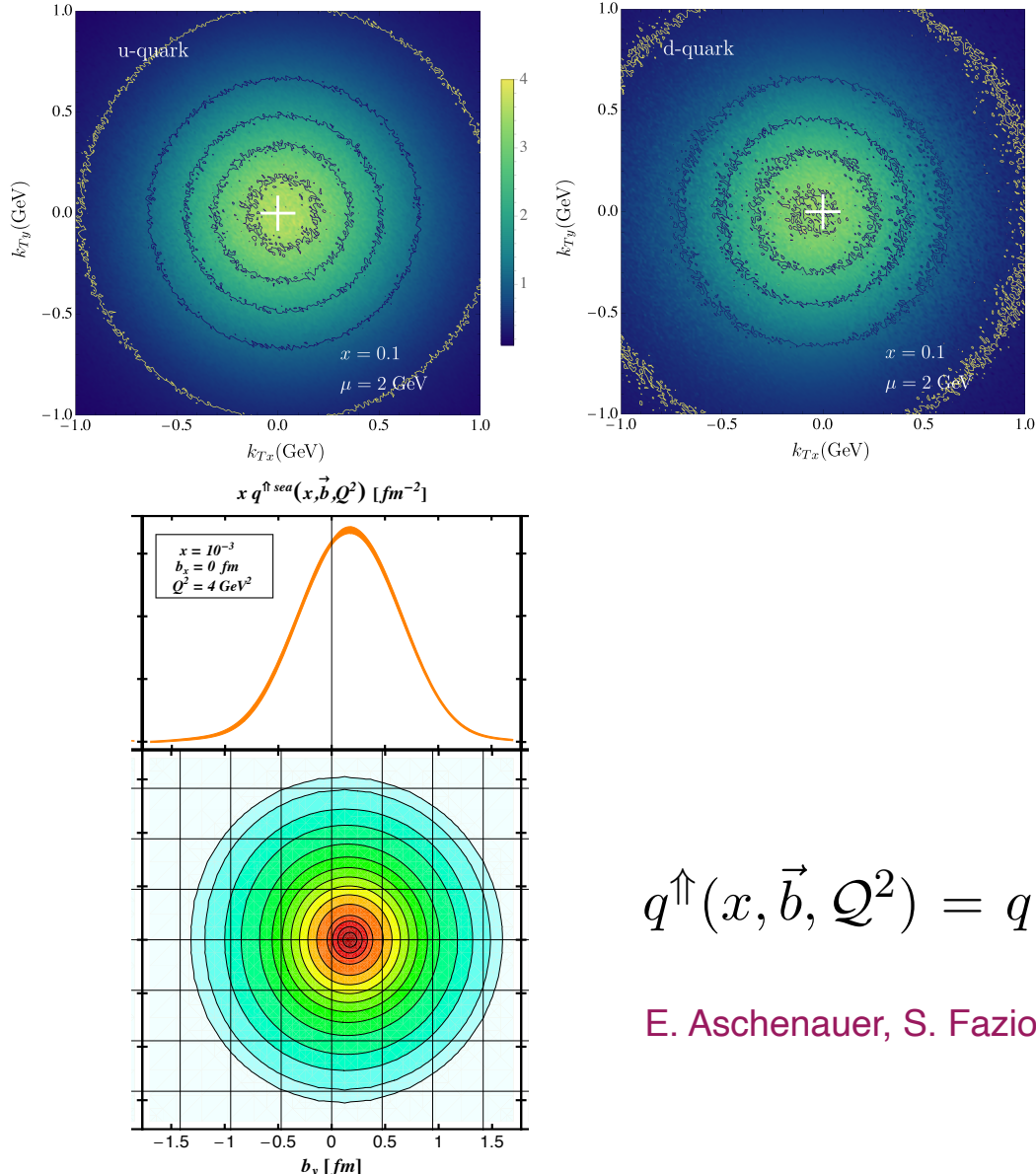
M. Bury, A. Prokudin, A. Vladimirov, Phys.Rev.Lett. 126 (2021)



A. Bacchetta, F. Delcarro, C. Pisano, M. Radici (2020)

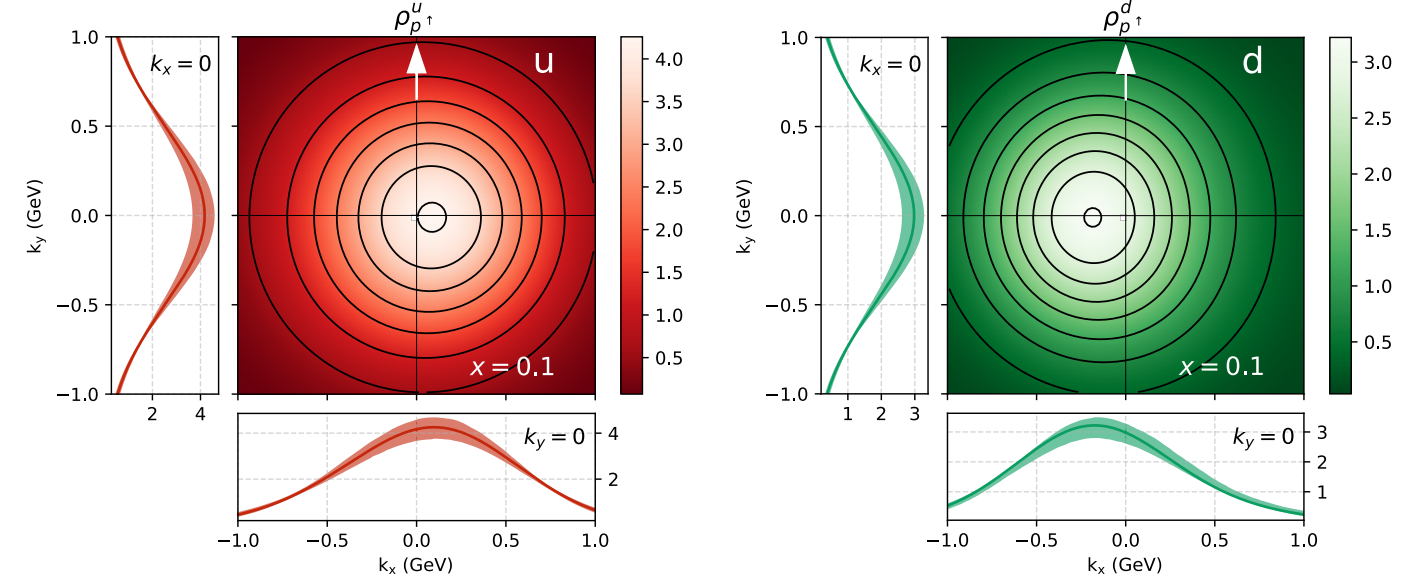
NUCLEON TOMOGRAPHY – THE FINAL GOAL OF THE EIC

$$\rho_{1;q \leftarrow h^\uparrow}(x, \mathbf{k}_T, \mathbf{S}_T, \mu) = f_{1;q \leftarrow h}(x, k_T; \mu, \mu^2) - \frac{k_T x}{M} f_{1T;q \leftarrow h}^\perp(x, k_T; \mu, \mu^2)$$



M. Bury, A. Prokudin, A. Vladimirov, Phys.Rev.Lett. 126 (2021)

A. Bacchetta, F. Delcarro, C. Pisano, M. Radici (2020)



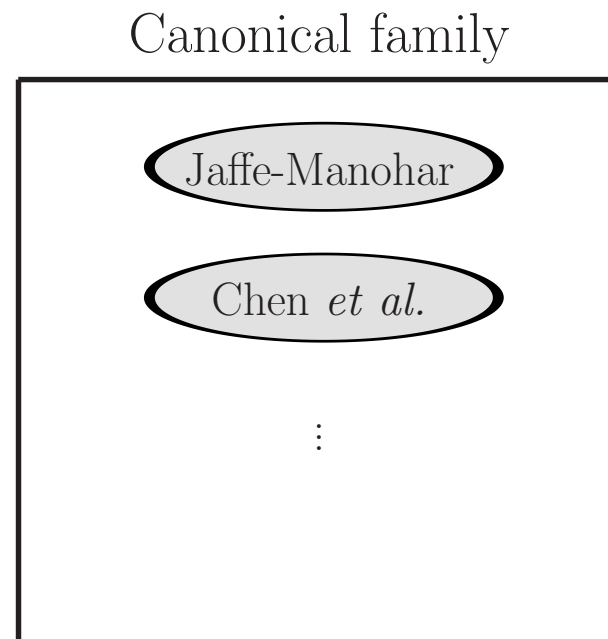
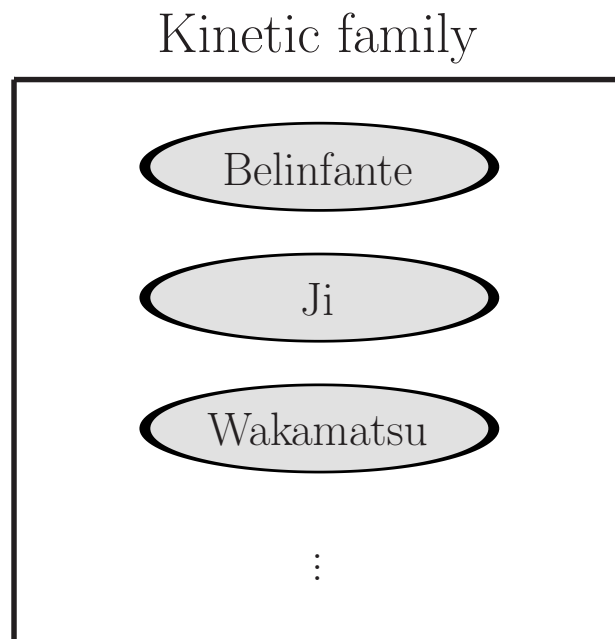
$$q^{\uparrow\uparrow}(x, \vec{b}, Q^2) = q(x, \vec{b}, Q^2) - \frac{1}{2M_p} \frac{\partial}{\partial b_y} E(x, \vec{b}, Q^2)$$

E. Aschenauer, S. Fazio, K. Kumericki, D. Mueller, JHEP 09 (2013) 093

- The shift in the transverse plane is generated by the Sivers function and GPD E that cannot exist without OAM
- The opposite signs of the shift is consistent with lattice QCD findings on the opposite signs of the OAM for u and d quarks

SPIN DECOMPOSITION

- The nucleon is a composite system. The spin is carried by its constituents: quarks, anti-quarks and gluons and the angular momentum generated by their motion.
- The nucleon at rest has spin 1/2, however its decomposition in terms of spin and orbital contributions associated with quarks and gluons is not unique.
- There are two types of decompositions of the proton spin operator: kinetic (also known as mechanical) and canonical. These two types differ by how the OAM operator is split into the quark and gluon contributions. They share the same quark spin operator.



R. L. Jaffe and A. Manohar, Nucl. Phys. B337, 509 (1990)
S. Bashinsky and R. L. Jaffe, Nucl. Phys. B 536 (1998)
X. Ji, Phys. Rev. Lett. 78 (1997)
X. -S. Chen, X. -F. Lu, W. -M. Sun, F. Wang and T. Goldman, Phys. Rev. Lett. 100 (2008)
M. Wakamatsu, Phys. Rev. D 83 (2011)
Y. Hatta, Phys. Rev. D 84 (2011)
E. Leader and C. Lorce, Phys.Rept. 541, 163 (2014)
C. Lorcé and B. Pasquini, JHEP 09 (2013)
C. Lorcé and B. Pasquini, Phys. Rev. D 84, (2011)
C. Lorcé, B. Pasquini, X. Xiong and F. Yuan, Phys. Rev. D 85, (2012)
L. Adhikari and M. Burkard, Phys.Rev.D 94 (2016)

- Kinetic family is related to Generalized Parton Distributions, while canonical in light cone gauge is related to collinear helicity distribution functions

LONGITUDINAL SPIN

When the proton or the neutron are polarized, quarks and gluons are polarized as well. Helicity distribution functions: number of quarks/gluons with spin parallel to the nucleon momentum minus the number of quarks/gluons with the spin opposite to the nucleon momentum

$$\Delta f(x, Q^2) = g_1(x, Q^2) \equiv f^+(x, Q^2) - f^-(x, Q^2)$$

The relevant spin decomposition is by Jaffe and Manohar

R. L. Jaffe and A. Manohar, Nucl. Phys. B337, 509 (1990)

$$\frac{1}{2} = S_q + \mathcal{L}_q + S_g + \mathcal{L}_g$$

Related to measured observables:

Quark spin contribution

$$S_q = \frac{1}{2} \int_0^1 \Delta \Sigma(x, Q^2) dx \equiv \frac{1}{2} \int_0^1 (\Delta u + \Delta \bar{u} + \Delta d + \Delta \bar{d} + \Delta s + \Delta \bar{s})(x, Q^2) dx$$

Difficult to measure in experiment:

$$\mathcal{L}_q + \mathcal{L}_g$$

quark and gluon orbital angular momenta (OAM)
via twist-3 GPDs, Wigner functions

D.V. Kiptily, M.V. Polyakov, Eur. Phys. J. C 37 (2004)

A. Courtoy, G. R. Goldstein, J. O. Gonzalez Hernandez, S. Liuti, A. Rajan, PLB 731 (2014)

Y. Hatta, Phys. Lett. B 708 (2012);

Y. Hatta, S. Yoshida, J. High Energy Phys. 1210 (2012)

WIGNER DISTRIBUTIONS AND THE SPIN

- Wigner distributions have information on both position and motion

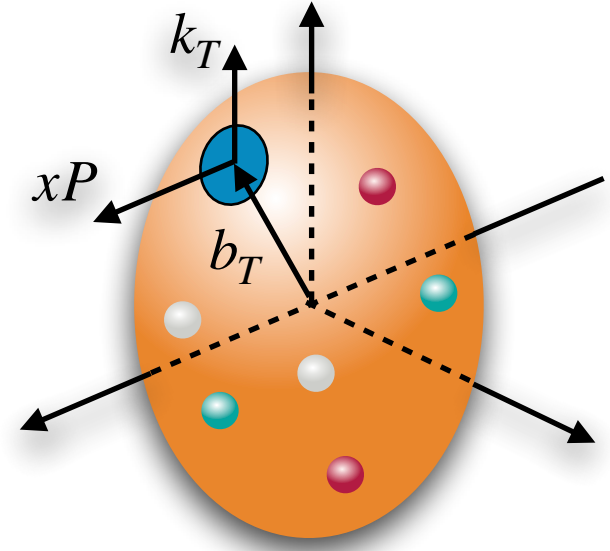
$$W(x, \vec{k}, \vec{b}) = \int \frac{dz^- d\vec{z}}{2(2\pi)^3} \int \frac{d\vec{\Delta}}{(2\pi)^2} e^{ixP^+ z^- - i\vec{k}\cdot\vec{z}} \langle P' S | \bar{\psi}(\vec{b} - \vec{z}/2) \gamma^+ \psi(\vec{b} + \vec{z}/2) | PS \rangle$$

- The most intuitive definition of OAM involves Wigner functions

$$L_z = \int dx d^2\vec{b} d^2\vec{k} (\vec{b} \times \vec{k})_z W(x, \vec{b}, \vec{k})$$

C. Lorcé, B. Pasquini, Phys. Rev. D 84, (2011)

C. Lorcé, B. Pasquini, X. Xiong and F. Yuan, Phys. Rev. D 85, (2012)



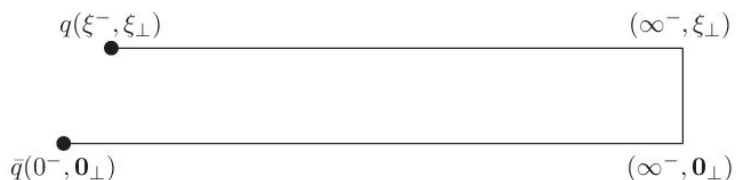
- The gauge link makes this definition gauge invariant and the two choices:

Straight link - kinetic OAM, Ji: L_q

X. Ji, X. Xiong and F. Yuan, Phys. Rev. D 88, no. 1, (2013)

Y. Hatta, PLB 708 (2012) 186

Stapple-like link - canonical OAM, Jaffe-Manohar: \mathcal{L}_q



- The difference between the two $\mathcal{L}_q - L_q$ is related to the torque force experienced by the struck quark and generated by the final state interactions M. Burkardt, Phys. Rev. D 88 (2013)
- How to fully access Wigner distributions in experiments is still to be explored

FRAGMENTATION TERMS

$$E_h \frac{d\Delta\sigma^{Frag}(S_T)}{d^3\vec{P}_h} = -\frac{4\alpha_s^2 M_h}{S} \epsilon_{PP_h S_T} \sum_i \sum_{a,b,c} \int_0^1 \frac{dz}{z^3} \int_0^1 dx' \int_0^1 dx \delta(\hat{s} + \hat{t} + \hat{u}) \frac{1}{\hat{s}} \\ \times h_1^a(x) f_1^b(x') \left\{ \left[H_1^{\perp(1),\pi/c}(z) - z \frac{dH_1^{\perp(1),\pi/c}(z)}{dz} \right] \tilde{S}_{H_1^\perp}^i + \left[-2H_1^{\perp(1),\pi/c}(z) + \frac{1}{z} \tilde{H}^{\pi/c}(z) \right] \tilde{S}_H^i \right\},$$

$$\begin{aligned} \tilde{S}_{H_1^\perp}^{qg \rightarrow qg} &= -\frac{1}{N_c^2} \frac{1}{\hat{t}} + \frac{1}{N_c^2 - 1} \frac{\hat{s}(\hat{u} - \hat{s})}{\hat{t}^3} - \frac{\hat{s}^2}{\hat{t}^2 \hat{u}}, \quad \tilde{S}_H^{qg \rightarrow qg} = \frac{1}{N_c^2 - 1} \frac{\hat{s}(\hat{u} - \hat{s})}{\hat{t}^3} + \frac{1}{N_c^2} \frac{\hat{s} - \hat{u}}{2\hat{t}\hat{u}} + \frac{(\hat{s} - \hat{u})(\hat{t}^2 - 2\hat{t}\hat{u} - 2\hat{u}^2)}{2\hat{t}^3 \hat{u}}, \\ \tilde{S}_{H_1^\perp}^{qq' \rightarrow qq'} &= \frac{1}{N_c^2} \frac{\hat{s}(\hat{u} - 2\hat{t})}{\hat{t}^3} + \frac{\hat{s}}{\hat{t}^2}, \quad \tilde{S}_H^{qq' \rightarrow qq'} = \frac{1}{N_c^2} \frac{\hat{s}(2\hat{u} - \hat{t})}{\hat{t}^3} - \frac{\hat{s}\hat{u}}{\hat{t}^3}, \\ \tilde{S}_{H_1^\perp}^{qq \rightarrow qq} &= \frac{1}{N_c^3} \frac{\hat{s}(\hat{t} - \hat{u})}{\hat{t}^2 \hat{u}} + \frac{1}{N_c^2} \frac{\hat{s}(\hat{u} - 2\hat{t})}{\hat{t}^3} + \frac{\hat{s}}{\hat{t}^2}, \quad \tilde{S}_H^{qq \rightarrow qq} = \frac{1}{N_c^3} \frac{\hat{s}(\hat{t} - 3\hat{u})}{2\hat{t}^2 \hat{u}} + \frac{1}{N_c^2} \frac{\hat{s}(2\hat{u} - \hat{t})}{\hat{t}^3} - \frac{1}{N_c} \frac{\hat{s}^2}{2\hat{t}^2 \hat{u}} - \frac{\hat{s}\hat{u}}{\hat{t}^3}, \\ \tilde{S}_{H_1^\perp}^{q\bar{q} \rightarrow q\bar{q}} &= \frac{1}{N_c^3} \frac{\hat{s}}{\hat{t}^2} + \frac{1}{N_c^2} \frac{\hat{s}(\hat{t} - \hat{s})}{\hat{t}^3} - \frac{1}{N_c} \frac{1}{\hat{t}}, \quad \tilde{S}_H^{q\bar{q} \rightarrow q\bar{q}} = \frac{1}{N_c^3} \frac{3\hat{s} - \hat{t}}{2\hat{t}^2} + \frac{1}{N_c^2} \frac{\hat{s}(\hat{t} - 2\hat{s})}{\hat{t}^3} + \frac{1}{N_c} \frac{\hat{u}}{2\hat{t}^2} + \frac{\hat{s}^2}{\hat{t}^3}, \\ \tilde{S}_{H_1^\perp}^{\bar{q}q \rightarrow \bar{q}q} &= \frac{1}{N_c^3} \frac{\hat{s}}{\hat{t}\hat{u}} - \frac{1}{N_c} \frac{1}{\hat{t}}, \quad \tilde{S}_H^{\bar{q}q \rightarrow \bar{q}q} = \frac{N_c^2 + 1}{N_c^3} \frac{\hat{s} - \hat{u}}{2\hat{t}\hat{u}}, \\ \tilde{S}_{H_1^\perp}^{q\bar{q}' \rightarrow q\bar{q}'} &= \frac{1}{N_c^2} \frac{\hat{s}(\hat{t} - \hat{s})}{\hat{t}^3}, \quad \tilde{S}_H^{q\bar{q}' \rightarrow q\bar{q}'} = \frac{1}{N_c^2} \frac{\hat{s}(\hat{t} - 2\hat{s})}{\hat{t}^3} + \frac{\hat{s}^2}{\hat{t}^3}. \end{aligned}$$

that shown in Ref. [59]. The reason is that in the forward region, where \hat{t} becomes very small, the $qg \rightarrow qg$ channel dominates, and the hard function $S_{H_1^\perp}^{qg \rightarrow qg} \propto 1/\hat{t}^3$ compensates the twist-3 $(P_{hT})^{-1}$ fall off of the asymmetry. Again, one